



01485

**UNIVERSIDAD NACIONAL AUTONOMA
DE MEXICO**

FACULTAD DE ODONTOLOGIA

FACTORES QUE REGULAN EL PROCESO DE LA
MINERALIZACION DURANTE LA CEMENTOGENESIS
IN VITRO

T E S I S
QUE PRESENTA
MARCO ANTONIO ALVAREZ PEREZ
PARA OPTAR POR EL GRADO DE:
DOCTOR EN CIENCIAS

DIRECTOR: DR. HIGINIO ARZATE



MEXICO, D. F.

2005

m. 340885



UNAM – Dirección General de Bibliotecas

Tesis Digitales
Restricciones de uso

DERECHOS RESERVADOS ©
PROHIBIDA SU REPRODUCCIÓN TOTAL O PARCIAL

Todo el material contenido en esta tesis está protegido por la Ley Federal del Derecho de Autor (LFDA) de los Estados Unidos Mexicanos (Méjico).

El uso de imágenes, fragmentos de videos, y demás material que sea objeto de protección de los derechos de autor, será exclusivamente para fines educativos e informativos y deberá citar la fuente donde la obtuvo mencionando el autor o autores. Cualquier uso distinto como el lucro, reproducción, edición o modificación, será perseguido y sancionado por el respectivo titular de los Derechos de Autor.

Jurado Asignado

Dr. Edgar Zenteno Galindo

Dr. José Reyes Gasga

Dr. Higinio Arzate

Dr. Luis Felipe Jiménez García

Dr. Jesús Chimal Monroy

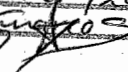
Dr. Abraham Landa Piedra

Dr. Juan Carlos Hernández Guerrero

Autorizo a la Dirección General de Bibliotecas de la UNAM a difundir en formato electrónico e impreso el contenido de mi trabajo recepcional.

NOMBRE: MARCO ANTONIO ALVAREZ PEREZ

FECHA: 31 FEBRERO 2005

FIRMA: 

Universidad Nacional Autónoma de México

Facultad de Odontología

Cualquier tesis no publicada postulando para el grado de Doctor en Ciencias y depositada en la Biblioteca de la Universidad, Facultad de Odontología, queda abierta para inspección, y solo podrá ser usada con la debida autorización. Las referencias bibliográficas pueden ser tomadas, pero ser copiadas sólo con el permiso del autor y el crédito se da posteriormente a la escritura y publicación del trabajo.

Esta tesis ha sido utilizada por las siguientes personas, que firman y aceptan las restricciones señaladas.

La biblioteca que presta esta tesis deberá asegurarse de recoger la firma de cada persona que la utilice.

Nombre y Dirección

Fecha

Dedico este trabajo a mis padres

Agradecimientos

Al Dr. Higinio Arzate por su apoyo y disposición para dirigir este trabajo. Además por compartir sus conocimientos y acertados comentarios de constante motivación que contribuyeron al desarrollo de este trabajo de investigación.

Agradezco a mi comité tutorial: Dr. Armando Báez Pedrajo, Dr. José Reyes Gasga, por su guía, asesoramiento y comentarios durante el transcurso de esta investigación.

Al Dr. Jaime Ortiz López de la Escuela Superior de Física y Matemáticas del IPN por permitirme trabajar en su laboratorio y darme las facilidades para utilizar el equipo (Microscopio de Fuerza Atómica), así como su apoyo y disposición en la realización de los experimentos.

Al Dr. Julio Juárez por su apoyo otorgado durante el desarrollo de este trabajo doctoral, así como al Dr. José Guzmán por sus acertados puntos y asesoramiento en los experimentos de microscopía de barrido.

Mi más sincero reconocimiento al jurado por darse el tiempo de revisar este documento pese a su apretada agenda de trabajo y por sus valiosos consejos, aclaraciones y comentarios para mejorar en varios puntos el contenido de esta tesis, así como del olvidado español bien escrito.

A todos aquellos que no aparecen en estos agradecimientos pero que participaron de una u otra manera en la realización de esta tesis.

Indice

Resumen	1
Abstract	3
Introducción	5
Antecedentes	9
Hipótesis	15
Objetivos	16
Metodología	17
Resultados	24
Discusión	37
Conclusiones	43
Bibliografía	44
Apéndice A (Tablas)	53
Apéndice B (Publicaciones)	55

Resumen

En esta tesis doctoral se estudia el efecto de inhibir la función de la proteína de adhesión del cemento radicular durante el proceso de la cementogenesis *in vitro*, secretada por las células derivadas de un cementoblastoma humano por medio del anticuerpo anti-CP.

Los cultivos celulares tratados con 5 µg/ml del anticuerpo anti-CP revelan una disminución en la actividad de la fosfatasa alcalina de 40% ($p < 0.005$), 44% ($p < 0.001$), 49% ($p < 0.1$) y 45% ($p < 0.02$) a los 9, 11, 13 y 15 días de cultivo cuando se comparan con los cultivos celulares control incubados con el anticuerpo normal de conejo a concentración de 5 µg/ml.

La inmunooexpresión de las proteínas involucradas en la formación de la matriz mineralizada en los cultivos tratados con 5 µg/ml del anticuerpo anti-CP, mostraron que el número de células que dieron una señal positiva para osteopontina se redujo en un 87, 83, 69 y 52% a los 5, 7, 9 y 11 días de cultivo. Asimismo, el número de células positivas para la sialoproteína ósea disminuyó en 80, 51, 60, 80, 83, y 87% a los 5, 7, 9, 11 y 15 días de cultivo, cuando se compararon con los cultivos celulares control incubados con el anticuerpo normal de conejo a concentración de 5 µg/ml.

El microanálisis del mineral depositado *in vitro* por las células derivadas del cementoblastoma nos indican que la razón Ca/P en los cultivos control es de 1.45 y 1.61 a los 5 y 15 días de cultivo, mientras que en los cultivos experimentales la razón Ca/P disminuye a 0.50 y 0.79 a los 5 y 15 días de cultivo respectivamente. Aunque la composición inorgánica disminuye en los cultivos experimentales, los patrones de difracción de rayos X a manera de anillos concéntricos que representan los espacios D-interplanares del cristal, tanto en los cultivos control como en los cultivos experimentales, demuestra que el mineral es hidroxiapatita. Estas disminuciones en la composición

inorgánica del mineral depositado se traduce en la formación de aglomerados esféricos sin un patrón organizado, que no forma las placas características del tejido mineral de cemento -como en el caso de las células control tratadas sólo con el anticuerpo normal de conejo-, determinadas por microscopía de fuerza atómica y microscopía electrónica de barrido. Sin embargo, estos patrones macroscópicos del mineral depositado, al ser analizados por microscopía electrónica de alta resolución, nos indican que la cristalinidad del mineral de hidroxiapatita muestra un arreglo preferencial de los cristales en ambos cultivos - control y experimental- a los 15 días de cultivo. Estos resultados concluyen que la proteína de adhesión de cemento es un factor importante que regula y/o participa en el proceso de la cementogénesis al afectar la actividad y función de diversas proteínas y que puede ser asociada al crecimiento del cristal así como a las características composicionales y morfológicas del mineral depositado durante el proceso de mineralización *in vitro*.

Abstract

In this thesis work, we study the inhibitory effect by a polyclonal antibody anti-CP raised against the cementum attachment protein secreted by human cementoblastoma-derived cells during cementogenesis process *in vitro*.

Cultures treated with 5 µg/ml of CP antibody from day 3 to day 15 revealed a significant decrease in alkaline phosphatase activity of 40% ($p < 0.005$), 44% ($p < 0.001$), 49% ($p < 0.1$) y 45% ($p < 0.02$) at 9, 11, 13 and 15 days respectively. Immunoexpression analysis of the proteins implicated in mineral deposition in the experimental cultures treated with 5 µg/ml of anti-CP antibody revealed that number of cementoblastoma cells expressing osteopontin was reduced by 87, 83, 69 and 52% at 5, 7, 9 y 11 days, respectively. Bone sialoprotein immunoexpression showed a decrease in positive cells of 82, 51, 60, 80, 83 and 87% at 5, 7, 9, 11 and 15 days, respectively when compared to controls. Microanalysis examination of the mineral-like tissue deposited by cementoblastoma-derived cells revealed that control cultures had a Ca/P ratio of 1.45 and 1.61 at 5 and 15 days, whereas experimental cultures revealed that Ca/P ratio was reduced to 0.50 and 0.79 at 5 and 15 days respectively. Although, the mineral-like tissue deposition process was affected in the experimental cell cultures, the mineral-like tissue corresponds to hydroxiapatite as revealed by electron diffraction pattern that showed as inner double rings representing D-spacing, which, were consistent with those of the hydroxiapatite in both control and experimental cultures. This decreased value in the inorganic composition of the mineral-like tissue was associated with a tiny, granular and spherical morphology without a special organization of needle like crystal to form plaque-like structures features of the cementum-like tissue as revealed in control cultures analyzed by atomic force microscopy and scanning electron

microscopy. However, the examination of these macroscopic patterns of the mineral-like tissue by high resolution transmission electron microscopy showed that the crystallinity of the hydroxiapatite crystal had a homogeneous and preferential spatial arrangement of the hydroxiapatite crystallites in both control and experimental cultures at 15 days of culture. Based in these observations, we suggest that the cementum attachment protein has a provocative role during cementogenesis process by affecting the activity and function of several proteins and it can be associated to the crystal growth, compositional and morphological features of the mineral-like tissue deposited by the cementoblastoma-derived cells during the mineralization process *in vitro*.

Introducción

Periodonto

El periodonto o tejido de sostén del diente, esta formado por los siguientes tejidos:

- 1) Encía
- 2) Ligamento Periodontal
- 3) Hueso alveolar
- 4) Cemento radicular

La función principal del periodonto es unir el diente al tejido óseo de la cavidad bucal y conservar la integridad de la mucosa masticatoria de la boca.

Encía

La encía es la parte de la mucosa masticatoria que rodea las porciones cervicales de los dientes. Anatómicamente esta dividida en encía marginal y encía insertada.

La encía esta formada por tejido epitelial y tejido conjuntivo, este ultimo es el tejido predominante de la encía. Sus componentes principales son fibras de colágena (60%), fibroblastos (5%), vasos sanguíneos y nervios (~ 35%).

Ligamento Periodontal

El ligamento periodontal es el tejido conectivo blando que rodea las raíces dentarias y se une a hueso. Esta compuesto principalmente por fibras de colágena dispuestas en haces que se insertan en hueso y en el cemento radicular, representando el 50% del peso seco de todo el tejido.

Hueso Alveolar

El hueso alveolar es la parte dura de los maxilares superiores e inferiores que forma y sostiene a los dientes.

El hueso alveolar junto con el ligamento periodontal y el cemento radicular constituyen el aparato de inserción de los dientes, cuya función principal es distribuir y reabsorber las fuerzas generadas por los contactos dentarios.

El hueso alveolar esta formado por las células osteoblásticas encargadas de depositar la fase osteoide, constituida por fibras de colágena y una matriz que contiene proteínas no colágenas y proteoglucanos. Esta fase osteoide experimenta una mineralización por depósitos de sales minerales de fosfato de calcio que se transforma en cristales de hidoxiapatita.

En el proceso de mineralización del hueso alveolar, los osteoblastos quedan atrapados en la matriz mineralizada convirtiéndose en los osteocitos, los cuales se nutren y comunican por medio de sus prolongaciones citoplasmicas^{1,2}.

Cemento Radicular

El cemento radicular fue descrito por primera vez en 1835 por los discípulos de Purkinje como un tejido mineralizado que cubre la superficie radicular de los órganos dentarios. Sus principales funciones son el proveer el anclaje para las fibras de colágena del ligamento periodontal (fibras de Sharpey), mediar en la inserción del diente al hueso alveolar, distribuir las fuerzas masticatorias y jugar un papel primordial en la reparación de la superficie radicular. Estas funciones se pierden cuando el cemento es afectado por la enfermedad crónica episódica e inflamatoria, la periodontitis, la cual es considerada un problema de salud pública a nivel mundial¹.

Estructura

En el cemento radicular pueden diferenciarse dos tipos de cemento: el acelular y el celular. El término cemento acelular no es muy apropiado ya que como tejido vivo, las células son parte integral del cemento en todo momento. No obstante, algunas capas de cemento

radicular no incorporan células en su matriz mineralizada, característica que les da su nombre. Este tipo de cemento cubre la dentina radicular desde la unión cemento-esmalte hasta el tercio medio de la superficie radicular.

A partir del tercio medio y hasta el ápice, donde el cemento es en su totalidad de tipo celular debido a que los cementoblastos (unidades estructurales) encargados de sintetizar la matriz tanto orgánica como inorgánica del cemento quedan atrapados en la matriz mineralizada que ellos mismos producen y se denominan cementocitos. Los cementoblastos son células cuboidales que presentan características ultraestructurales únicas: numerosas mitocondrias, un aparato de Golgi bien desarrollado y grandes cantidades de retículo endoplásmico granular, lo que revela su intensa actividad biológica.

El cementocito típico posee numerosas prolongaciones celulares o canículos que se irradian a partir de su cuerpo celular. Estas prolongaciones pueden ramificarse y con frecuencia establecer anastomosis con las de una célula vecina. El citoplasma del cementocito contiene escasas mitocondrias, mientras que el retículo endoplásmico parece dilatado y el núcleo es pequeño, revelando involución y picnosis, indicando que los cementocitos son células en proceso de degeneración y se propone que presentan una escasa actividad biológica^{3,4}.

Propiedades físico-químicas

El cemento radicular se asume que es idéntico al hueso, porque presenta similitudes con este:

- 1) Las enfermedades que afectan las propiedades del hueso, a menudo alteran las propiedades del cemento. Por ejemplo, la enfermedad ósea de Paget resulta en hipercementosis; la hipofosfatasa resulta en la no-formación de cemento, con la exfoliación dentaria y el hipopituitarismo que esta asociado con la disminución de cemento.⁵

2) La composición inorgánica de cemento radicular es similar a hueso alveolar. Tanto el cemento como el hueso se componen aproximadamente del 50% de fosfatos de calcio que se encuentra en forma de cristales de hidroxiapatita $[Ca_{10}(PO_4)_6(OH)_2]$. Además, en el cemento se encuentran elementos trazas, entre los que podemos mencionar al magnesio (0.5 al 1.4%), flúor, sodio, cobre, azufre y zinc, y que actualmente; tanto en su distribución y significado biológico no han sido estudiados a detalle.⁶

3) La matriz orgánica de cemento es considerada similar al hueso: consiste primariamente de colágenas Tipo I (95%) y Tipo III (5%), las cuales en su conjunto, desempeñan un papel tipo estructural. Moléculas no colágenas como fibronectina (FN), sialoproteína ósea (BSP), osteopontina (OPN), fosfatasa alcalina (ALP), etc., diversos factores de crecimiento como IGF-I, FGFa, FGFb, PDGF y TGF β ^{7, 8}, proteoglucanos y glucosaminoglucanos como el dermatan sulfato, hialurona, condroitina sulfato, lumican, entre otros, que han sido identificados bioquímicamente e histoquímicamente como las especies dominantes, pero no son cemento específicas^{9, 10}.

A pesar de estas similitudes, el cemento radicular tiene características únicas que lo pueden diferenciar del hueso: presenta un color amarillo, una baja microdureza, un recambio metabólico bajo, carece de inervación, de irrigación sanguínea directa, drenaje linfático, a diferencia del hueso alveolar no sufre procesos de remodelación de un modo fisiológico, presenta una formación activa caracterizada por un depósito continuo durante toda la vida, que se observa a manera de líneas de crecimiento; y posee - hasta el momento- moléculas específicas de matriz como la proteína de adhesión de cemento (CP) y el factor de crecimiento del cemento radicular (CGF) que se ha reportado ser similar al factor de crecimiento insulínico tipo I (IGF-I)^{11, 12}.

Antecedentes

La investigación desde 1835 sobre la histología y composición del cemento radicular ha demostrado que el cemento es un tejido único. Mientras, los estudios sobre las proteínas específicas expresadas por los cementoblastos, así como, la localización de las células progenitoras de los cementoblastos durante el desarrollo, y en el estadio adulto, permanece como un paradigma oscuro^{13, 14}.

Durante el desarrollo, se sugiere que las células ectomesenquimatosas, células del folículo y células de la papilla dental, cuando se estimulan correctamente tienen la capacidad de actuar como cementoblastos^{15, 16}. En el estadio adulto, se propone que una pequeña población de las células del ligamento periodontal maduro tiene la capacidad para diferenciarse hacia un fenotipo osteoblástico o cementoblástico con la consiguiente formación de tejido mineralizado^{17, 18}.

Los estudios para dilucidar el origen de las células progenitoras de los cementoblastos se han basado en un modelo animal (ratón), indicando que las células de los espacios endosteales del hueso alveolar migran y adoptan una localización paravascular en el ligamento periodontal, convirtiéndose posteriormente en células formadoras de tejido mineral^{19, 20}, sin embargo, es preciso establecer, que, el proceso de la cementogénesis en ratón no constituye un modelo paralelo a la cementogénesis en humanos^{21, 22}.

Alternativamente, se ha propuesto que diferentes factores suministrados por las células epiteliales dentro de un ambiente local, pueden en parte influenciar la diferenciación de las células del folículo dentario hacia cementoblastos, de tal modo que, secretan la matriz mineralizada de cemento^{23, 24}, o bien, se propone una hipótesis en que las mismas células de la vaina epitelial radicular de Herwig se encuentren bajo una transformación generativa

hacia cementoblastos (transformación ectomesenquimática) y así proveer la apropiada matriz para la formación del tejido cementoide²⁵.

Por tal motivo, los factores que disparan la proliferación de los precursores de los cementoblastos, los que controlan la migración celular dirigida hacia la superficie radicular y los que regulan su diferenciación en el periodonto adulto permanecen como preguntas abiertas. Las anteriores interrogantes se pueden abordar al identificar, aislar y caracterizar poblaciones celulares que expresen el fenotipo del cemento radicular. Sin embargo, existen dificultades para lograr este objetivo:

- 1) Los laboriosos procedimientos de disección requeridos para obtener suficiente tejido para estudiar sus propiedades bioquímicas y moleculares.
- 2) A la fecha no existe un marcador biológico específico de la matriz extracelular del cemento radicular.
- 3) La población celular del ligamento periodontal es heterogénea, lo cual implica que existen linajes osteoblásticos, cementoblásticos y fibroblásticos, que impiden aislar una población puramente cementoblástica²⁶.

Observaciones recientes indican que el 40% del total de las poblaciones del ligamento periodontal expresan un fenotipo asociado a la formación de tejido mineralizado y solo el 7% de esta población expresa el fenotipo cementoblástico con alta actividad específica de ALP, lo que revela estadios de diferenciación²⁷.

A este respecto, nuestro laboratorio desarrolló una estrategia de investigación tendiente a contribuir al conocimiento de la biología del cemento radicular, la cual consistió en aislar, expandir y caracterizar parcialmente una línea celular a partir de un cementoblastoma de humano²⁸.

La Organización Mundial de la Salud considera al cementoblastoma como un raro tumor odontogénico de origen mesenquimatoso descrito por primera vez por Norberg en 1930. La lesión es solitaria, presentando un crecimiento lento asociada a la raíz de dientes permanentes (premolares y/o molares). Radiográficamente, la lesión esta bien delimitada y la parte central es radio-opaca y comúnmente rodeada por una zona radio-luminosa de anchura uniforme, la cual representa el tejido no mineralizado que corresponde a las capas celulares en formación, es decir, cementoblastos²⁹.

Los cultivos de las células derivadas del tumor de cemento, estudiadas en nuestro laboratorio, manifestaron, inicialmente, una morfología fibroblástica, y después del pasaje 4^{to} a 5^{to} asumieron una morfología distinta; consistente en células más anchas, aplanadas y multipolares, especialmente cuando llegaban a confluencia.

La caracterización de las células derivadas del cementoblastoma, muestran que esta línea celular parece ser homogénea, así como expresar el fenotipo del cemento celular humano, dado que expresan marcadores asociados a tejidos mineralizados como:

- 1) La fosfatasa alcalina (ALP) enzima reconocida como un marcador biológico en el complejo proceso de la diferenciación de osteoblastos y cementoblastos, participando en la mineralización de la matriz extracelular, probablemente, regulando las concentraciones extracelulares de fosfatos^{30, 31}
- 2) Proteínas no colágenas como la osteopontina (OPN) y la sialoproteína ósea (BSP): "Proteínas que se encuentran en la respectiva matriz mineralizada de cemento e implicadas en la deposición del mineral y en las interacciones matriz-matriz durante el desarrollo radicular"^{32, 33}.

El estudio de la naturaleza y propiedades estructurales del tejido mineral depositado *in vitro* por las células derivadas del cementoblastoma en nuestro laboratorio, muestran que es

diferente al compararlo con el tejido mineralizado depositado por células derivadas de hueso alveolar *in vitro*. Además, el tejido mineralizado tiene características similares al cemento radicular humano *in vivo*, tanto en morfología, como en composición y ultraestructura; por lo cual, estas células las hemos considerado como una línea de cementoblastos putativos^{34, 35}. Resultados preliminares, sugieren que las células derivadas del cementblastoma humano, aunque probablemente comparten un progenitor común con las células osteoblásticas, siguen diferentes vías en el proceso de mineralización y por lo tanto, en la diferenciación, ofreciendo una oportunidad única para dilucidar como el proceso de la cementogénesis es regulado *in vitro*.

Por otro lado, esta línea celular derivada del cementblastoma -de un modo importante- también ha mostrado producir una proteína relacionada a la proteína de adherencia del cemento radicular (CP por sus siglas en inglés: cementum attachment protein), la cual al parecer es el único marcador biológico de este tejido a la fecha¹³. Los estudios de secuencias parciales de aminoácidos obtenidas de la proteína CP, han revelado que se trata de una proteína de tipo colágena, debido a que cuatro de las seis secuencias obtenidas presentan cierta homología en su estructura primaria con colágena tipo I y XII dado que contienen la repetición Gly-X-Y característica de la estructura de triple hélice de la colágena, aunque algunos de los péptidos obtenidos muestran que no son triple-helicoidales³⁶.

Algunas de las posibles explicaciones para encontrar ambos tipos de secuencias son que CP podría contener secuencias no colágenas y colágenas y alternativamente CP podría ser una proteína de adherencia de tipo colágena localizada en el cemento radicular, aunque esto parece improbable, ya que, los anticuerpos contra colágena tipo I, V, XII, y XIV no presentaron reacción cruzada contra CP por medio de inmunotransferencias³⁷.

El análisis por computadora de las secuencias parciales de aminoácidos de CP revelaron que no están presentes en fibronectina, laminina, osteopontina, sialoproteína ósea, y vitronectina, lo que muestra que la CP es una molécula única y probablemente específica para el cemento radicular³⁸.

Los estudios dirigidos para entender cual es la función de esta proteína, han demostrado que es capaz de promover la expresión de ALP, inducir la formación de nódulos mineralizados en células mesenquimatosas embrionarias sin un fenotipo definido *in vitro*, promover la adherencia celular, mostrar afinidad por la hidroxiapatita. Se sugiere que CP es un factor importante en la quimioatracción, adhesión y diferenciación celular en el proceso de la cementogénesis y posiblemente en la regeneración de las estructuras periodontales^{39, 40, 41}.

La producción de CP por las células del cementoblastoma humano, nos indica que; esta línea celular es una fuente significativa para la obtención, purificación y caracterización del marcador biológico del cemento radicular. En nuestro laboratorio, se llevó a cabo la producción de un anticuerpo policlonal contra esta proteína obtenida a partir del medio condicionado. Las inmunotransferencias han mostrado que este anticuerpo policlonal (anti-CP), reconoce una proteína relacionada con cemento con un peso molecular de 56 kDa tanto de extractos de cemento radicular humano como de las células derivadas del cementoblastoma humano *in vitro*.

Para determinar la especificidad celular del anticuerpo se utilizaron secciones transversales y longitudinales de dientes de humano así como cultivos celulares derivados del ligamento periodontal, hueso alveolar y células del cementoblastoma humano.

Los resultados de los ensayos inmunohistoquímicos nos muestra que este anticuerpo reconoce cemento, cementoblastos, cementocitos, células progenitoras en los espacios

endosteales de hueso alveolar y células de localización paravascular en el ligamento periodontal. Lo que nos indica la especificidad en la expresión y distribución de la proteína derivada de cemento en el periodonto.

Por otro lado, estudiamos si la proteína immunopurificada a partir de las células aisladas del cementoblastoma tenía la propiedad de promover la adhesión celular. Los ensayos muestran que la proteína promueve la adherencia de las células del ligamento periodontal, de hueso alveolar y de fibroblastos gingivales de manera creciente en la concentración⁴².

Juntos, todos estos datos preliminares, indican que la proteína derivada por nosotros, del cementoblastoma, podría ser una molécula relacionada a CP y servir como un marcador biológico para el tejido mineralizado del cemento radicular y probablemente encargada de regular en parte el proceso de mineralización durante la cementogénesis. Sin embargo, si esta proteína es específica para el cemento radicular, esto debe determinarse en el futuro con la disponibilidad de la secuencia de ADNc para determinar las células que expresan esta proteína durante el desarrollo, maduración y regeneración de las estructuras periodontales.

Hipótesis

La proteína de adhesión derivada del cemento (CP) regula la expresión de factores y/o marcadores que juegan un papel importante en la formación de tejido mineral, tales como: la fosfatasa alcalina (ALP), osteopontina (OPN) y sialoproteína ósea (BSP), asimismo participa en la regulación de la naturaleza y características morfológicas del tejido mineral depositado durante el proceso de la cementogenesis *in vitro*.

Objetivos

Objetivo General

El propósito de este trabajo es estudiar el papel regulador de CP en la expresión de ALP, OPN y BSP, así como sobre la naturaleza y características del tejido mineral depositado *in vitro* durante el proceso de la cementogénesis.

Objetivo Específico

- 1) Inhibir CP por medio del anticuerpo anti-CP para correlacionar dicha molécula con la expresión de ALP, OPN y BSP durante el proceso de la cementogénesis *in vitro*.
- 2) Determinar y caracterizar el tejido mineral depositado al inhibir CP durante el proceso de la cementogénesis *in vitro*.

Metodología

Cultivo celular

Las células derivadas del cementoblastoma humano, se mantuvieron en un medio de cultivo DMEM suplementado con 10% de suero fetal bovino (SFB), una solución de antibióticos (penicilina 100 U/ml, estreptomicina 100 µg/ml y fungizona 0.3 µg/ml). Los cultivos se mantuvieron a una temperatura de 37°C y en una atmósfera de 95% de aire y 5% de CO₂ en un ambiente con 100% de humedad. Para el trabajo experimental se utilizaron cultivos celulares en el segundo pasaje.

Ensayo de proliferación

Para determinar si el anticuerpo normal de conejo y el anticuerpo policlonal que reconoce a la proteína de adhesión de cemento (anti-CP) afecta la proliferación celular, las células derivadas del cementoblastoma humano fueron cultivadas en placas de cultivo de 48 pozos a una densidad celular de 2×10^4 e incubadas en 10% de SFB, toda la noche, en las condiciones mencionadas anteriormente. Al día siguiente (designado como día cero), el medio fue cambiado y los cultivos celulares fueron incubados con un medio de cultivo con 10% de SFB más 5 µg/ml del anticuerpo policlonal anti-CP. Los cultivos controles fueron incubados con 10% de SFB más 5 µg/ml el anticuerpo normal de conejo. El medio fue cambiado cada tercer día. Las células fueron colectadas con 0.05% de tripsina porcina - 0.02% de EDTA. Una vez obtenido el botón, las células se contabilizaron utilizando un contador Coulter Counter (Coulter electronics, Hialeah, Florida). El número de células fue evaluado a los 1, 3, 5 y 10 días de cultivo celular. Los experimentos se realizaron por triplicado repitiéndose dos veces.

Ensayo de viabilidad celular

Para estudiar si el anticuerpo anti-CP que reconoce a la proteína de adhesión, derivada de cemento (CP), afecta a la viabilidad celular; se realizó un ensayo de azul de trizol (MTT) basado en la habilidad de la enzima deshidrogenasa mitocondrial para oxidar la sal de tetrazolio (3-[4,5-dimetiltiazol-2-y]-2-5 bromuro difeniltetrazolio) a un producto insoluble de color azul. Las células del cementoblastoma fueron cultivadas en placas de 96 pozos a una densidad de 1×10^4 por triplicado e incubadas con 5 $\mu\text{g}/\text{ml}$ del anticuerpo anti-CP (experimentales) y con 5 $\mu\text{g}/\text{ml}$ del anticuerpo normal de conejo (control) por 1, 3, 5 y 10 días de cultivo. Después de cada periodo experimental, las células fueron incubadas con MTT (120 mg/ml) a 37°C por 3 h. Pasado este tiempo, el sobrenadante fue removido y a cada pozo de cultivo se le adicionó una solución con 0.04 M de ácido clorhídrico (HCl) en isopropanol y la placa se llevó a un lector para análisis de inmunoabsorción unida a enzimas (ELISA) para obtenerse la densidad óptica a una longitud de onda de 570 nm. Los experimentos se realizaron por triplicado repitiéndose dos veces.

Inhibición de CP

Para estudiar que CP es una proteína reguladora del proceso de la cementogenesis, probamos el efecto de inhibir a CP por medio de ensayos de inhibición, incubando las células derivadas de un cementoblastoma humano con el anticuerpo polyclonal (anti-CP) sobre la actividad de moléculas involucradas en el proceso de la cementogenesis y en la capacidad de formación del tejido mineral.

Las células fueron cultivadas en los siguientes tiempos 5, 7, 9, 11, 13 y 15 días en medio DMEM suplementado con 10 % SFB, antibióticos (penicilina 100 U/ml, estreptomicina

100 µg/ml y fungizona 0.3 µg/ml), 10 mM de β -glicerofosfato, 50 µg/ml de ácido ascórbico y 10^{-7} M de dexametasona.

Los cultivos experimentales se trataron con 5 µg/ml del anticuerpo anti-CP y los cultivos control con 5 µg/ml del anticuerpo normal de conejo. En cada punto experimental se procedió a examinar la actividad específica de la fosfatasa alcalina, la presencia de osteopontina y sialoproteína ósea, así como, el mineral formado, como se describe a continuación.

Ensayo de la actividad específica de la fosfatasa alcalina

Se sembraron células en placas de 24 pozos a una densidad de 2×10^4 como se describió anteriormente, cambiándose el medio y el anticuerpo cada 72 h. La actividad de la enzima fosfatasa alcalina (AP) se determinó de acuerdo al método de Lowry⁴³. Las células se sometieron a sonicación para extraer las capas celulares en una solución amortiguadora con 10 mM de Tris-HCL pH 7.4 más 0.1% de tritón X-100. Los ensayos de la actividad enzimática se llevaron a cabo utilizando el sustrato p-nitrofenil fosfato (PNP) a una concentración de 8 mM y como activador enzimático 2 mM de cloruro de magnesio ($MgCl_2$) en una solución amortiguadora con 10 mM de tris-HCl pH 9.8 e incubado a 37°C por 30 min. La reacción enzimática se detuvo adicionando 50 µL de 0.05 N de hidróxido de sodio (NaOH) y entonces, se hicieron las mediciones de la absorbancia a una longitud de onda de 405 nm. La concentración de proteínas se determinó por el método de Bradford⁴⁴ usando como control estándar albúmina sérica bovina (BSA). Los ensayos fueron por triplicado y se repitieron al menos tres veces.

Detección de OPN y BSP por Inmunofluorescencia

Se utilizaron cultivos celulares a una densidad de 5×10^2 en placas Lab-Tek de 8 pozos. Al término de cada tiempo experimental, las células se fijaron con 3.7% de formaldehído y se incubaron con el primer anticuerpo contra OPN (LF-123) y BSP (LF-100) donado por el Dr. Larry Fisher (NHI), para determinar la presencia de OPN y BSP. La concentración de los anticuerpos primarios fue de 1:300 en un amortiguador salino de fosfatos (PBS), conteniendo 1 mg/ml de BSA e incubados toda la noche a 4°C. Los portaobjetos se lavaron con PBS frío por 10 min. e incubados con el segundo anticuerpo cabra anti-conejo IgG conjugado con FITC (3mg/ml, Sigma chemical Co., St, Louis, Mo.) durante 1 h. a 4°C diluido a una concentración de 1:50 en PBS. Por último, los portaobjetos se lavaron con PBS más 0.1% de triton X-20 y cubiertos con glicerol-PBS (1:9 v/v) conteniendo 20 mg/ml 1,2, diazabiciclo (2,2,2) octano (DABCO). La inmunotinción se visualizó por inmunofluorescencia indirecta en un microscopio Axiophot, Carl Zeiss. El número de células que reaccionaron positivamente con el anticuerpo que reconoce a OPN y BSP fue determinado escogiendo cinco campos al azar con el objetivo 20x. Los resultados son expresados como media ($n=5$) ± error estándar de tres experimentos independientes. Los controles negativos fueron las células incubadas con suero pre-inmune de conejo o aquellos cultivos a los cuales no se les adicionó el primer anticuerpo.

Análisis de OPN y BSP por medio de Inmunotransferencia

Para determinar los niveles de proteínas asociadas al proceso de mineralización se vieron afectados al inhibir CP por el anticuerpo anti-CP, los cultivos experimentales fueron comparados contra los tratamientos con el anticuerpo normal de conejo. Las células fueron sembradas a una densidad de 5×10^4 en platos de cultivo de 35 mm³ como se menciono

anteriormente. En cada tiempo (5, 7, 9,11, 13 y 15 días) las células fueron recuperadas y resuspendidas en PBS frío y centrifugadas a 2000 rpm durante 5 min. Los botones celulares de ambos tratamientos, fueron lisados en amortiguador de lisis (1mM de EDTA (pH 8) 10 mM Hepes, 50 mM NaCl, 0.05% 2-mercaptoetanol, 0.5% triton X-100, 1mM fenilmetilsulfonilfluoruro, 5 µM de leupeptina y 10 de µM aprotinina). Después de centrifugar el botón celular a 14000 rpm durante 10 min. a 4°C, los sobrenadantes fueron almacenados a – 20°C. La concentración de proteínas se determinó de acuerdo al método de Bradford⁴⁴ y se utilizó albúmina sérica bovina como estándar. Para cada anticuerpo (OPN y BSP), las mismas cantidades de proteína (10 µg/línea) fueron cargadas en los geles de poliacrilamida-SDS al 12%. Las proteínas fueron electroforéticamente transferidas sobre una membrana PVDF y posteriormente bloqueada con 5% de leche descremada más 0.1% de Tween 20 en PBS pH 7.6 durante 1 h. Las membranas fueron incubadas con cada uno de los anticuerpos mencionados (anti-OPN y anti-BSP) a una concentración 1:300 por 1 h. a temperatura ambiente. Después de lavar, las membranas se incubaron con un anticuerpo cabra anti-conejo IgG conjugado a peroxidasa de rábano a una concentración 1:1000 durante 1 h., lavados con PBS y revelados con diaminobenzidina (DAB). La membrana fue capturada por un escáner y analizada con un programa de análisis y documentación de electroforesis EDAS 290, Kodak. El nivel relativo de cada proteína se determinó midiendo la intensidad relativa integrada de todos los píxeles en cada banda de proteína, excluyendo el fondo local. Los resultados se expresan como porcentajes de la intensidad obtenida en los cultivos control.

Caracterización de tejido mineral depositado

Para determinar el patrón de mineralización del tejido mineral generado por los cultivos celulares, se utilizaron técnicas de microscopía de alta resolución, tales como: microscopía de fuerza atómica (MFA), microscopía electrónica de barrido (MEB) y de transmisión (MET), ya que todas en su conjunto son complementarias.

Microscopía de fuerza atómica

Esta técnica se utilizó para determinar la acción de CP en la homogeneidad y morfología del mineral formado por las células del linaje cementoblástico. Se empleó un microscopio Park Scientific Instruments con autosonda en modalidad de contacto y modo constante de fuerza de 5 nN. Las células fueron cultivadas a una densidad de 2×10^4 en placas Costar de 24 pozos sobre un substrato de silicio y los cultivos se mantuvieron durante 5 y 15 días en medio DMEM suplementado con 10 % SFB, antibióticos (penicilina 100 U/ml, estreptomicina 100 µg/ml y fungisona 0.3 µg/ml), 10 mM de β-glicerofosfato, 50 µg/ml de ácido ascórbico y 10^{-7} M de dexametasona. Los cultivos experimentales se incubaron con 5 µg/ml del anticuerpo anti-CP y los cultivos control con 5 µg/ml del anticuerpo normal de conejo, cambiándose el medio y el anticuerpo cada 76 h. Al término de este tiempo, los cultivos se lavaron con PBS, fijados *in situ* con etanol y secados al aire.

Microanálisis de energía dispersiva electrónica con rayos X (EDS)

La composición del tejido mineral formado por las células del linaje cementoblástico cultivadas como se mencionó en el apartado anterior, a los 5 y 15 días, se analizaron utilizando un microscopio electrónico de barrido (SEM Leica-Cambridge 440) equipado con el aditamento Pentafet y la microsonda para el microanálisis de composición química con rayos X (EDS). Los análisis se llevaron a cabo a 20 KeV por 300 segundos.

Microscopía electrónica de transmisión

Con el propósito de determinar las características estructurales y cristalográficas de la fase mineral generada por las células, estas fueron cultivadas únicamente por 15 días como se mencionó anteriormente, sobre rejillas de cobre recubiertas con una delgada capa de carbón para determinar el patrón de difracción electrónica. Los patrones de difracción de los espacios interplanares-D fueron calibrados contra aquellos obtenidos con el estándar de oro en idénticas condiciones de difracción para la hidroxiapatita. La fase mineral fue analizada con un MET Jeol 100 CX a 100 KeV. La información nos permitió determinar las etapas de maduración de los cristales de hidroxiapatita y su arreglo espacial.

Análisis estadístico

Los datos obtenidos de los ensayos de proliferación y viabilidad celular fueron evaluados por análisis de varianza. Para los demás ensayos se llevó a cabo un análisis de *t de student* usando un programa de estadística Sigma Stat versión 2.0 (Jandel Scientific).

Resultados

Ensayo de proliferación y de viabilidad celular

Para determinar si el anticuerpo normal de conejo y el anticuerpo anti-CP alteran a las células derivadas del cementoblastoma; el índice de proliferación fue analizado durante un periodo de 10 días. Como se observa en la figura 1 (A), no existe una diferencia estadísticamente significativa entre los tratamientos con el anticuerpo normal de conejo, el anticuerpo anti-CP y el control tratado solo con 10 % de SFB.

Por otro lado, el anticuerpo anti-CP no afectó la viabilidad celular basado en la actividad de oxidación del MTT por la enzima deshidrogenasa en las células del cementoblastoma comenzando en el día 3 y continuando hasta el día 10 sin mostrar cambios estadísticos significativos entre el anticuerpo normal de conejo, con respecto al medio control que solo presenta 10% de SFB, lo cual se ilustra en la Figura 1B. La dosis utilizada de los anticuerpos fue similar a los estudios realizados *in vitro* por Shakibaei⁴⁵.

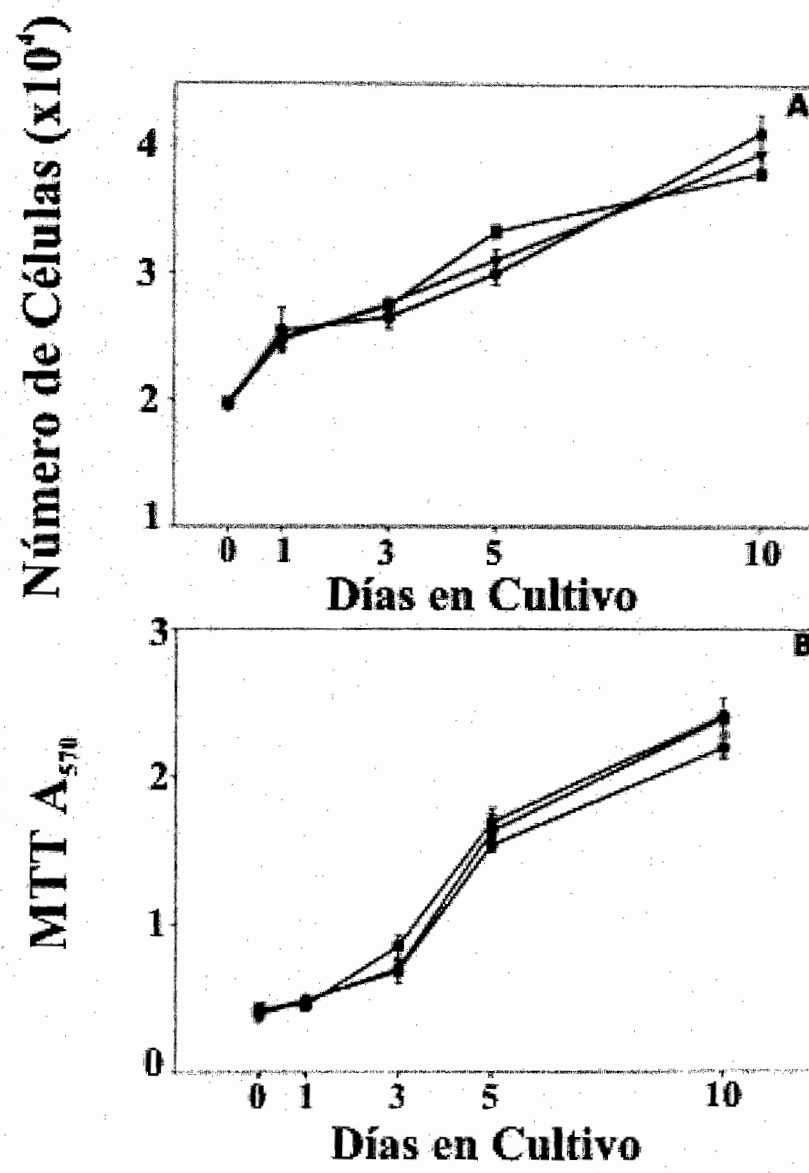


Figura 1. (a) Ensayos de proliferación y viabilidad celular de las células derivadas del cementoblastoma tratadas con el anticuerpo normal de conejo (●), con el anticuerpo anti-CP (■), ambos anticuerpos a una concentración de 5 $\mu\text{g}/\text{ml}$. La concentración de 10% de SFB fue usada como medio control (•). (b) actividad de oxidación.

Ensayo de la actividad de la fosfatasa alcalina

La fosfatasa alcalina (ALP) se determinó en los diferentes tiempos de cultivo celular al medir su actividad enzimática en la capa celular. Dicha actividad se registró en los primeros días, sin ninguna diferencia estadística entre los tratamientos a los 3, 5 y 7 días. Por otro lado, la actividad de la ALP muestra una disminución en su actividad del 40% ($p < 0.005$), 44% ($p < 0.001$), 49% ($p < 0.1$) y 45% ($p < 0.02$) con respecto a los cultivos tratados con el anticuerpo normal de conejo a los 9, 11, 13, y 15 días de cultivo. Estos resultados muestran que la actividad enzimática de ALP se ve inhibida durante los estados iniciales de la mineralización, como se indica en la figura 2.

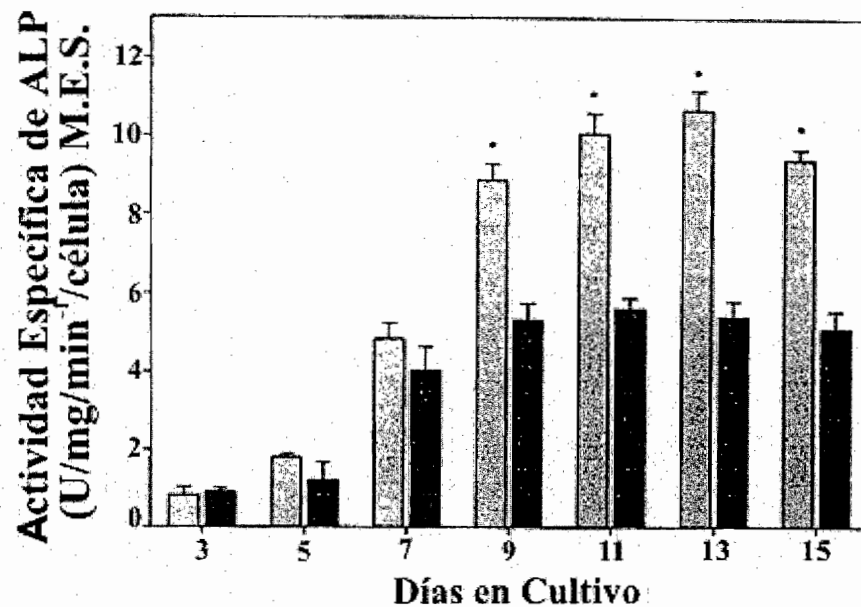


Figura 2. Ensayo de la actividad de la fosfatasa alcalina de los cultivos control (□) tratados con 5 $\mu\text{g}/\text{ml}$ del anticuerpo normal de conejo y los cultivos experimentales (■) tratado con 5 $\mu\text{g}/\text{ml}$ del anticuerpo anti-CP. Los asteriscos indican las diferencias estadísticas entre los tratamientos a $p < 0.05$.

Detección de OPN y BSP por Inmunofluorescencia

La presencia de osteopontina identificada por el anticuerpo específico contra OPN (LF-123) por medio inmunofluorescencia reveló que el porcentaje de células positivas a OPN fue más bajo en los cultivos experimentales por 87, 83, 69 y 52 % a los 5, 7, 9 y 11 días de cultivo cuando se compararon con el número de células positivas a OPN en los cultivos control como se observa en la figura 3A y en la tabla I (ver apéndice). Sin embargo, a los 13 y 15 días, los porcentajes de células positivas a OPN en los cultivos experimentales fueron similares a los porcentajes de células positivas observados en los cultivos control.

El análisis por inmunofluorescencia de las células positivas a sialoproteína ósea utilizando el anticuerpo LF-100 específico contra BSP, disminuyó en los cultivos experimentales conforme transcurrieron los tiempos de cultivo celular, a diferencia de los cultivos control, donde, se observó un aumento gradual en las células positivas para esta proteína. La disminución del porcentaje de células positivas para BSP fue de 82, 51, 60, 80, 83 y 87% con respecto a las células positivas en los cultivos control a los 5, 7, 9, 11, 13 y 15 días como se observa en la figura 3B y en la tabla II (ver apéndice).

Microscopía de fuerza atómica

Las imágenes de microscopía de fuerza atómica, muestran una secuencia de disposición morfológica en tres dimensiones del tejido mineral depositado por los cultivos celulares.

Las características del tejido mineral depositado a los 5 días en los cultivos control incubados con el anticuerpo normal de conejo, se observa como una acumulación de granos con tamaños de $1.5 - 0.30\mu\text{m}$, lo que favorece la formación de placas cristalinas con un patrón tipo laminar. Estas placas individuales tienen una longitud de $0.36\mu\text{m}$ y un ancho de $0.18\mu\text{m}$, la cual, representa una estructura cristalina anisotrópica de 2:1 (l/w) (Fig. 5 A). A una mayor resolución, estas placas cristalinas se observan como estructuras en forma de agujas con una orientación preferencial y con una altura de 6 \AA (Fig. 5 E).

El tejido mineral depositado por los cultivos experimentales tratados con el anticuerpo anti-CP a los 5 días de cultivo, muestra una morfología granular que conlleva a la formación de aglomerados cristalinos con un tamaño de $1.3 - 0.25\mu\text{m}$ (Fig. 5 B) y en una mayor resolución a observar la formación esférica de dichos aglomerados (Fig. 5F).

El mineral depositado en los cultivos control a los 15 días de cultivo se observa como estructuras tipo placa bien organizada y orientada con longitud de $20\mu\text{m}$ y una anchura de $1.6\mu\text{m}$, representando una razón anisotrópica de 12.5 (l/w), con tamaños de partícula de $2.6 - 0.9\mu\text{m}$ y a mayor resolución, cristales en forma de aguja característico de la hidroxiapatita (Fig. 5 C y G). Por ultimo, en los cultivos experimentales a los 15 días de cultivo, el tejido mineral es depositado a manera de aglomerados con similitud a los observados en los cultivos de 5 días, con una morfología esférica bien definida, sin una organización para formar estructuras tipo laminar. Sin embargo, los aglomerados presentan un tamaño de partícula más grande $\sim 1.5 \mu\text{m}$ (Fig. 5 D y H).

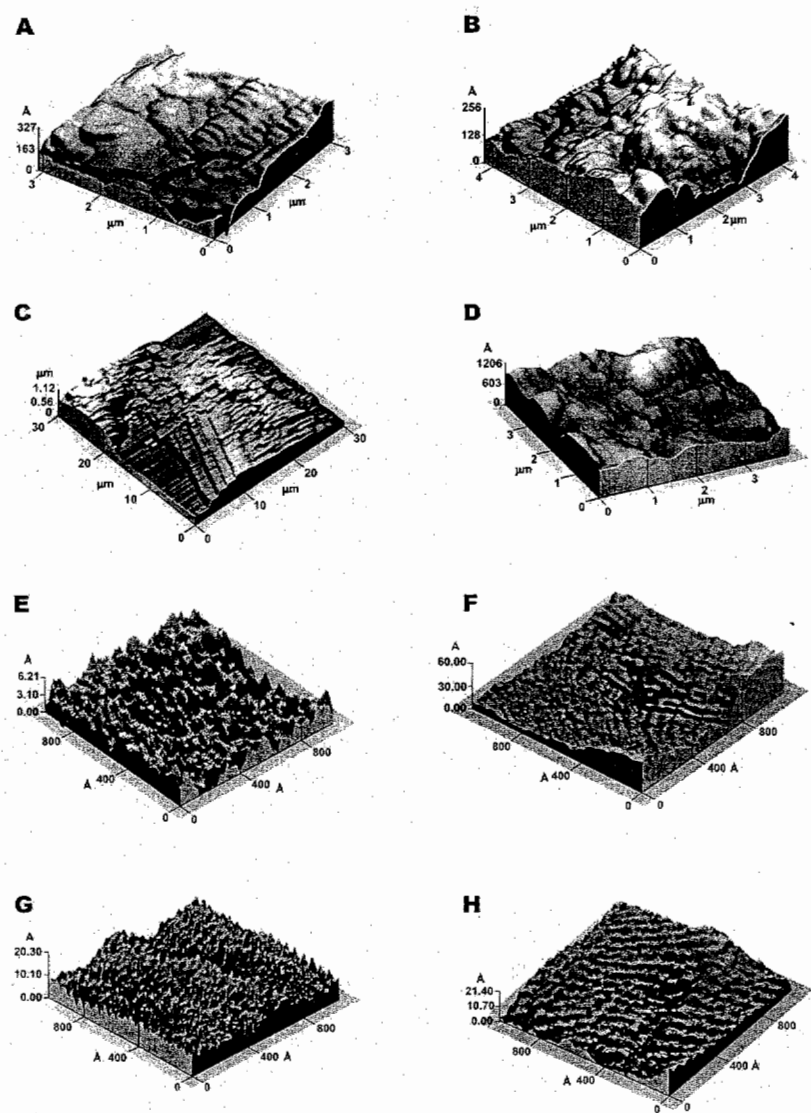


Figura 5. Morfología del tejido mineral depositado por los cultivos celulares a los 5 y 15 días de cultivo. Las imágenes (A y C) son representativas del mineral formado con un arreglo laminar y las imágenes (E y G) son representativas del mineral formado a manera de agujas a mayor aumento por los cultivos control incubados con 5 μ g/ml del anticuerpo normal de conejo. Las imágenes (B y D) representan el mineral formado con morfología esférica sin organización. Las imágenes (F y H) son representativas del patrón globular a mayor aumento del mineral depositado por los cultivos experimentales tratados con 5 μ g/ml del anticuerpo anti-CP.

Microanálisis de energía dispersiva electrónica con rayos X (EDS)

La composición y la razón Ca/P del mineral depositado *in vitro* por las células derivadas del cementoblastoma humano, fueron analizadas a los 5 y 15 días de cultivo por microanálisis de energía dispersiva con rayos X. Los cultivos control a los 5 días mostraron un porcentaje atómico de 56.1% para el calcio (Ca) y 38.7% para el fósforo (P) respectivamente (Fig. 6C). Otros elementos como potasio (2.5%) y Mg (2.4%) estuvieron presentes en la composición global del tejido. La razón Ca/P de 1.45 corresponde con los valores de la hidroxiapatita biológica.

Los cultivos experimentales a los 5 días muestran una disminución en los picos de energía para el Ca y P con porcentajes atómicos de 29.9% y 58.5% respectivamente. Los demás elementos como el K y el Mg no fueron detectados en el espectro. El valor de la razón Ca/P fue de 0.50 (Fig. 6A). A los 15 días los cultivos control exhiben un porcentaje atómico de 55.4% para el Ca y 34.4% para el P. Los iones potasio y magnesio también estuvieron presentes en el tejido depositado con porcentajes atómicos de 6.1% y 3.8%. La razón Ca/P fue de 1.61 (Fig. 6D).

Por ultimo, los cultivos experimentales a los 15 días mostraron los siguientes porcentajes atómicos: 38.5% para el calcio, 48.3% para el fósforo, 2.0% para el magnesio y 4.5% para el potasio y el valor de la razón Ca/P para los 15 días de cultivo experimental fue de 0.79 (Fig. 6B).

El microanálisis de energía dispersiva con rayos X determina los valores composicionales de la hidroxiapatita biológica, aunque los espectros de EDS de las muestras control muestran mejor definición en los picos de energía cuando se comparan con los cultivos experimentales, esto nos indica una mayor densidad de cristales en los cultivos control que en los cultivos experimentales (Fig.6).

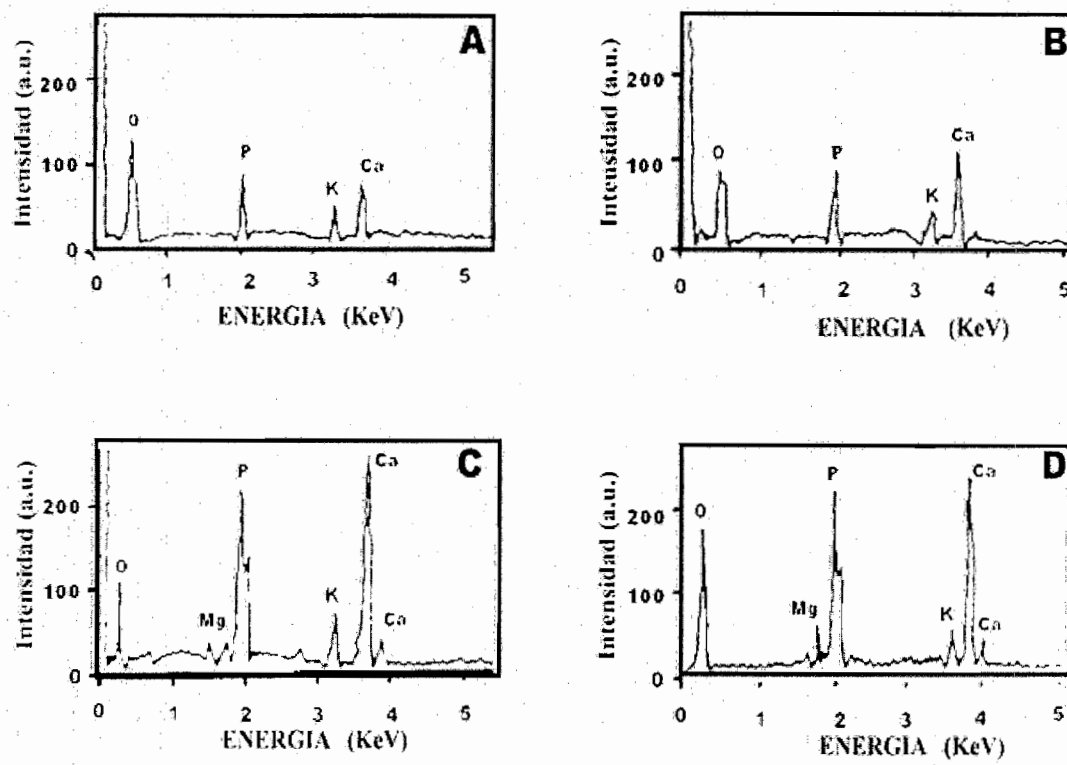


Figura 6. Espectros emitidos por el microanálisis de energía dispersiva con rayos X del tejido mineral depositado por los cementoblastos putativos *in vitro*. Cultivos experimentales a los 5 (A) y 15 (B) días muestran picos débiles para calcio (Ca) y fósforo (P). Cultivos control muestran picos prominentes de Ca y P a los 5 y 15 días de cultivo.

Patrones de difracción electrónica

El análisis del mineral depositado únicamente a los 15 días de cultivo tanto en los cultivos control como experimental indican que las muestras son policristalinas por lo que se revelan como patrones de anillos concéntricos. El valor de los anillos es de 2.34 \AA y 2.98 \AA que corresponde con los espacios interplanares-D para la hidroxiapatita (2.29 \AA y 3.08 \AA). El semi-anillo interior muestra un claro crecimiento preferencial de los cristales de hidroxiapatita (Fig. 7 A y B).

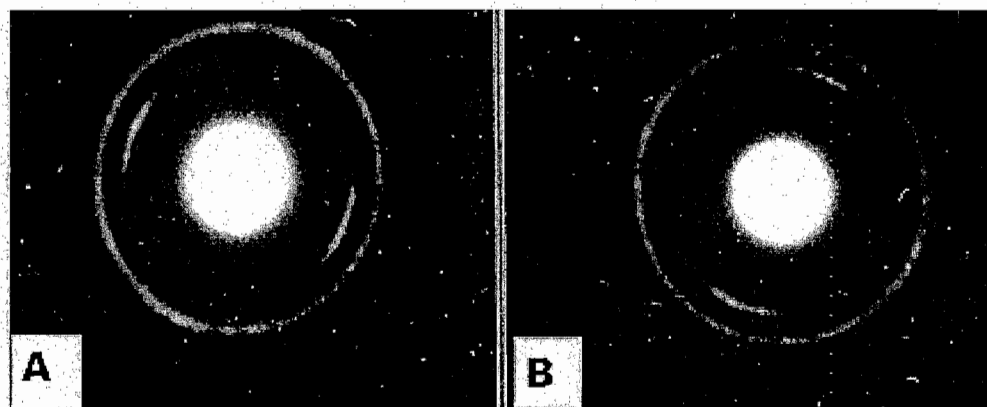


Figura 7. Patrón de difracción electrónica obtenido del tejido mineral depositado por las células derivadas del cementoblastoma a los 15 días de cultivo para el control (A) y experimental (B). Nótese que son anillos que indican que el material es policristalino y además, los semi-anillos nos informan que existe una dirección preferencial de crecimiento en los cristales de hidroxiapatita.

Microscopía electrónica de alta resolución (HRTEM)

Al examinar la cristalinidad de las muestras por HRTEM, se observa que ambos cultivos celulares a los 15 días revelan una formación de cristales de hidroxiapatita homogéneos y con una orientación preferencial. Por otro lado, la densidad de cristales de hidroxiapatita es más grande y homogénea en los cultivos control, como se observa en las imágenes de alta resolución, con valores que corresponden a sus distancias interatómicas de 7.1 Å que es debido al plano de difracción ($h k l$: 1 0 0), 3.8 Å ($h k l$: 1 1 1) y 3.1 Å ($h k l$: 2 1 0). Revelando que en los cultivos experimentales los cristales son más pequeños y con un crecimiento amortiguado, con valores en sus distancias interatómicas de: 2.27 Å ($h k l$: 2 1 2), 2.42 Å ($h k l$: 3 0 1) y 3.53 Å ($h k l$: 2 0 1). Los patrones obtenidos se compararon con los estándares de la hidroxiapatita: JCPDS N° de archivo 9-432⁴⁶.

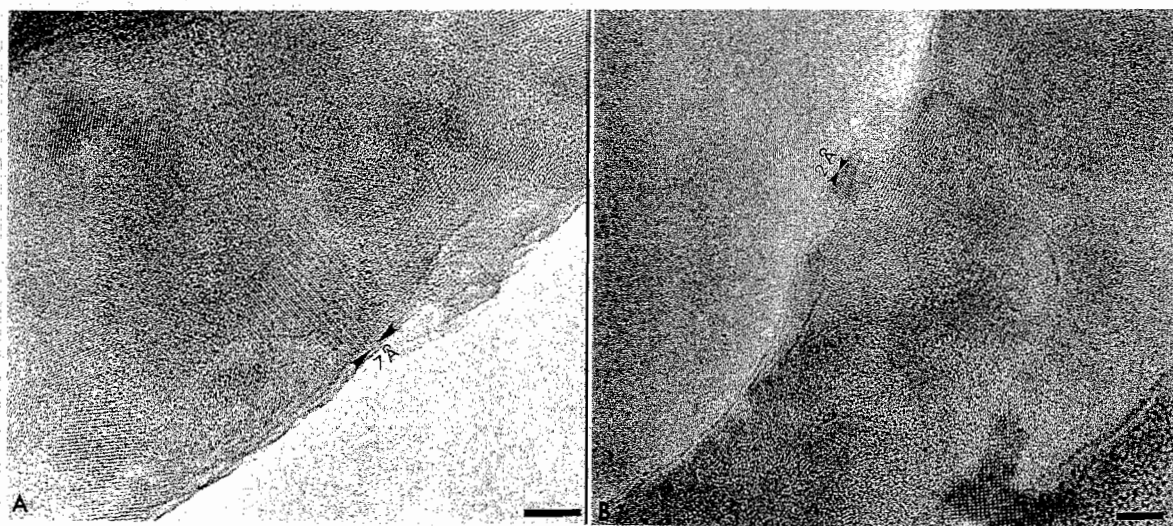


Figura 8. Alta resolución de los cristales de hidroxiapatita a los 15 días de cultivo. Los cultivos control (A) muestran un crecimiento homogéneo y preferencial de los cristales. Los cultivos experimentales presentan un crecimiento no homogéneo con cristales más pequeños (B). La barra en A = 1.7 nm y en B = 1.4 nm

Microscopía electrónica de barrido (SEM)

El análisis de los cultivos control a los 5 días de cultivo revela áreas mineralizadas constituidas por aglomerados y estructuras tipo aguja (Fig. 9C), confirmando los análisis de difracción electrónica y las imágenes obtenidas por microscopía de fuerza atómica. A los 15 días de cultivo, los cultivos control muestran estructuras formadas a manera de placas (Fig. 9D) y los cultivos experimentales a los 5 y 15 días de cultivo se observan aglomerados con formas esféricas de tamaños homogéneos (Fig. 9 A y B).

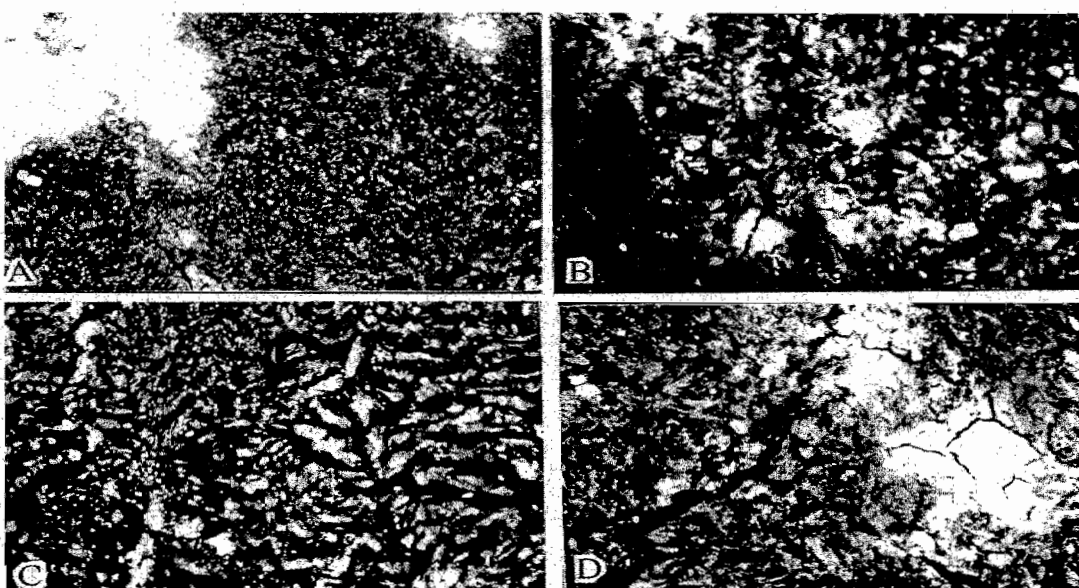


Figura 9. Imágenes de microscopía electrónica de barrido (SEM) donde se observa la morfología del tejido mineral depositado a manera de aglomerados y estructuras tipo aguja a los 5 (A) y 15 (B) días de los cultivos control. Los cultivos experimentales a los 5 (C) y 15 (D) días muestran aglomerados en forma esférica y de tamaño homogéneo. Barra = 30 μm .

Discusión

Los resultados, indican que la inhibición de CP por la presencia del anticuerpo anti-CP en los cultivos experimentales, puede afectar la actividad de ALP, los niveles de las proteínas OPN y BSP, así como la cantidad y calidad del mineral depositado, sin interferir con la proliferación y viabilidad celular que fue de más del 90% para todos los tratamientos.

Actividad de la fosfatasa alcalina

La fosfatasa alcalina juega un papel importante en la mineralización al regular las concentraciones extracelulares de fosfatos por catalizar la hidrólisis de compuestos de ésteres de fosfatos y su actividad ha sido asociada con las primeras fases del proceso de mineralización, aunque su papel durante la mineralización no esta completamente entendida^{47, 48, 49}. La actividad de ALP, puede propicias las condiciones para iniciar la mineralización por incrementar las concentraciones locales de fosfatos y una vez que se ha completado la deposición del mineral esta tiende a disminuir; por ende, el progreso de la mineralización de la matriz extracelular es asociado con la retención de la actividad de ALP^{50, 51}.

Los cultivos experimentales revelaron una disminución del 49% en la actividad de ALP a los 9-15 días, sugiriendo que la ausencia de CP, inhibe parcialmente las fases primarias y tardías de la mineralización en los cultivos experimentales. Estos resultados confirman nuestros datos previos, lo cual apunta a la capacidad de CP en promover la mineralización en células mesenquimatosas no diferenciadas⁴¹ y en incrementar la actividad de ALP en la línea derivada del cementoblastoma³⁴.

Análisis de OPN y BSP

Las principales fosfoproteínas sintetizadas por los cementoblastos son OPN y BSP⁵². Dichas moléculas han recibido substancial atención como reguladores potenciales de la nucleación y crecimiento de los cristales de hidroxiapatita^{53, 54}. Aunque, los mecanismos por los cuales la mineralización es llevada a cabo no está bien entendida. Diversos autores sugieren que las fosfoproteínas, junto con el ordenamiento de las fibras de colágeno tipo I podrían llevar a cabo la nucleación de los cristales de hidroxiapatita^{55, 56}.

Los resultados de este estudio revelaron una disminución de la proteína OPN durante las primeras fases del cultivo experimental, como se observa en los ensayos de inmunofluorescencia e inmunotransferencias, lo cual afectó la calidad del mineral depositado en los cultivos celulares, como se observó en las imágenes obtenidas por MFA, SEM y HRTEM.

La asociación entre la disminución de la proteína OPN y la morfología del mineral, está fundamentada por diversos estudios que reportan que OPN está asociada a los estadios tempranos de mineralización del cemento radicular, donde se indica un papel para OPN en regular el crecimiento de los cristales de hidroxiapatita^{57, 58}.

OPN tiene la habilidad de unirse y potencialmente orientar significativas cantidades de calcio, lo que sugiere que puede funcionar como un promotor de la calcificación^{59, 60}. Sin embargo, OPN se maneja como una proteína multifuncional debido a que los estudios realizados en solución de fosfatos de calcio *in vitro* y libre de células, reportan que OPN puede inhibir la formación y crecimiento de la apatita. Aunque dicho cristal al ser analizado por difracción de rayos X, mostró ser un cristal de hidroxiapatita pobre y análogo al cristal del mineral oseo⁶⁰.

La función de OPN en la formación del tejido mineral y en la probable inhibición del crecimiento del cristal durante el proceso de mineralización *in vitro* no puede ser atribuida a la sola presencia de OPN, sin considerar, el posible papel de ALP sobre la desfosforilación de esta proteína.

En la literatura se maneja que la desfosforilación de OPN es requerida para su efecto inhibitorio en un sistema *in vivo*, porque al adicionar OPN fosforilada en matrices mineralizadas, se observó que no tiene efecto alguno en la formación y crecimiento del cristal de hidroxiapatita, indicando la importancia de los residuos de fosfato en su función y explicando en parte porque diferentes OPNs de diferentes tejidos presentan diversos efectos sobre la formación del mineral y su crecimiento⁶¹. Por tal motivo, que residuos son fosforilados y cuales dominios son requeridos para que actúen como un inhibidor y/o como regulador del crecimiento del cristal, permanecen como preguntas abiertas.

Es claro que la ausencia de CP podría afectar en alguna manera el inicio y el progreso de la matriz mineralizada en el tejido de cemento. Esto sugiere que CP podría regular los estados iniciales de la mineralización de cemento por influenciar la disponibilidad de OPN durante el crecimiento y la maduración del cristal.

BSP es otra fosfoproteína importante de la matriz mineralizada del cemento radicular y esta asociada con los primeros agregados minerales, actuando como un potente nucleador para la hidroxiapatita en sistemas *in vivo* e *in vitro*^{62, 63, 64}.

Los datos obtenidos, sugieren que BSP fue parcialmente disminuida durante el periodo experimental, que corresponde a los estadios medio y tardíos del proceso de mineralización, como se observa en las imágenes de inmunofluorescencia e inmunotransferencias. Así, el proceso de nucleación del mineral fue afectado en los cultivos experimentales, explicando los agregados globulares en el mineral y la no-formación de estructuras laminares como se

observó al determinar la homogeneidad y morfología del mineral de hidroxiapatita, por la microscopia de fuerza atómica y de barrido.

Hay que considerar que las proteínas que se unen a la hidroxiapatita pueden afectar la mineralización en diversas vías, tales como: 1) estabilizar el núcleo del cristal y actuar como nucleadores externos/epitaxiales, negando la demanda de energía del proceso de nucleación y facilitando el crecimiento del cristal, como en el caso de BSP; y 2) pueden unirse a una cara en particular del cristal, previniendo el crecimiento de esta cara y por ello cambiando la forma del cristal y/o aislar el cristal entero previniendo su crecimiento y proliferación de forma similar a como lo sería en el caso de OPN. Por esto, parece razonable considerar que la acción combinada de BSP y OPN en los focos de calcificación temprana, determinan en parte, el subsiguiente patrón espacial y temporal de mineralización del cemento radicular.

Microanálisis y patrón de mineralización

Los datos de composición del tejido mineral depositado por los cultivos experimentales a los 5 y 15 días revelan que la falta de CP afecta la composición iónica del tejido mineral con respecto a su contenido de Ca^{2+} , P, K y Mg^{2+} . Esta suposición se basa en las reducidas razones Ca/P cuando se compara con los cultivos controles, lo que da a entender que al inhibir CP por el anticuerpo anti-CP, este retarda la salida de calcio y con ello la generación del mineral, ya que los cultivos experimentales presentan un bajo valor de Ca^{2+} . Aunque los patrones de difracción electrónica a manera de dobles anillos concéntricos nos indican que en ambos cultivos celulares a los 15 días el material formado es hidroxiapatita. Estos resultados podrían estar relacionados a la disminución de las proteínas OPN, BSP y a la disminución en la actividad de ALP, explicando la presencia de los agregados globulares en

la deposición del mineral y la no formación de estructuras de forma laminar en los cultivos experimentales.

Otros elementos, tales como: el potasio y magnesio juegan un papel importante en el crecimiento del cristal. Aunque el potasio se reporta como la segunda impureza más predominante en los estudios de biominerización de fosfato de calcio, su papel preciso en la mineralización aún no esta bien entendida, pero se sugiere que el mineral formado está más relacionada a una hidroxiapatita que al fosfato de calcio amorfo⁶⁵. Por otro lado, se reporta que el magnesio se une a la superficie del cristal, compitiendo por el mismo sitio de unión del calcio en la hidroxiapatita, retardando la nucleación en su forma precrystalina de fosfato de calcio amorfo y modulando el crecimiento del cristal en los procesos de mineralización y en su maduración^{66, 67}.

Nuestros resultados revelan que en los cultivos experimentales no hay presencia de magnesio, lo cual, nos lleva a pensar que el magnesio podría dictar que sólo los cristales correctos de hidroxiapatita puedan ser aquellos que se sigan formando y que los que presentan defectos sean los que se vean afectados en su desarrollo, lo que se traduce en un decremento del crecimiento del cristal de hidroxiapatita, que es fundamentado por los análisis de HRTEM donde se observan cristales de hidroxiapatita mas pequeños comparados con los cultivos control.

En los cultivos controles se observó un arreglo organizado de la fase mineral con un patrón definido de líneas de crecimiento, que puede estar asociado a la actividad de ALP y a un alto grado de organización y orientación espacial de las fibras de colágeno⁶⁸, porque se ha reportado que existe una correlación entre la alta actividad de ALP y el grosor del tejido mineral de cemento^{69, 70}.

En los cultivos experimentales esta correlación se vio afectada, ya que la fase mineral es más delgada y al parecer, la ausencia de CP impide un arreglo organizado, manteniendo una apariencia globular. Esto podría ocurrir dentro de una matriz que pierde la orientación de las fibras de colágena por el efecto en la disminución de la actividad de ALP; por la disminución de la proteína BSP que no afecta la habilidad de la pequeña proporción de proteína BSP para promover la formación inicial de agregados cristalinos de forma esférica y con una distribución al azar, que puede ser atribuida a la disminución de OPN, ya que esta proteína es necesaria para inhibir el crecimiento erróneo de los cristales de hidroxiapatita.

Descubrimientos recientes sugieren que las capas en el cemento dental humano pueden estar relacionadas a la orientación de los cristales de hidroxiapatita^{71, 72, 73}.

Los estudios de los cristales de hidroxiapatita -por las diferentes técnicas de microscopía apoyan esta idea, ya que los cultivos control a los 15 días indicaron que la celda unitaria de la hidroxiapatita tiene un arreglo preferencial, reflejándose en la formación de mineral a manera de láminas, mientras que los cristales de hidroxiapatita en los cultivos experimentales -a los 15 días- presentan alteraciones en su arreglo espacial, lo cual se reflejó en su morfología del tipo globular. La razón de este efecto no es clara, pero estos datos en conjunto suponen que CP puede ser clave en la maduración y morfología del tejido mineral depositado por las células al afectar las funciones y disponibilidad de ALP, OPN y BSP, así como la salida de calcio⁷⁴; originando las diferencias morfológicas encontradas en la composición y orientación de los cristales de hidroxiapatita.

Conclusiones

A partir de nuestros resultados podemos concluir que:

- 1) La proteína de adhesión derivada de cemento es un factor importante que regula y participa, en el proceso de la cementogenesis *in vitro*.
- 2) CP está correlacionada a la actividad de ALP, OPN y BSP.
- 3) Los microanálisis por EDS, las imágenes de alta resolución por HRTEM y las imágenes de SEM y MFA permitieron caracterizar, medir y evaluar los cambios morfológicos del mineral depositado por los cultivos celulares.
- 4) CP está asociada al crecimiento del cristal, así como a las características de composición y morfológicas del mineral depositado durante el proceso de mineralización *in vitro*.
- 5) Nuestras observaciones y los datos experimentales combinados, sugieren que CP participa en el proceso de biominerilización del cemento radicular. En consecuencia, es claro que esta investigación propone realizar más estudios para determinar de forma concluyente cual es el papel biológico de CP en el desarrollo de la mineralización por medio de las células cementoblásticas.

Bibliografía

1. Lindhe Jan. Peri odontología clínica e implantología odontológica. Editorial Médica Panamericana. España, 2000.
2. Genco J. R. Periodoncia. Editorial Interamericana, McGraw-Hill, México, 1993.
3. Page RC. Oral health status in the United States: Prevalence of inflammatory periodontal diseases. *J Dent Educ* 49:354-364, 1985.
4. McCulloch CAG., Nemeth HE., Lowenberg B., Melcher AH. Paravascular cells in endosteal spaces of alveolar bone contribute to periodontal ligament cell populations. *Anat Rec* 21:592-612, 1987.
5. Pitaru S, McCulloch CAG, Narayanan AS. Cellular origins and differentiation control mechanisms during periodontal development and wound healing. *J Periodont Res* 29: 81-94, 1994.
6. Schroeder HE. Biological problems of regenerative cementogenesis: Synthesis and attachment of collagenous matrices on growing and established root surfaces. In: Jean, Friedman, eds. *Int Rev of Cytology*, vol. 142: pp 1-59, 1993.
7. Paynter KJ, Pudy G. A study of the structure, chemical nature, and development of cementum in the rat. *Anat Rec* 131:233-251, 1958.
8. Birkedal-Hansen H, Butler WT, Taylor RC. Proteins of the periodontium. Characterization of the insoluble collagens of bovine dental cementum. *Calcif Tissue Int* 23:39-44, 1977.
9. Chovelon A, Carmichael DJ, Pearson CH. The composition of the organic matrix of bovine cementum. *Arch Oral Biol* 20:537-541, 1975.

10. Christner P, Robinson P, Clark CC. A preliminary characterization of human cementum collagen. *Calcif Tissue Int* 23:147-150, 1977.
11. Reichert T, Storkel S, Becker K, Fisher LW. The role of osteonectin in human tooth development: An immunohistological study. *Calcif Tissue Int* 50:468-472, 1992.
12. Bronckers AL, Farach-Carson MC, Van Waveren E, Butler WT. Immunolocalization of osteopontin, osteocalcin, and dentin sialoprotein during dental root formation and early cementogenesis in rat. *J Bone Miner Res* 9:833-841, 1994.
13. McAllister B, Narayanan AS, Miki Y, Page RC. Isolation of a fibroblast attachment protein from cementum. *J Periodont Res* 25: 99-105. 1990.
14. Lynch SE, Williams RC, Polson AM, Howell TH *et al.* Combination of platelet-derived and insulin-like growth factors enhances periodontal regeneration. *J Clin Periodontol* 16:545-548, 1989.
15. Amar S. Implications of cellular and molecular biology advances in periodontal regeneration. *Anat Rec* 245:361-373, 1996.
16. Lin WL, McCulloch CAG, Cho MI. Differentiation of periodontal ligament fibroblasts into osteoblasts during socket healing after tooth extraction in the rat. *Anat Rec* 240:492-506, 1994.
17. Giniger MS, Norton I, Sousa S, Lorenzo JA, Bronner E. A human periodontal ligament fibroblasts clone releases a bone resorption inhibition factor in vitro. *J Dent Res* 70:99-101, 1991.
18. Somerman MJ, Archer SY, Shteyer A, Foster RA. Protein production by human gingival fibroblasts is enhanced by guanidine extracts from cementum. *J Periodont Res* 22: 75-77, 1987.

19. Somerman MJ, Archer SY, Hassel TM, Shteyer A, Foster RA. Enhancement by extracts of mineralized tissues of protein production by human gingival fibroblasts *in vitro*. *Archs Oral Biol* 12: 879-883, 1987.
20. Somerman MJ, Foster RA, Imm GM, Sauk JJ, Archer SY. Periodontal ligament cells and gingival fibroblasts respond differently to attachment factors *in vitro*. *J Periodontol* 60: 73-77, 1989.
21. Somerman MJ, Argraves WS, Foster RA, Dickerson K, Norris K, Sauk JJ. Cell attachment activity of cementum: bone sialoprotein II identified in cementum. *J Periodont Res* 26: 10-16, 1991.
22. Melcher AH, On the repair potential of the periodontal tissues. *J Periodontol* 47: 256-260, 1976.
23. Slavkin HC, Bringas PJr, Bessem C, Santos V, et al. Hertwig's epithelial root sheath differentiation and initial cementum and bone formation during long-term organ culture of mouse mandibular first molar using serumless, chemically-defined medium. *J Periodont Res* 23:28-40, 1988.
24. Slavkin HC., Bessem C., Fincham AG., Bringas P., Santos V, et al. Human and mouse cementum proteins immunologically related to enamel proteins. *Biochimica et Biophysica Acta* 991:12-18, 1989.
25. Zeichner-David M, Oishi K, Su Z, Zakartchenko V, Chen LS, Arzate H, Bringas P Jr. Role of Hertwig's epithelial root sheath cells in tooth root development. *Dev Dyn.* 228(4):651-63, 2003.
26. Mina M., Kollar EJ. The induction of odontogenesis in non-dental mesenchyme combined with early murine mandibular arch epithelium. *Arch Oral Biol* 32:123-127, 1987.

27. Melcher AH. Does the developmental origin of cementum, periodontal ligament and bone predetermine their behavior in adults?. In: Guggenheim B, ed. *Periodontology Today*. Basel:Krager AG., pp 6-14, 1988.
28. Arzate H., Olson S., Page RC. and Narayanan AS., Isolation of human tumor cells that produce cementum protein in culture. *Bone and Mineral*, 18:15-30,1992.
29. Ohki K, Kumamoto H, Nitta Y, Nagasaka H, Kawamura H, Ooya K. Benign cementoblastoma involving multiple maxillary teeth: report of a case with a review of the literature *Oral Surg Oral Med Oral Pathol Oral Radiol Endod*.97:53-8, 2004.
30. Cheng SL, Yang JW, Rifas L, Zhang SF, Avioli LV. Differentiation of human bone marrow osteogenic stromal cells *in vitro*: Induction of the osteoblast phenotype by dexamethasone. *Endocrinology* 134:277-286, 1994.
31. Ramakrshnan PR, Lin WL, Sodek J, Cho IL. Synthesis of noncollagenous extracellular matrix proteins during development of mineralized nodules by rat periodontal ligament cells *in vitro*. *J Periodont Res* 30:52-59;1995.
32. Gould TRL, Melcher AH, Brunette DM. Location of progenitor cells in periodontal ligament of mouse molar stimulated by wounding. *Anat Rec* 180:133-142, 1977.
33. Piche JE, Carnes DL, Graves DT. Initial characterization of cells derived from human periodontium. *J Dent Res* 68:761-767, 1989.
34. Arzate H., Alvarez-Pérez MA., Aguilar Mendoza ME., Alvarez-Fregoso O. Human cementum tumor cells have different features from human osteoblastic cells *in vitro*. *J Periodont Res* 33: 249-258, 1998.
35. Arzate H, Alvarez-Pérez MA, Alvarez-Fregoso O, Wusterhaus-Chavez A, Reyes-Gasga J, Ximenes-Fylie LA, Electrón microscopy, micro-analysis and Xray diffraction

characterization of mineral-like tissue deposited by human cementum tumor-derived cells.

J Dent Res 79: 28-34, 2000.

36. Wu D, Ikezawa K, Parker T, Saito M, Arzate H, Narayanan AS. Characterization of a collagenous cementum-derived attachment protein. *J Bone Min Res* 11:686-692, 1996.
37. Somerman MJ, Sauk JJ, Agraves WS, Morrison G, et al. Expression of attachment proteins during cementogenesis. *J Biol Buccale* 18: 207-214, 1990.
38. Nakae H, Narayanan AS, Raines E, Page RC. Isolation and partial characterization of mitogenic factors from cementum. *Biochem* 30: 7047-7052, 1991.
39. Narayanan AS, Ikezawa K, Wu D, Pitaru S. Cementum specific components which influence periodontal connective tissue cells. *Connec Tissue Res*; 33: 1-3, 1995.
40. Pitaru S, Narayanan AS, Olson S, Savion N, Hekmati H, Alt I, Metzger Z. Specific cementum attachment protein enhances selectively the attachment and migration of periodontal cells to root surfaces. *J Periodont Res* 30:360-368, 1995.
41. Arzate H, Chimal MJ, Hernández LL, Díaz LL. Human cementum protein extract promotes chondrogenesis and mineralization in mesenchymal cells. *J Periodont Res* 31: 144-148; 1996.
42. Arzate H, Jiménez-García LF, Alvarez-Pérez MA, Landa A, Bar-Kana I, Pitaru S . Immunolocalization of human cementoblastoma conditioned medium-derived protein. *J Dent Res* 81: 541-546, 2002.
43. Lowry, O.H., Roberts, N.R., Wu, M.-L., Hixon, W.S., Crawford, E.J., 1954. The quantitative histochemistry of brain I. Enzyme measurement. *J Biol. Chem.* 207, 19-37.
44. Bradford, M.M., 1976. A rapid and sensitive method for the quantitation of microgram quantities of protein utilizing the principle of protein-dye binding. *Ann. Biochem.* 72, 248-254.

**ESTA TESIS NO SALI
DE LA BIBLIOTECA**

45. Shakibaei, M., 1998. Inhibition of chondrogenesis by integrin antibody in vitro. *Exp. Cell Res.* 240, 95–106.
46. JCPDS, 1995. Joint Committee on Powder Diffraction Standards No. 9-432 file for calcium hydroxyapatite.
47. Linde, A. On enzymes associated with biological calcification. In: Veis, A. (Ed.), *The Chemistry and Biology of Mineralized Connective Tissue*. Elsevier, New York, pp. 559–570, 1982.
48. Boyan, BD., Schwarz, Z., Bonewald, LF., Swain, LD. Localization of 1,25-(OH)₂D₃ responsive alkaline phosphatase in osteoblast-like cells and growth cartilage cells in culture. *J Biol Chem.* 264:11, 879-886, 1989.
49. Harrison, G., Shapiro, I.M., Golub E. The phosphatidylinositol-glycolipid anchor on alkaline phosphatase facilitates mineralization initiation in vivo. *J Bone Miner Res.* 10, 568-573, 1995.
50. Bianco, P. Structure and mineralization of bone. In: Bonucci, E. (Ed.), *Calcification in Biological Systems*. CRC Press, Boca Raton, FL, pp. 244–268, 1992.
51. Torii, Y, Hitomi K., Yamagashi Y., Tsukagoshi N. Demonstration of alkaline phosphatase participation in the mineralization of osteoblasts by antisense RNA approach. *Cell Biol Int.* 20:7, 459-464, 1996.
52. Manara, MC., Baldini N., serra M., Lollini PL., De Giovanni C., Vaccari M., Argnani A., Benini S., Maurici., Picci P., and Scotland K. Reversal of malignant phenotype in human osteosarcoma cells transduced with the alkaline phosphatase gene. *Bone.* 26:3, 215-220, 2000.

53. Bosshardt, D.D., Zalzal, S., McKee, M.D., Nanci, A. Developmental appearance and distribution of bone sialoprotein and osteopontin in human and rat cementum. *Anat. Rec.* 250, 13–33, 1998.
54. Nanci, A. Content and distribution of noncollagenous matrix proteins in bone and cementum: relationship to speed of formation and collagen packing density. *J Struct. Biol.* 126, 256–269, 1999.
55. Roach, H.I. Why does bone matrix contain non-collagenous proteins? The possible roles of osteocalcin, osteonectin, osteopontin and bonesialoprotein in bone mineralization and resorption. *Cell Biol. Int.* 18, 617–628, 1994.
56. Chen, J., Zhang, Q., McCulloch, C.A., Sodek. Immunohistochemical localization of bone sialoprotein in foetal porcine bone tissues: comparisons with secreted phosphoprotein I (SSP-I, osteopontin) and SPARC (osteonectin). *Histochem. J.* 23, 281–289, 1991.
57. Hunter, G.K., Hauschka, P.V., Poole, R.A., Rosenberg, L.C., Goldberg, H.A. Nucleation and inhibition of Hydroxyapatite formation by mineralized tissue proteins. *Biochem. J.* 317, 59–64, 1996.
58. Butler, W.T., Ridall, A.L., McKee, M.D. Osteopontin. In: Bilezikian, J.P., Raisz, L.G., Rodan, G.A. (Eds.), *Principles of Bone Biology*. Academic Press, San Diego, CA, pp. 167–181, 1996
59. Gorski, J. Acidic phosphoproteins from bone matrix: a structural rationalization of their role in biominerlization. *Calcif. Tissue Int.* 50, 391–396, 1992
60. Hunter, GK., Kyle, CL. And Goldberg HA. Modulation of crystal formation by bone phosphoprotein: structural specificity of the osteopontin-mediated inhibition of hydroxiapatite formation. *Biochem J.* 300, 723–728, 1994.

61. Butler, W.T., Ridall, A.L., McKee, M.D. Osteopontin. In: Bilezikian, J.P., Raisz, L.G., Rodan, G.A. (Eds.), *Principles of Bone Biology*. Academic Press, San Diego, CA, pp. 167–181, 1996.
62. Chen, J.K., Shapiro, H.S., Wrana, J.L., Reimers, S., Heersche, J.N., Sodek, J. Localization of bone sialoprotein (BSP) expression to sites of mineralized tissue formation in fetal rat tissues by *in situ* hybridization. *Matrix* 11, 133–143, 1991.
63. Chen, J., Shapiro, H.S., Sodek, J. Developmental expression of bone sialoprotein mRNA in rat mineralized connective tissues. *J. Bone Miner. Res.* 7, 987–997, 1992.
64. Hunter, G.K., Goldberg, H.A. Nucleation of hydroxyapatite by bone sialoprotein. *Proc. Natl. Acad. Sci. USA*, 90, 8562–8565, 1993.
65. Hayakawa T; Yoshinari M, Sakae T and Remoto K. Calcium phosphate formation on the phosphorylated dental bonding agent in electrolyte solution. *J Oral Rehabilitation* 31; 67–73, 2004.
66. Amjad, Z., Koutsoukos PG., Nancollas GH. The crystallization of hidroxiapatite and fluorapatite in the presence of magnesium ions. *J Colloid Interface Sci.* 101, 250-256, 1984.
67. Weismann, H.P., Tkotz, T., Joos, U., Zierold, K., Stratmann, U., Szuwart, T., Plate, U., Hohling, H.J. Magnesium in newly formed dentin mineral of rat incisor. *J. Bone Miner. Res.* 12, 380–383, 1997.
68. Boyde, A., Hobdell, M.H. Scanning electron microscopy of lamellar bone. *Z. Zelforsch. Mikrosk. Anat.* 93, 213–231, 1969.
69. Groeneveld, M.C., Everts, V., Beertsen, W. Alkaline phosphatase activity in the periodontal ligament and gingival of the rat molar: its relation to cementum formation. *J. Dent. Res.* 74, 1374–1381, 1995.

70. Vandenbos, T., Beertsen, W. Alkaline phosphatase activity in human periodontal ligament: age effect and relation to cementum growth rate. *J. Periodont. Res.* 34, 1–6, 1999.
71. Beertsen, W., van den Bos, T., Everts, V. Root development in mice lacking functional tissue non-specific alkaline phosphatase gene: inhibition of acellular cementum formation. *J. Dent. Res.* 78, 1221–1229, 1999.
72. Cool, S.M., Forwood, M.R., Campbell, P., Bennett, M.B. Comparisons between bone and cementum compositions and the possible basis for their layered appearances. *Bone* 30, 386–392, 2002.
73. Tesch, W., Vandenbos, T., Roschgr, P., Fratzl-Zelman, N., Klaushofer, K., Beertsen, W., Fratzl, P. Orientation and mineral crystallites and mineral density during skeletal development in mice deficient in tissue nonspecific alkaline phosphatase. *J. Bone Miner. Res.* 18, 117–125, 2003.
74. Fukayama, S., Tashjian Jr., A.H. Stimulation by parathyroid hormone of $^{45}\text{Ca}_{2+}$ uptake in osteoblast-like cells: possible involvement of alkaline phosphatase. *Endocrinology* 126, 1941–1949, 1990.

Apéndice A (Tablas)

Tabla - I

Expresión de OPN en los cultivos de las células derivadas del cementoblastoma tratados con 5 µg/ml del anticuerpo anti-CP.

Días	Cultivo control ^{a, d}	Cultivo Experimental ^{b, d}	% ^c
5	55.4 ± 1.14*	7.2 ± 0.83	13.0
7	62.8 ± 2.16*	10.4 ± 1.34	16.6
9	65.2 ± 2.16*	20.2 ± 1.30	31.0
11	66.2 ± 1.30*	31.2 ± 2.58	47.2
13	70.8 ± 2.16*	67.4 ± 1.14	95.2
15	71.6 ± 1.81	69.6 ± 1.14	97.3

^aCultivos celulares tratado con 5µg/ml de la fracción IgG de conejo.

^bCultivos celulares tratado con 5µg/ml del anticuerpo anti-CP.

^cPorcentajes de las células positivas en los cultivos experimentales comparadas con los cultivos control.

^dPromedio ± error estándar de tres experimentos

* p < 0.001 (Prueba de *t* de student)

Tabla II

Expresión de BSP en los cultivos de las células derivadas del cementoblastoma tratados con 5 µg/ml del anticuerpo anti-CP.

Días	Cultivo control ^{a, d}	Cultivo Experimental ^{b, d}	% ^c
5	47.4 ± 2.40*	8.40 ± 0.89	17.8
7	54.2 ± 1.48*	26.4 ± 2.07	48.8
9	55.2 ± 1.09*	22.0 ± 1.58	39.8
11	68.8 ± 0.83*	13.4 ± 1.14	19.5
13	76.4 ± 1.14*	12.4 ± 1.34	16.7
15	79.8 ± 1.48*	9.8 ± 1.64	12.3

^aCultivo celular tratado con 5µg/ml de la fracción IgG de conejo.

^bCultivo celular tratado con 5µg/ml del anticuerpo anti-CP.

^cPorcentajes de las células positivas en los cultivos experimentales comparadas con los cultivos control.

^dPromedio ± error estándar de tres experimentos

* p < 0.001 (Prueba de *t* de student)

Apéndice B

Publicaciones:

- Alvarez-Pérez MA, Pitaru S, Alvarez-Fregoso O, Reyes-Gasga J and Arzate H., Anti-cementoblastoma-derived protein antibody partially inhibits mineralization on a cementoblastic cell line. *J Structural Biol* 143: 1-13, (2003).
- Arzate H, Jiménez-García LF, Alvarez-Pérez MA, Landa A, Bar-Kana I, Pitaru S. Immunolocalization of human cementoblastoma conditioned medium-derived protein. *J Dent Res* 81: 541-546, 2002.
- Arzate H, Alvarez-Pérez MA, Alvarez-Fregoso O, Wusterhaus-Chavez A, Reyes-Gasga J, Ximenes-Fylie LA, Electrón microscopy, micro-analysis and Xray diffraction characterization of mineral-like tissue deposited by human cementum tumor-derived cells. *J Dent Res* 79: 28-34,2000.

Anti-cementoblastoma-derived protein antibody partially inhibits mineralization on a cementoblastic cell line

Marco Antonio Alvarez Pérez,^a Sandu Pitaru,^b Octavio Alvarez Fregoso,^c
José Reyes Gasga,^d and Higinio Arzate^{a,*}

^a Laboratorio de Biología Celular y Molecular, Facultad de Odontología, UNAM, Mexico

^b The Maurice and Gabriela Goldschleger, School of Dental Medicine, Tel Aviv University, Israel

^c Instituto de Investigación en Materiales, UNAM, Mexico

^d Instituto de Física, UNAM, Mexico

Received 23 October 2002, and in revised form 30 April 2003

Abstract

The effect of human anti-cementoblastoma-derived protein antibody during cementogenesis in vitro was investigated by using human cementoblastoma-derived cells. Cultures treated with 5 µg/ml of CP antibody from day 1 to day 15 revealed a significant decrease in alkaline phosphatase activity (ALP) 40% ($p < 0.005$), 44% ($p < 0.001$), 49% ($p < 0.1$), and 45% ($p < 0.02$) at 9, 11, 13, and 15 days, respectively. Immunoexpression of osteopontin revealed that in cultures treated with anti-CP antibody, the positive number of cementoblastoma cells was reduced by 87, 83, 69, and 52% at 5, 7, 9, and 11 days, respectively. Bone sialoprotein immunoexpression showed a decrease in positive cells of 82, 51, 60, 80, 83, and 87% at 5, 7, 9, 11, 13, and 15 days, respectively, as compared to controls. The Ca/P ratio of the mineral-like tissue deposited in vitro by cementoblastoma cells revealed that control cultures had a Ca/P ratio of 1.45 and 1.61 at 5 and 15 days, whereas experimental cultures revealed a Ca/P ratio of 0.50 and 0.79 at 5 and 15 days, respectively. Electron diffraction patterns showed inner double rings representing D-spacing that were consistent with those of hydroxyapatite in both control and experimental cultures. Examination of the crystallinity with high resolution transmission electron microscopy showed homogeneous and preferential spatial arrangement of hydroxyapatite crystallites in control and experimental cultures at 15 days. Atomic force microscopy images of control cultures at 5 and 15 days revealed small granular particles and grain agglomeration that favored the formation of crystalline plaques with a lamellar-like pattern of the mineral-like tissue. Experimental cultures at 5 and 15 days showed tiny and homogeneous granular morphology. The agglomerates maintained spherical morphology without organization of needle-like crystals to form plaque-like structures. Based on these findings, it is hypothesized that cementoblastoma-derived protein may be associated to crystal growth, compositional and morphological features during the mineralization process of cementum in vitro.

© 2003 Elsevier Science (USA). All rights reserved.

Keywords: Cementum; Cementoblastoma-derived protein; Bone sialoprotein; Hydroxyapatite; Mineralization; Osteopontin

1. Introduction

Cementum is a unique avascular mineralized connective tissue that surrounds the root dentine and provides the interface through which the root surface is anchored to the collagen Sharpey's fibers of the periodontal ligament. Cementum matrix consists of collagen types I and III, fibronectin, osteopontin (OPN), bone

sialoprotein (BSP) (Bosshardt et al., 1998; Nanci, 1999), and osteocalcin (OCN) (D'Errico et al., 2000; Kagayama et al., 1997; MacNeil et al., 1998).

OPN and BSP have been implicated in mineral deposition and cell- and matrix-matrix interactions (Boskey, 1995). These proteins have been proposed to be potential regulators of the hydroxyapatite crystal nucleation and/or growth. OPN has a poly-Asp and BSP two poly-Glu domains, whose repetitive sequences are known to bind calcium to mineral surfaces. OPN is a highly phosphorylated and sulfated sialoprotein with an

* Corresponding author. Fax: +52(55)56225563.
E-mail address: harzate@servidor.unam.mx (H. Arzate).

RGD motif attachment that recognizes the vitronectin type of the integrin receptor. Periodontium cells in close contact with acellular cementum and cellular cementum, express OPN as well as cementocytes (Bronckers et al., 1994).

BSP is also an RGD-containing sialoprotein with cell attachment properties (Oldberg et al., 1988). It has been suggested that it is involved in controlling the formation and resorption of mineralized tissues as well as in the nucleation of hydroxyapatite crystals at the mineralizing front of bone (Chen et al., 1992a). BSP is believed to play a critical regulatory role during the process of cementogenesis and this molecule might be involved in the processes of precementoblast chemoattraction, adhesion, and differentiation (MacNeil et al., 1995).

Recent studies suggest that cementum may contain unique molecules that are specific for this tissue (McAllister et al., 1990). The cementum attachment protein (CAP) has been characterized as a collagenous protein with an M_r of 56 000 (Wu et al., 1996), and its location appears to be restricted to cementum (Arzate et al., 1992). This molecule has been shown to promote adhesion and spreading of mesenchymal cell types (Olson et al., 1991), and alkaline phosphatase expression and mineralization in undifferentiated mesenchymal cells (Arzate et al., 1996). CAP promotes selectively the attachment of mineralized tissue forming periodontium lineages (Pitaru et al., 1995), serves as a marker for putative cementoblastic progenitors of the adult human periodontal ligament (Bar-Kana et al., 1999; Liu et al., 1997), and affects the differentiation of these progenitors *in vitro* (Saito et al., 2001).

Recently, we isolated and characterized a human cementoblastoma-derived cell line that expresses the cementum phenotype. The physical, morphological and chemical features of the cementum-like tissue deposited by these cells appeared to be different from the mineral-like tissue deposited by human osteoblastic cells *in vitro*, and is similar to human cellular cementum (Arzate et al., 1998, 2000). This cell line produces a cementum protein species of 56 kDa that has been purified from its conditioned media. The cementoblastoma-derived protein (CP) promotes attachment on human gingival fibroblasts, human periodontal ligament cells, and alveolar bone-derived cells in a dose-dependent manner. CP has also been postulated to be related to CAP since a monoclonal antibody against bovine CAP cross-reacted with immunopurified CP as a 70 kDa species (Arzate et al., 2002). A polyclonal antibody raised against CP revealed that CP is widely distributed throughout cementum and is able to identify putative cementoblastic populations both *in vivo* and *in vitro* (Arzate et al., 2002). Thus, the antibody raised against CP could serve as an *in vitro* model to study the mineralization process in this characterized cementoblastic cell line.

2. Materials and methods

Rabbit polyclonal antiserum to human OPN (LF-123), and human BSP (LF-100) were kindly donated by Dr. Larry Fisher from NIH.

2.1. Antibody preparation

CP's partial purification was performed as described by McAllister et al. (1990). Three liters of conditioning media obtained from human cementoblastoma-derived cells were dialyzed against PBS and lyophilized, then reconstituted in PBS and loaded into a DEAE-cellulose column. The 0.5 M NaCl fraction was loaded on SDS-PAGE gel and the CP band with an M_r of 56 000 was excised from the gel. Gel slices were electroeluted in 50 mM NH₄HCO₃ containing 0.1% SDS. SDS was removed by extracting with acetone at -20 °C and lyophilized. New Zealand rabbits were immunized through subcutaneous (s.c.) injections with a 5-μg dose of CP mixed with Al(OH)₃ (v/v), in the muscle of the right hind leg every two weeks for two months (Dunbar and Schwoebel, 1990). Seven days after the last immunization, the rabbits were bled, sera pooled, and frozen. Antibody production was monitored by ELISA and Western blot. Antiserum was purified through protein A-Sepharose chromatography. Antibodies bound to Protein A were washed with PBS and eluted with a solution of 0.2 M glycine-HCl, pH 2.6. Eluted antibodies were immediately neutralized with 10× PBS, and dialyzed against PBS. The specificity of the anti-CP antibody was tested by immunoblotting and immunostaining as described previously in detail (Arzate et al., 2002). The antibody fraction will be referred to as anti-CP antibody.

2.2. Cell culture and anti-CP treatment

Cell cultures were derived from a human cementoblastoma, a neoplasm accepted as being essentially cementogenic by the World Health Organization (Kramer et al., 1992), through the conventional explant technique; cells were characterized as previously described (Arzate et al., 1998, 2000). Cementoblastoma cells were cultured in 75 cm² cell culture flasks containing DMEM, supplemented with 10% FBS and antibiotic solution (100 μg/ml streptomycin and 100 U/ml penicillin, Sigma Chemical). The cells were incubated in a 100% humidified environment at 37 °C in a 95% air and 5% CO₂ atmosphere. Human cementoblastoma-derived cells at the second passage were used for all the experimental procedures.

2.3. Proliferation assay

To determine whether IgG or anti-CP antibodies affected cell proliferation, human cementoblastoma-de-

rived cells were plated at 2×10^4 into 48-well culture plates and incubated overnight in 10% FBS. The following day, designated as day 0, the medium was changed and cultures were treated with 10% FBS plus anti-CP antibody (5 µg/ml). Control cultures were treated with a normal rabbit IgG antibody (5 µg/ml). Medium and antibodies were changed every other day. Cells were harvested by trypsinization (0.05% trypsin and 0.02% EDTA) and counted in a model ZBI Coulter Counter (Coulter Electronics, Hialeah, FL). Cell numbers were assessed at days 1, 3, 5, and 10. Experiments were performed in triplicate and repeated twice.

2.4. Cell viability assay

Cementoblastoma-derived cells viability in the presence of anti-CP antibodies was determined through the MTT assay. This assay is based on the ability of mitochondrial dehydrogenases to oxidize thiazolyl blue (MTT), a tetrazolium salt (3-[4,5-dimethylthiazolyl-2-yl]-2,5-diphenyltetrazolium bromide), to an insoluble blue formazan product. Cells were plated at 1×10^4 into a 96-well plate by triplicate and incubated for 1, 3, 5, and 10 days. After each term, cells were incubated with MTT (120 mg/ml) at 37 °C for 3 h. After the supernatant was removed, 0.04 M HCl in isopropanol was added to each well and the optical density of the solution was read at 570 nm in an enzyme-linked immunoassay (ELISA) plate reader. Since generation of the blue product is proportional to the dehydrogenase activity, a decrease in absorbance at 570 nm provides a direct measurement of the number of viable cells. Experimental cultures were treated with 5 µg/ml of anti-CP antibody. Controls were treated with 5 µg/ml of IgG antibody. Experiments were performed in triplicate and repeated separately twice.

To test the effect of anti-CP antibodies on the mineral tissue formation, human cementoblastoma-derived cells were cultured for 5, 7, 9, 11, 13, and 15 days in DMEM supplemented as described above. Immediately after plating the cells and every other day, experimental cultures were treated with anti-CP antibody (5 µg/ml) and control cultures were treated with normal rabbit IgG antibodies (5 µg/ml) as described by Shakibaei (1998). At each time point cultures were tested for alkaline phosphatase activity and expression of OPN and BSP as described below.

2.5. Alkaline phosphatase activity

Human cementoblastoma-derived cells were plated in triplicate at 2×10^4 in 24-well culture plates (Costar, Cambridge MA, USA). Cells were cultured in DMEM, supplemented with 10% FBS, antibiotic solution, 10 mM β-glycerophosphate, 50 µg/ml ascorbic acid, and 10⁻⁷ M dexamethasone. Control and experimental cultures were treated as described above immediately after plating the

cells. Fresh medium and antibody were added to the cultures every other day. Alkaline phosphatase activity (ALP) was determined according to Lowry et al. (1954). Cell layers were extracted in 10 mM Tris-HCl buffer, pH 7.4, containing 0.1% Triton X-100 and then sonicated. Enzyme activity was assessed using 8 mM disodium *p*-nitrophenyl phosphate (PNP) as the substrate and 2 mM MgCl₂ in 0.1 M Tris-HCl buffer, pH 9.8, and incubated at 37 °C for 30 min. The reaction was stopped by adding 50 µl of 0.05 N NaOH and absorbances were measured at 405 nm. Samples were assayed under conditions that ensured linearity with respect to time and protein concentrations. Protein concentrations were determined according to the Bradford (1976) assay using BSA as standard. Assays were repeated at least three times.

2.6. Immunofluorescence

Human cementoblastoma-derived cells were plated at low density (5×10^2) in 8-well Lab-Tek chamber slides; allowed to attach overnight and cultured for the time periods mentioned above. At each term, cells were then fixed in 3.7% formaldehyde, and screened for the expression of BSP and OPN. Slides were incubated with anti-human OPN (LF-123) and anti-human BSP (LF-100), diluted 1:300 in PBS containing 1 mg/ml BSA and incubated overnight at 4 °C. Slides were washed with ice-cold phosphate-buffered saline (PBS) for 10 min at room temperature and incubated for 1 h at 4 °C with the secondary antibody goat-anti-rabbit immunoglobulin conjugated with FITC (3 mg/ml, Sigma Chemical, St. Louis, MO), diluted 1:50 in PBS. Slides were rinsed with PBS plus 0.1% Triton X-20 and coverslipped in glycerol-PBS (1:9 v/v) containing 20 mg/ml of 1,2-diazabicyclo (2.2.2) octane (DABCO; triethylenediamine). Immunostaining was visualized by indirect immunofluorescence (Axiphot, Carl Zeiss).

The number of cells cross-reacting with anti-OPN and anti-BSP was determined by scoring five different microscopic fields with a 20× lens. Results are expressed as means ($n = 5$) ± SE of three independent experiments. Slides incubated with pre-immune rabbit serum or lacking first antibody were used as negative controls.

2.7. Western blot analysis

The relative levels of OPN and BSP of cementoblastoma cells treated with anti-CP antibody were compared with those treated with IgG antibody. Cementoblastoma-derived cells were plated in triplicate at 5×10^4 density on 35 mm culture dishes. Experimental and control cultures were treated as described above and cultured during 5, 7, 9, 11, 13, and 15 days. At each term, cells were scraped with a policeman, re-suspended with ice-cold PBS, and centrifuged for 5 min at 2000 rpm. Pellets were lysed in ice-cold lysis buffer (1 mM

EDTA, pH 8.0), 10 mM Hepes, 50 mM NaCl, 0.5% Triton X-100, 1 mM phenylmethylsulfonyl fluoride, 5 µM leupeptin, and 10 µg/ml aprotinin). After centrifugation at 8000 rpm for 10 min at 4 °C, supernatants were collected and stored at –20 °C. Crude protein concentrations were determined as described above. For each antibody (OPN and BSP), equal amounts of protein (10 µg/lane) were subjected to SDS-PAGE on 12% polyacrylamide gels. The proteins were then electrophoretically transferred onto Immobilon-P (PVDF) nitrocellulose membranes (Millipore, Bedford, MA). Membranes were blocked with 5% skim milk for 1 h and then incubated with 1:300 diluted rabbit polyclonal antiserum to human OPN (LF-123) and human BSP (LF-100) for 1 h at room temperature. After washing, membranes were incubated with 1:1000 diluted horse-radish peroxidase-conjugated-goat anti-rabbit IgG secondary antibody for 1 h, washed with PBS and developed with diaminobenzidine. Blots were scanned and analyzed with a Kodak Electrophoresis Documentation and Analysis System (EDAS) 290. The relative level of each protein was assessed by measuring the integrated intensity of all pixels in each band, excluding the local background. Results are expressed as percentages of protein intensity obtained in control cultures.

2.8. Atomic force microscopy

Atomic force microscopy (AFM) was used to determine the morphology and homogeneity of the mineral-like tissue deposited by cementoblastoma-derived cells in the presence of 5 µg/ml normal rabbit IgG antibody (5 µg/ml) or anti-CP antibody (5 µg/ml). AFM (Park Scientific Instruments) was used with an AutoProbe in contact mode with a constant applied force (10 nN) at 1 Hz scan rate in wet samples. Cementoblastoma-derived cells were plated at 2×10^4 in 24-well culture plates (Costar, Cambridge, MA, USA) onto silicon (111) monocrystal substrate and cultured for 5 and 15 days in DMEM supplemented with 10% FBS, antibiotics, 50 µg/ml ascorbic acid, 10 mM β-glycerophosphate, and 10^{-7} M dexamethasone. Experimental and control cultures were treated every other day with fresh medium and fresh antibody. The cultures were monitored at 5 and 15 days to detect calcium salts precipitation by using Alizarin red S staining. Upon termination of the culture times, cementoblastoma-derived cells were rinsed thrice with ice-cold PBS and culture plates were fixed in situ with 70% ethyl alcohol and air-dried.

2.9. Energy dispersive X-ray microanalysis

The composition of the mineral-like tissue formed by the cementoblastoma-derived cells plated onto silicon (111) monocrystal substrate at an initial density of

2×10^4 in 24-well plates was analyzed at 5 and 15 days. Control and experimental cultures were maintained in DMEM supplemented as described. Upon termination, the cultures were washed with PBS, fixed in 70% ethyl alcohol, air-dried and covered with a thin gold film, 100 nm thick, to avoid electron disturbances that could interfere with the microanalysis. Cell cultures were analyzed by using a Leica-Cambridge 440 scanning electron microscope fitted with a Pentafet energy dispersive X-ray microanalysis microprobe. All analyses were performed at 20 kV for 300 s (Cuisinier et al., 1991; van Dijk et al., 1995) on different areas with different probe sizes.

2.10. Electron diffraction analysis

Human cementoblastoma-derived cells, control and experimental cultures treated as described during 15 days, were tested for mineral phase formation. To do this, cells were cultured on copper grids of 200 mesh covered with a plastic film and coated with a carbon thin film for TEM observation. D-spacing of diffraction patterns was calibrated to correspond to those for the gold standard obtained with identical diffraction conditions. The mineral phase was analyzed using a Jeol 100 CX analytical transmission microscope. All analyses were performed at 100 kV. A Jeol 4000 EX TEM was used at 400 kV for the high-resolution (HRTEM) analysis of the experimental and control cultures at 15 days.

2.11. Statistical analysis

Data for the proliferation and viable cell number assays were evaluated by variance analysis followed by multiple comparisons using a corrected Bonferroni *p* value. Statistics for all other assays were performed with the Student's *t* test, using Sigma Stat V 2.0 software (Jandel Scientific).

3. Results

3.1. Cell proliferation and cell viability

To determine whether IgG and anti-CP antibodies contributed to alter human cementoblastoma cells, their proliferation rate was determined during a 10-day period. There were no statistical differences between treatments and 10% FBS-treated controls (Fig. 1A). Cell viability was not affected by either IgG or anti-CP antibodies over the 10-day period as illustrated in Fig. 1B. MTT activity of cementoblastoma cells began to increase on day 3 and continued until day 10. No statistical significances in MTT activity were seen between IgG and anti-CP antibodies with respect to 10% FBS control medium.

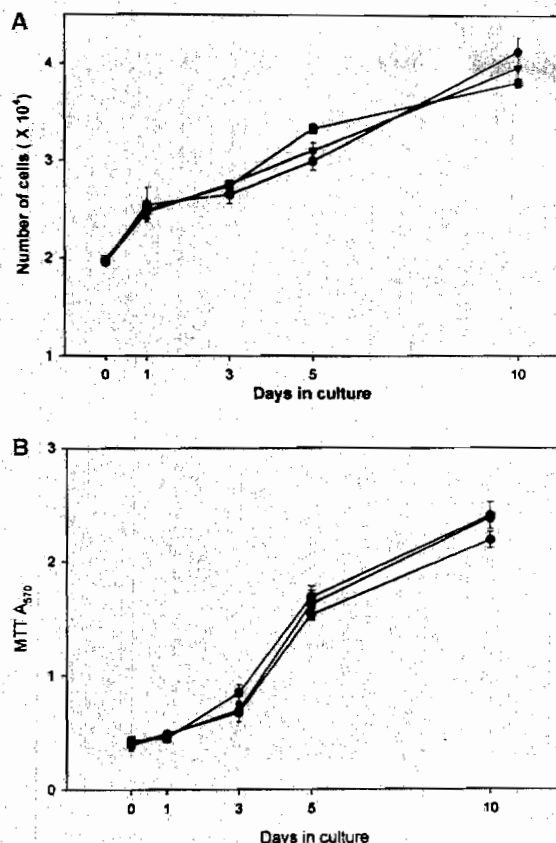


Fig. 1. Effects of IgG, anti-CP antibodies and 10% FBS on cell growth and cell viability. Shown are pooled data from two independent growth curves (A) and from two independent viability curves (B) of cementoblastoma-derived cells treated with IgG (●) and anti-CP antibodies (■), at a concentration of 5 μ g/ml each. Ten percent FBS was used as a control media (▼). There were no statistical differences between treatments.

3.2. Alkaline phosphatase activity

ALP activity was assessed at different culture times by measuring the enzymatic activity in the cell layer. ALP activity was detected in the cell layers of experimental and control cultures as early as 72 h. No statistical differences between treatments were observed at days 3 and 7. However, alkaline phosphatase activity of cementoblastoma-derived cell cultures treated with anti-CP was 40% ($p < 0.005$), 44% ($p < 0.001$), 49% ($p < 0.1$), and 45% ($p < 0.02$) lower than their counterparts treated with normal rabbit IgG antibody at 9, 11, 13, and 15 days, respectively. These results show that anti-CP antibody inhibited ALP enzymatic activity during the initial stages of mineralization (Fig. 2).

3.3. Effect of anti-CP treatment on in vitro expression of OPN and BSP

Analysis of OPN expression reveals that the number of OPN positive cells was lower in the experimental

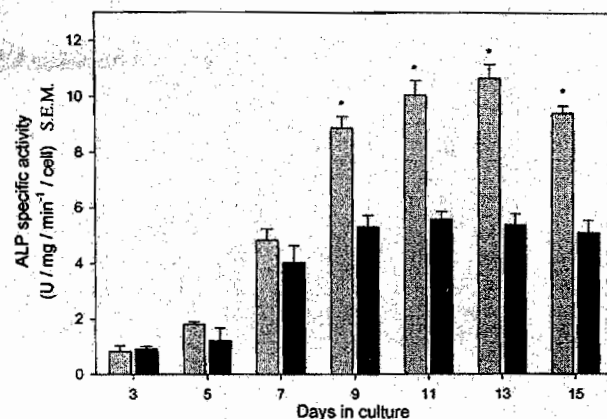


Fig. 2. Alkaline phosphatase activity of human cementoblastoma-derived cells taken at 3, 5, 7, 9, 11, 13, and 15 days. Control cultures (▨) treated with 5 μ g/ml of IgG antibody and experimental cultures (■), treated with 5 μ g/ml of anti-CP antibody. An asterisk indicates statistical difference between treatments at $p < 0.05$.

cultures by 87, 83, 69, and 52% at 5, 7, 9, and 11 days, than their control counterparts (Fig. 3A and Table 1). However, at 13 and 15 days the values of OPN positive cells in the experimental cultures were similar to those observed in control cultures.

BSP expression was decreased in the cultures treated with anti-CP antibody throughout the entire culture period as compared to controls. BSP positive cell percentages were 82, 51, 60, 80, 83, and 87% lower in experimental cultures than in the control ones at 5, 7, 9, 11, 13, and 15 days (Fig. 3B, Table 2). In the control cultures, a gradual increase in the percentage of BSP positive cells was observed throughout the experimental period. In the experimental cultures the number of BSP positive cells increased 3-fold between days 5–7 and after day 9 decreased gradually to the initial level of day 5.

3.4. Immunoblotting

Western analysis showed that, in the experimental cultures, the relative levels of OPN were reduced by 60, 58, 30, 57, 56, and 39% at 5, 7, 9, 11, 13, and 15 days of culture as compared to controls. These results indicate that OPN protein expression was highly inhibited during early stages of the mineralization process (Fig. 4A). BSP relative levels of experimental cultures as compared to control cultures were 30, 18, 50, 16, 17, and 42% at 5, 7, 9, 11, 13, and 15 days, respectively, indicating that anti-CP antibody influenced BSP protein levels at mid and late stages of mineralization (Fig. 4B).

3.5. AFM

AFM images showed a sequence of the three-dimensional morphological disposition of the mineral-like

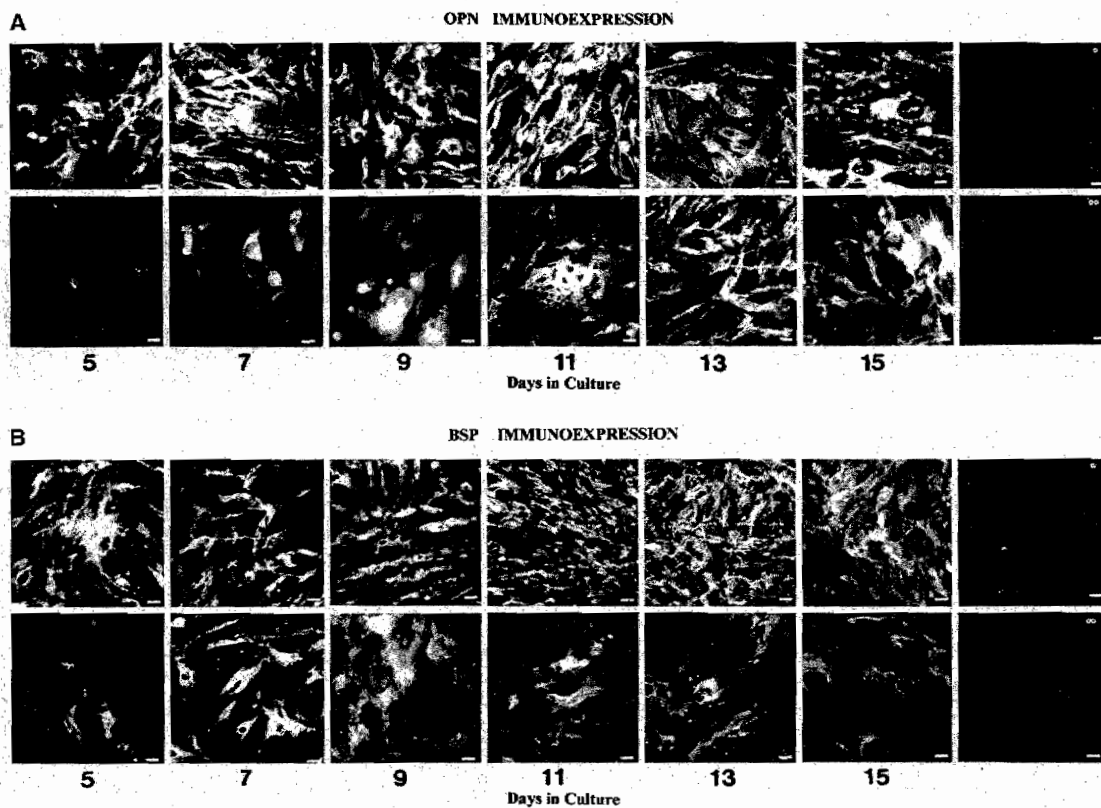


Fig. 3. Immunostaining of cementoblastoma-derived cells with rabbit anti-human OPN polyclonal antibody (A). Experimental cultures treated with 5 µg/ml of anti-CP antibody (lower row) revealed that the number of OPN positive cells was lower by 87, 83, 69, and 52% at 5, 7, 9, and 11 days, than their control counterparts at 5, 7, 9, 11, 13, and 15 days (upper row). Representative negative control with pre-immune rabbit serum for control (°) and experimental (°°) cultures. Original magnification 20×. Bar = 12 µm. Immunostaining of cementoblastoma-derived cells with rabbit anti-human BSP polyclonal antibody (B). Experimental cultures (lower row) treated with 5 µg/ml of anti-CP antibody at 5, 7, 9, 11, 13, and 15 days revealed that BSP expression was dramatically decreased throughout the entire culture period as compared to the control cultures (upper row). Representative negative control with pre-immune rabbit serum for control (°) and experimental (°°) cultures. Original magnification 20×. Bar = 12 µm.

Table 1
Expression of OPN in cementoblastoma-derived cells treated with anti-CP antibody

Days	Control cultures ^{a,d}	Experimental cultures ^{b,d}	% ^c
5	55.4 ± 1.14*	7.2 ± 0.83	13.0
7	62.8 ± 2.16*	10.4 ± 1.34	16.6
9	65.2 ± 2.16*	20.2 ± 1.30	31.0
11	66.2 ± 1.30*	31.2 ± 2.58	47.2
13	70.8 ± 2.16*	67.4 ± 1.14	95.2
15	71.6 ± 1.81	69.6 ± 1.14	97.3

^a Cementoblastoma-derived cells treated with 5 µg/ml of normal rabbit IgG antibody.

^b Cementoblastoma-derived cells treated with 5 µg/ml of anti-CP antibody.

^c Represents percentages of experimental positive cells respect to control cultures.

^d Means ± SE of triplicates.

* p < 0.001 Student's t test.

tissue deposited by cementoblastoma cells. The features observed in control cultures, at 5 days, revealed granular agglomerates with a size range of 1.5–0.30 µm and

Table 2
Expression of BSP in cementoblastoma-derived cells treated with anti-CP antibody

Days	Control cultures ^{a,d}	Experimental cultures ^{b,d}	% ^c
5	47.4 ± 2.40*	8.40 ± 0.89	17.8
7	54.2 ± 1.48*	26.4 ± 2.07	48.8
9	55.2 ± 1.09*	22.0 ± 1.58	39.8
11	68.8 ± 0.83*	13.4 ± 1.14	19.5
13	76.4 ± 1.14*	12.4 ± 1.34	16.7
15	79.8 ± 1.48*	9.8 ± 1.64	12.3

^a Cementoblastoma-derived cells treated with 5 µg/ml of normal rabbit IgG antibody.

^b Cementoblastoma-derived cells treated with 5 µg/ml of anti-CP antibody.

^c Represents percentages of experimental positive cells respect to control cultures.

^d Means ± SE of triplicates.

* p < 0.001 Student's t test.

grain agglomeration that favored the formation of crystalline plaques with a lamellar-like pattern. These individual plaques were 0.18 µm wide and 0.36 µm

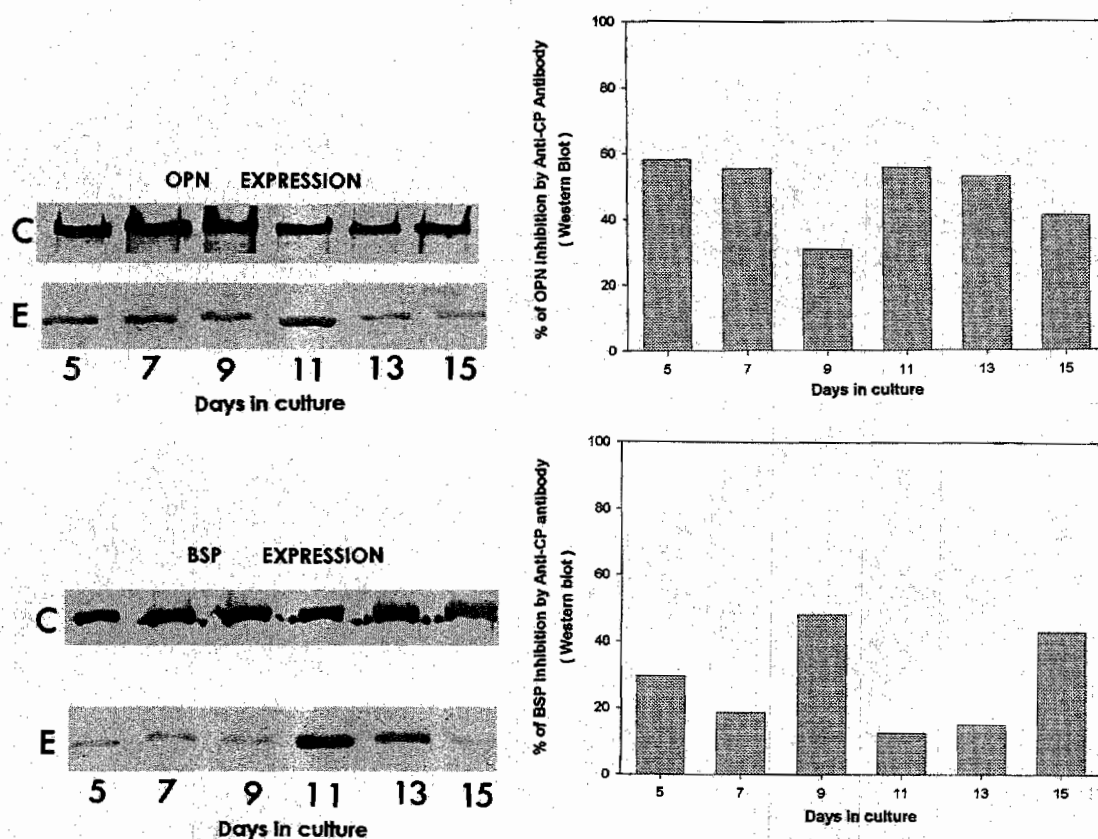


Fig. 4. Western blots for the detection of OPN and BSP in cementoblastoma-derived cells treated with IgG antibodies (C) and with anti-CP antibodies (E). Solubilized extracts from different culture times (5–15 days) were subjected to SDS-PAGE and then to immunodetection with antibodies to human OPN and BSP. Protein relative levels were assessed by measuring the integrated intensity of all pixels in each band, excluding the local background.

long, representing an anisotropic crystalline structure of 2:1 (l/w); with small granular particles (0.3 μm , and 300 Å high), (Fig. 5A). Tiny needle-shaped crystals 6 Å high with preferential orientation were observed (Fig. 5E). Experimental cultures treated during 5 days with anti-CP antibody showed a tiny granular morphology with a submicron size (0.1 μm) of granular particles that formed the agglomerates with a size range of 1.3–0.25 μm (Fig. 5B) and spherical agglomerates (Fig. 5F). Control cultures at 15 days showed well-oriented and organized plaque-like structures of 1.6 μm width and 20 μm length, representing an anisotropic ratio of 12.5 (l/w). These cultures also showed granular agglomerates with a size range of 2.6–0.9 μm . (Fig. 5C) and needle-shaped crystals (Fig. 5G). Experimental cultures at 15 days revealed almost the same features observed in experimental cultures at 5 days. The agglomerates maintained spherical morphology without organization of needle-like crystals to form plaque-like structures. However, the granular agglomerates were larger in size (1.5–0.30 μm), when compared to those observed at 5 days of experimental cultures (Figs. 5D and H)).

3.6. EDS

The Ca/P ratio and composition of the mineral-like tissue deposited in vitro by cementoblastoma-derived cells was assessed at 5 and 15 days of culture. Control cultures at 5 days showed 56.1 and 38.7 at.% of Ca^{2+} and P, respectively (Fig. 6C). Other elements such as K (2.5 at.%), and Mg^{2+} (2.4 at.%) were present in their global composition. The Ca/P ratio (1.45) corresponds well with the biological hydroxyapatite value (Fang et al., 1994). Cementoblastoma cell cultures treated with 5 $\mu\text{g}/\text{ml}$ of anti-CP antibody for 5 days showed low energy peaks for Ca^{2+} and P (Fig. 6A) with an atomic percentage of 29.9 and 58.5, respectively. Other elements such as K represented 5.4 of the atomic percentage. Mg^{2+} ions were not detectable in the spectrum. The Ca/P ratio value was of 0.50. At 15 days of culture, control cultures exhibited 55.4 and 34.4 at.% for Ca^{2+} and P (Fig. 6D). K and Mg^{2+} were present in the composition with 6.1 and 3.8 at.%. The Ca/P ratio was 1.61, which corresponds well with the biological hydroxyapatite value. Experimental cultures revealed 38.5, 48.3, and 4.5 at.% for Ca^{2+} , P, and K (Fig. 6B). The Ca/P ratio

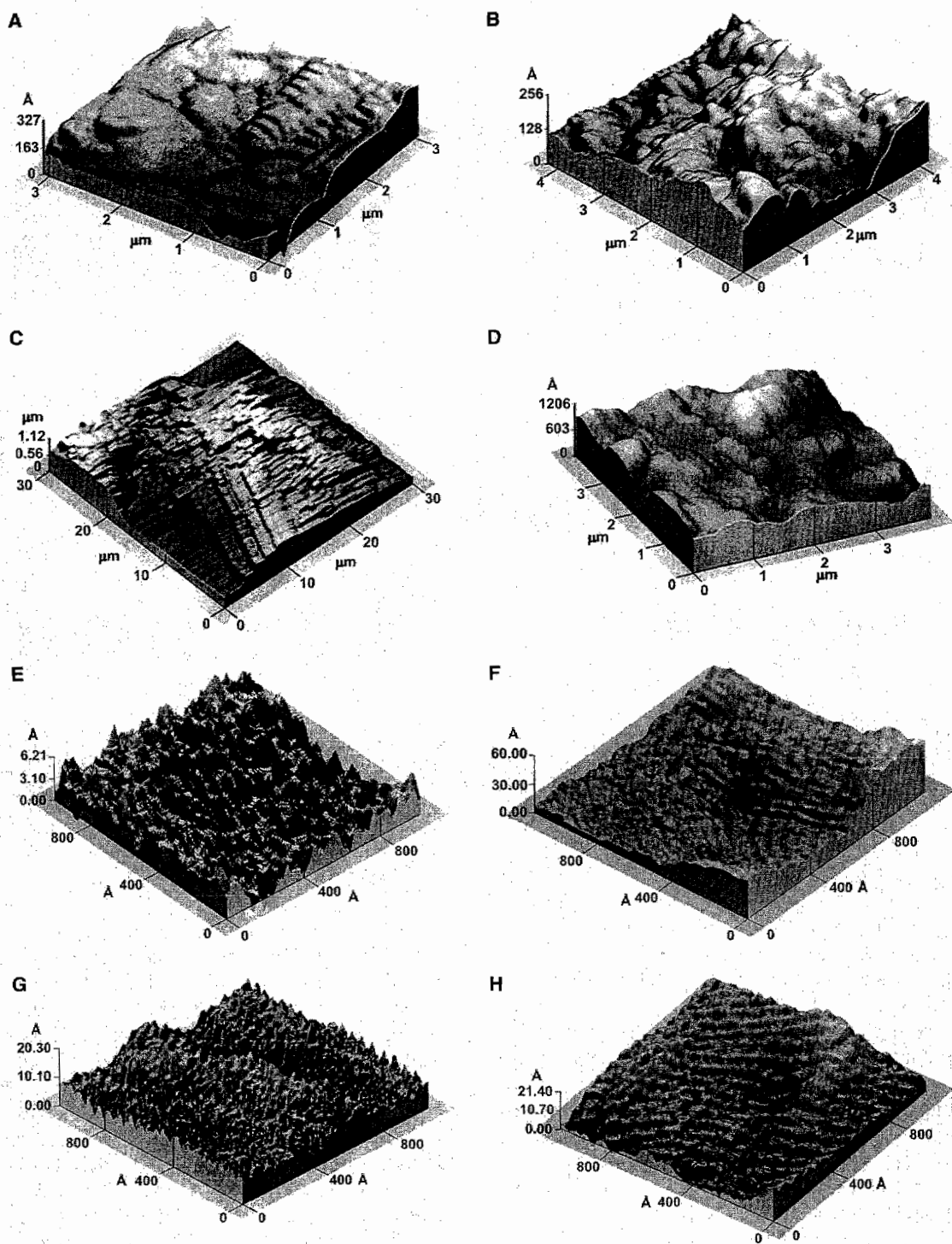


Fig. 5. Three-dimensional features observed by AFM showed globular, needle-shaped crystals and lamellar arrangement of the mineralized-like tissue deposited by cementoblastoma-derived cells in control cultures at 5 days (A and E), and 15 days of culture (C and G); Experimental cultures treated with 5 μ g/ml of anti-CP antibody revealed similar spatial disposition of globular-like structures at 5 days (B and F), and 15 days of culture without lamellar arrangement of the mineralized-like tissue deposited by cementoblastoma-derived cells (D and H).

was 0.79. Energy dispersive X-ray microanalysis (EDS) examination determined the biological hydroxyapatite values. Therefore, the EDS spectra from control samples

showed better peak definition than those of the experimental cultures which reveals that the crystal density was larger in the control cultures.

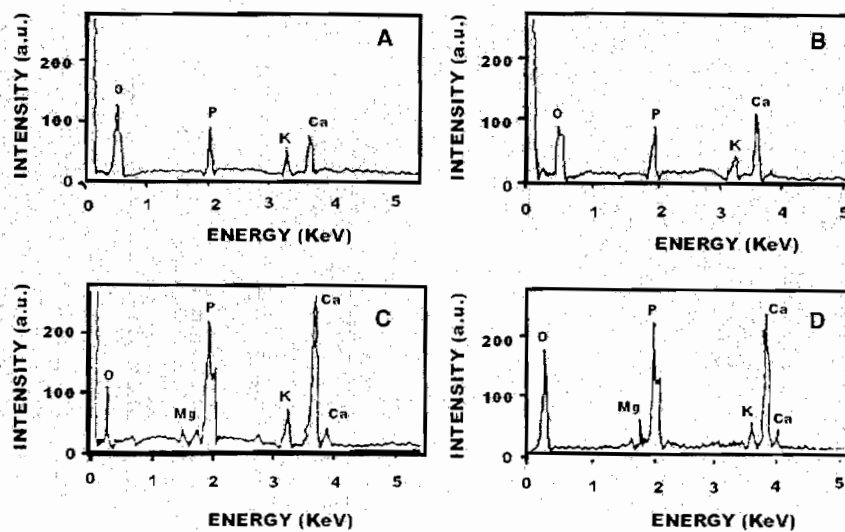


Fig. 6. Representative energy-dispersive x-ray microanalysis spectrum of a 1×1 mm area of mineralized areas deposited by putative human cementoblasts. Experimental cultures at 5 (A) and 15 (B) days showed low peaks for calcium (Ca^{2+}) and phosphorous (P). Control cultures showed prominent peaks of Ca^{2+} and P and peaks representing Mg^{2+} and K at 5 (C) and 15 (D) days of culture.

3.7. Electron diffraction

Cell cultures from cementoblastoma-derived cells were obtained for the analysis of mineral deposits at 15 days of culture. Control and experimental cultures showed crystals that revealed patterns of concentric double rings. The inner double rings correspond to D-spacing, 2.34 and 2.98 Å (Figs. 7A and B, respectively), which were consistent with those for hydroxyapatite (2.29 and 3.08 Å). The inner semi-ring in Fig. 7 shows a clear preferential growth of hydroxyapatite crystals.

Examination of the crystallinity of samples with HRTEM showed that both control and experimental cultures at 15 days revealed a homogeneous and preferential spatial arrangement of hydroxyapatite crystallites with a 7.1 Å ($\text{hkl}: 100$), 3.8 Å ($\text{hkl}: 111$), and 3.1 Å ($\text{hkl}: 210$) interatomic distances (Fig. 8). All the crystals were nanostructured with atomic distances of hydroxyapatite crystals values of d : 2.27 Å ($\text{hkl}: 212$), 2.42 Å ($\text{hkl}: 301$), 3.53 Å ($\text{hkl}: 201$) and 4.5 Å ($\text{hkl}: 110$). The patterns obtained are shown in Fig. 7 and

were indexed with the hydroxyapatite standard patterns of the JCPDS (Joint Committee on Powder Standards) No. 9-432 file for calcium hydroxyapatite (JCPDS, 1995).

3.8. Scanning electron microscopy

Examination of control cultures at 5 days revealed mineralized areas formed by agglomerates and needle-like structures (Fig. 9C), confirming the electron diffraction analysis and AFM images. At 15 days, control cultures formed plaque-like structures (Fig. 9D). However, experimental cultures at 5 and 15 days showed agglomerates with spherical shape and homogeneous size (Figs. 9A and B, respectively). It was evident that in the cultures treated with anti-CP antibody the growth of the mineralized area was retarded.

4. Discussion

The results of this study indicate that mineralization in a cementoblastic cell line was partially inhibited by anti-CP, indicating that the CP is among the factors that regulate mineral deposition of this lineage in vitro. Anti-CP antibody influenced the ALP activity and the protein levels of OPN and BSP as well as the amount and quality of mineral deposited in these cultures without interfering with cell proliferation and cell viability. Cell viability was greater than 90% for all treatment groups, eliminating the likelihood of cell toxicity caused by either IgG or anti-CP antibodies. The dosages of IgG and anti-CP antibodies were similar to those used for in vitro studies reported by Shakibaei, 1998). ALP activity,

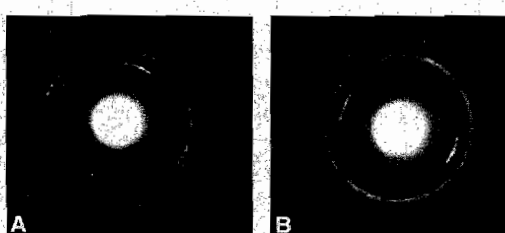


Fig. 7. Selected area electron diffraction pattern obtained from mineralized-like tissue deposited by cementoblastoma-derived cells. The inner semi-ring shows a clear preferential growth of hydroxyapatite crystals at 15 days for both, control (A) and experimental (B) cultures.

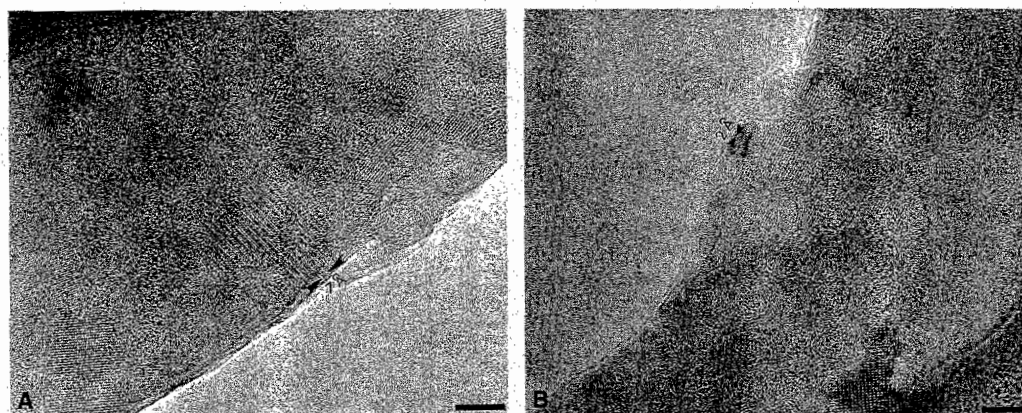


Fig. 8. High-resolution transmission electron microscopy (HRTEM) shows that crystallinity of the mineralized-like tissue in control cultures at 15 days was homogeneous and with a preferential spatial arrangement of hydroxyapatite crystallites (A). Experimental cultures at 15 days showed non-homogeneous hydroxyapatite crystallite arrangement (B). Bar in A = 1.7 nm. Bar in B = 1.4 nm.

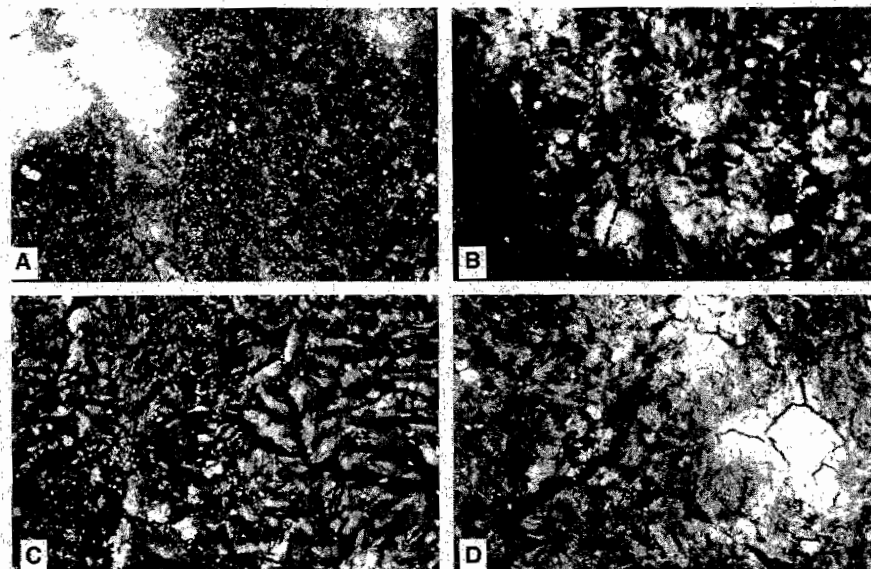


Fig. 9. SEM examination of the mineral-like tissue deposited by cementoblastoma-derived cells revealed agglomerate and needle-like structures at 5 (A) and 15 (B) days. Experimental cultures at 5 (C) and 15 (D) days show agglomerates with spherical shape and homogeneous size. Bar = 30 μ m.

expression of OPN and BSP are characteristic of early and late stages of mineral-like tissue deposition in osteoblastic and cementoblastic cell lines in vitro. Since the cementoblastic cell line used in this study has been shown to express CAP, which is immunologically related to CP (Arzate et al., 2002), and CAP has also been reported as a 65 kDa species in developing tooth germ (Saito et al., 2001), it is possible that CP represents a CAP-related molecular form. In addition anti-CP antibody has the capacity to identify putative cementoblastic populations both in vitro and in vivo.

ALP is thought to play a role in general phosphate metabolism and cementum formation, although its precise role during mineralization is not entirely clear

(Linde, 1982). ALP activity is related to the initial mineralization and once the phase of bulk matrix synthesis and mineralization has ceased, the further progression of mineralization of previously deposited matrix is associated with retention of ALP activity (Bianco, 1992). Our experimental cultures revealed an up to 49% decrease in ALP activity from 9 to 15 days, suggesting that anti-CP antibody partially inhibited ALP activity during mineralization in the experimental cultures. In addition to this, the thickness of the cementum-like tissue deposited by cementoblastoma-derived cells in the experimental cultures, as analyzed by AFM, was thinner than that observed in control cultures. The present results support previous work where a highly

significant positive correlation between ALP activity and cementum thickness has been demonstrated, i.e., the higher the activity of the enzyme, the thicker the cementum layer. Besides inhibition of ALP activity causes severe inhibition of cementum formation. Thus, ALP appears to be essential for the continuous growth of cementum (Beertsen et al., 1999; Groeneveld et al., 1995; Vandenbos and Beertsen, 1999). These results provide further support to our previous data, which point to the capability of CP to promote mineralization in undifferentiated mesenchymal cells (Arzate et al., 1996) and ALP activity in cementoblastoma cells (Arzate et al., 1998).

It has been suggested that non-collagenous proteins, such as OPN and BSP, have a major role in filling spaces created during collagen assembly, imparting cohesion to the mineral-like tissue by allowing mineral deposition to spread across the entire collagen meshwork (Bosshardt et al., 1998; Nanci, 1999). However, the means by which mineralization is achieved is still not well understood. Several authors suggest that phosphoproteins such as BSP and OPN are necessary for the initiation of crystal formation (Roach, 1994), and the large highly ordered fibrils of type I collagen. The major phosphoproteins in cementum are OPN and BSP and are synthesized by cementoblasts (Chen et al., 1991b; MacNeil et al., 1998; Shapiro et al., 1993). Our results revealed that OPN at the protein level was highly depressed in the experimental cultures during the initial stages of mineralization and the highest effect on BSP protein levels was observed at the mid and late stages of the experimental period as revealed by immunocytochemistry and Western blots. Since OPN is expressed at high levels in mineralized connective tissues (Bianco et al., 1991) and is related to the initial growth of hydroxyapatite crystals, it seems that the anti-CP antibody could have a secondary effect during initiation and progression of the mineralized matrix. Our results suggest that CP could mediate initial stages of mineralization probably by influencing OPN availability during crystal growth and maturation. Since, OPN's ability to bind and potentially orient significant amounts of Ca^{2+} which suggests that might function to promote calcification (Butler et al., 1996; Gorski, 1992). However, OPN is a multifunctional protein and indeed, in vitro studies support a role for OPN as an inhibitor of calcium oxalate crystals in the kidney and in cell-free systems, and acts principally on crystal growth (Hunter et al., 1996). It has been reported that OPN is abundant at sites of calcification in human atherosclerotic plaques and in calcified aortic valves, but is not found in normal arteries (Butler et al., 1996). However the function of OPN in hard tissue formation, mineralization and turnover is not yet clear, and the mineral inhibition during the mineralization process cannot be attributable to OPN acting solely as an inhibitor of crystal growth without considering the pos-

sible role of ALP on OPN's dephosphorylation, since phosphorylation of OPN is required for its inhibitory effect in an in vitro mineralization system (Jono et al., 2000). BSP plays an important role in mineral nucleation (Chen et al., 1991a, 1992b). BSP has a precise spatial association with early mineral aggregates, binds strongly to hydroxyapatite and acts as a specific and potent nucleator for hydroxyapatite formation in vitro (Hunter and Goldberg, 1993). Our findings demonstrate that BSP protein levels were partially depressed throughout the entire culture time. Thus, the process of mineral nucleation and growth was probably partially inhibited in the experimental cultures by affecting availability of OPN and ALP to regulate calcium uptake (Fukayama and Tashijan, 1990), crystal growth and maturation, and BSP crystal nucleation, explaining the globular mineral aggregates that did not develop to form lamellar structures in these cultures.

This statement is supported by the compositional data of the mineralized-like tissue deposited by cementoblastoma-derived cell cultures at 5 and 15 days as observed in the experimental cultures, since Ca/P ratio was lower when compared to controls and is related to a lesser crystal density. It appears that the calcium uptake deposition was retarded, since experimental cultures presented lower values of Ca^{2+} than control cultures at 5 and 15 days. This result could be related to the partial inhibition of OPN protein levels and ALP activity. It has been shown that other elements such as potassium and small concentrations of ions, like Mg^{2+} , slow crystal development by adsorbing to and blocking surface growth sites and hydroxyapatite crystal formation and maturation (Amjad et al., 1984; Serre et al., 1998; Weismann et al., 1997). Mg^{2+} ions are not directly incorporated into the apatite structure, but are rather accumulated in the hydration shell around the hydroxyapatite crystal, forming surface-bound ionic complexes (Posner, 1969). Our results revealed that magnesium was absent in the experimental cultures, which could contribute to the crystal growth retardation observed at 15 days of culture in cells treated with the anti-CP antibody. However, relatively high potassium concentrations and accumulation might be a common feature of mineralizing matrices. EDS examination of the mineralized-like tissue revealed that the material deposited by cementoblastoma-derived cells represents hydroxyapatite in both, control and experimental cultures at 15 days.

This is also supported by the analysis of HRTEM images. However, experimental cultures at 15 days had smaller crystallites in the range of nanocrystals and both control and experimental cultures have a preferential crystallographic orientation. This occurs within a matrix characterized by the lack of orientation of collagen fibrils in coherent directions and is characterized by the initial formation of randomly distributed, roughly

spherical, aggregates of crystals radiating from a center. In contrast, the control cultures showed the ordered mineralization pattern of lamellar-like mineralized tissue, matching a significant degree of collagen spatial organization and orientation (Boyde and Hobdell, 1969). Recent findings suggest that growth layers in human cementum may be related to altered mineral crystal orientation (Cool et al., 2002). Our observations strengthen the argument that mineral crystals are responsible for the layers observed in cementoblastoma control cultures and that the anti-CP antibody and the decreased ALP activity could contribute to the partial inhibition during the development of this morphological pattern and mineral crystal alignment (Tesch et al., 2003), presumably as a result of crystal density and impaired mineral maturation as revealed by EDS and HRTEM examination of the mineral phase in the experimental cultures.

Finally, our observations and combined data analysis suggest a provocative role of CP during the biological mineralization process of cementum-like tissue *in vitro*. Consistent with this idea, are the partial inhibition of ALP activity, decreased protein levels of OPN and BSP, compositional, morphological changes, and the retardation of the mineral phase by human putative cementoblastic cells, observed during the development of mineralized matrix. However, further studies are necessary to show the biological significance of CP among the factors that regulate cementum extracellular matrix mineralization *in vitro*, since its specific role cannot be determined conclusive at this time.

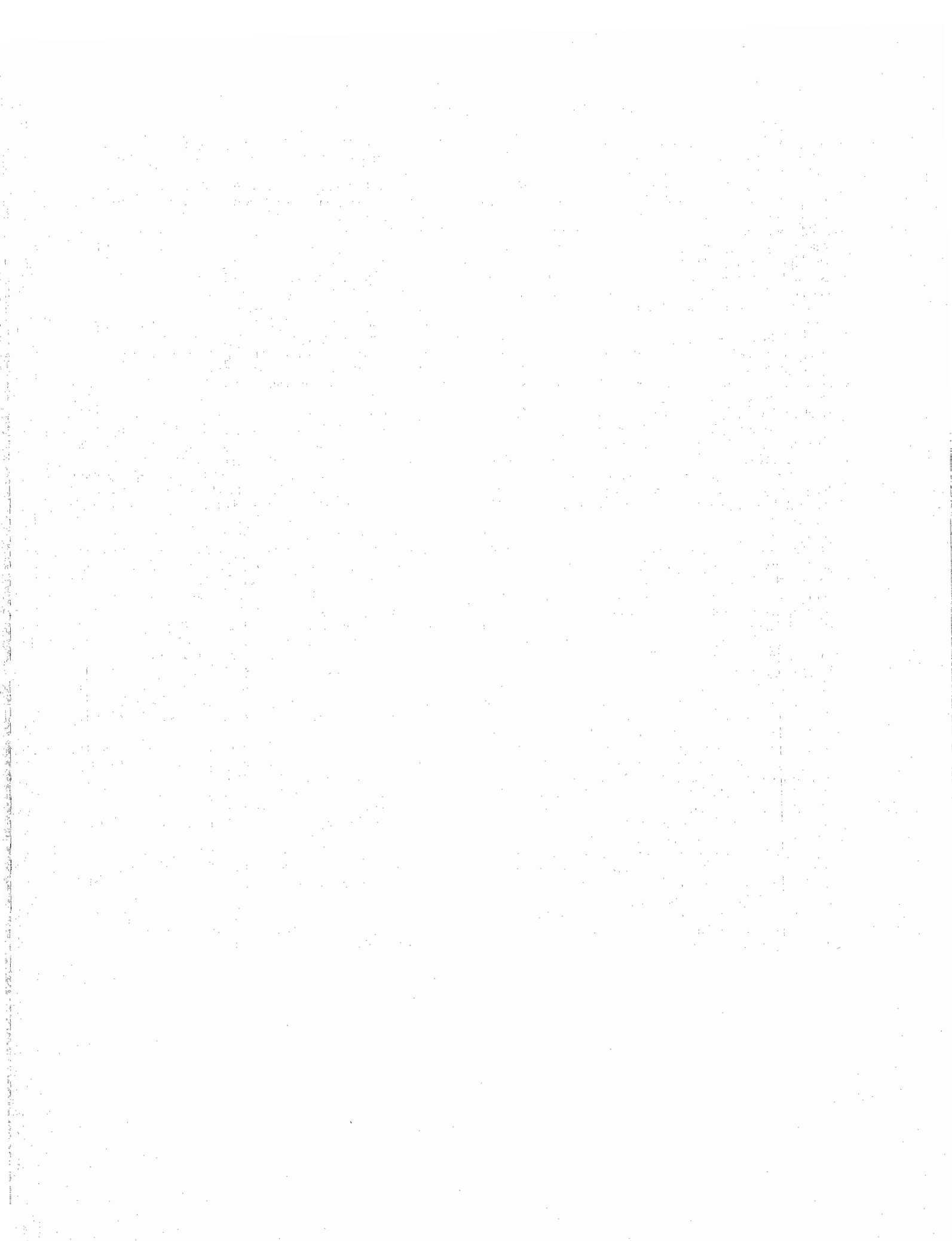
Acknowledgments

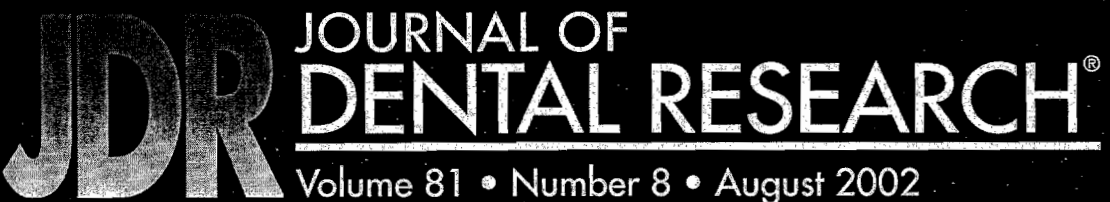
The authors wish to thank Dr. Larry W. Fisher for the gift of polyclonal antibodies against OPN (LF-123) and BSP (LF-100). Rogelio Fragozo from CINVESTAV-México, José Guzmán from IIM-UNAM, Luis Rendón, Pedro Mexia, Carlos Flores, and Roberto Hernández from IF-UNAM, for their technical assistance during the course of this study. Their support is greatly appreciated. This research was partially supported by DGAPA-UNAM (IN200599, IN200501) and CONACyT 30735-M.

References

- Amjad, Z., Koutsoukos, P.G., Nancollas, G.H., 1984. The crystallization of hydroxyapatite and fluoroapatite in the presence of magnesium ions. *J. Colloid Interface Sci.* 101, 250–256.
- Arzate, H., Olson, S.W., Page, R.C., Gown, A.M., Narayanan, A.S., 1992. Production of a monoclonal antibody to an attachment protein derived from human cementum. *FASEB J.* 6, 2990–2995.
- Arzate, H., Chimal-Monroy, J., Hernández-lagunas, L., Díaz de León, L., 1996. Human cementum protein extract promotes chondrogenesis and mineralization in mesenchymal cells. *J. Periodont. Res.* 31, 144–148.
- Arzate, H., Alvarez-Pérez, M.A., Aguilar-Mendoza, M.E., Alvarez-Fregoso, O., 1998. Human cementum tumor cells have different features from human osteoblastic cells *in vitro*. *J. Periodont. Res.* 33, 249–258.
- Arzate, H., Alvarez-Pérez, M.A., Alvarez-Fregoso, O., Wusterhausen-Chávez, A., Reyes-Gasga, J., Ximénez-Fyvie, L.A., 2000. Electron microscopy, micro-analysis and X-ray diffraction characterization of the mineral-like tissue deposited by human cementum tumor-derived cells. *J. Dent. Res.* 79, 28–34.
- Arzate, H., Jiménez-García, L.F., Alvarez-Pérez, M.A., Landa, A., Bar-Kana, I., Pitaru, S., 2002. Immunolocalization of a human cementoblastoma conditioned medium-derived protein. *J. Dent. Res.* 81, 541–546.
- Bar-Kana, I., Narayanan, A.S., Savion, N., Pitaru, S., 1999. Cementum attachment protein enriches the cementoblastic population on root surfaces *in vitro*. *J. Dent. Res.* 78, 213 (special Issue Abstr # 857).
- Beertsen, W., van den Bos, T., Everts, V., 1999. Root development in mice lacking functional tissue non-specific alkaline phosphatase gene: inhibition of acellular cementum formation. *J. Dent. Res.* 78, 1221–1229.
- Bianco, P., Fisher, L.W., Young, M.F., Termine, J.D., Robey, P.G., 1991. Expression of bone sialoprotein (BSP) in developing human tissues. *Calcif. Tissue Int.* 49, 421–426.
- Bianco, P., 1992. Structure and mineralization of bone. In: Bonucci, E. (Ed.), *Calcification in Biological Systems*. CRC Press, Boca Raton, FL, pp. 244–268.
- Bosshardt, D.D., Zalzal, S., McKee, M.D., Nanci, A., 1998. Developmental appearance and distribution of bone sialoprotein and osteopontin in human and rat cementum. *Anat. Rec.* 250, 13–33.
- Boskey, A.L., 1995. Osteopontin and related phosphorylated sialoproteins: effects on mineralization. *Ann. N.Y. Acad. Sci.* 760, 249–256.
- Boyde, A., Hobdell, M.H., 1969. Scanning electron microscopy of lamellar bone. *Z. Zelforsch. Mikrosk. Anat.* 93, 213–231.
- Bradford, M.M., 1976. A rapid and sensitive method for the quantitation of microgram quantities of protein utilizing the principle of protein-dye binding. *Ann. Biochem.* 72, 248–254.
- Bronckers, A.L., Farach-Carson, M.C., Van Waveren, E., Butler, W.T., 1994. Immunolocalization of osteopontin, osteocalcin, and dentin sialoprotein during dental root formation and early cementogenesis in the rat. *J. Bone Miner. Res.* 9, 833–841.
- Butler, W.T., Ridall, A.L., McKee, M.D., 1996. Osteopontin. In: Bilezikian, J.P., Raisz, L.G., Rodan, G.A. (Eds.), *Principles of Bone Biology*. Academic Press, San Diego, CA, pp. 167–181.
- Chen, J.K., Shapiro, H.S., Wrana, J.L., Reimers, S., Heersche, J.N., Sodek, J., 1991a. Localization of bone sialoprotein (BSP) expression to sites of mineralized tissue formation in fetal rat tissues by *in situ* hybridization. *Matrix* 11, 133–143.
- Chen, J., Zhang, Q., McCulloch, C.A., Sodek, 1991b. Immunohistochemical localization of bone sialoprotein in foetal porcine bone tissues: comparisons with secreted phosphoprotein I (SSP-I, osteopontin) and SPARC (osteonectin). *Histochem. J.* 23, 281–289.
- Chen, J., Shapiro, H.S., Sodek, J., 1992a. Developmental expression of bone sialoprotein mRNA in rat mineralized connective tissues. *J. Bone Miner. Res.* 7, 987–997.
- Chen, Y., Bal, B.S., Gorski, J.P., 1992b. Calcium and collagen binding properties of osteopontin, bone sialoprotein, and bone acidic glycoprotein-75 from bone. *J. Biol. Chem.* 267, 24871–24878.
- Cool, S.M., Forwood, M.R., Campbell, P., Bennett, M.B., 2002. Comparisons between bone and cementum compositions and the possible basis for their layered appearances. *Bone* 30, 386–392.
- Cuisinier, M.J., Glaisher, R.W., Voegel, J.C., Hutchinson, J.L., Brès, E.F., Frank, R.M., 1991. Compositional variations in apatites with respect to preferential ionic extraction. *Ultramicroscopy* 36, 297–305.

- D'Errico, J.A., Berry, J.E., Ouyang, H., Strayhorn, C.L., Windle, J.J., Somerman, M.J., 2000. Employing a transgenic animal model to obtain cementoblasts in vitro. *J. Periodontol.* 71, 63–72.
- Dunbar, B.S., Schwoebel, E.D., 1990. Guide to protein purification. Section XI. Immunological procedures. Preparation of polyclonal antibodies. *Methods Enzymol.* 182, 663–670.
- Fang, Y., Agrawal, D.K., Roy, D.M., 1994. Thermal stability of synthetic hydroxyapatite. In: *Handbook of Bioactive Ceramics*, vol. III. CRC Press, Boca Raton, FL, pp. 269–282.
- Fukayama, S., Tashjian Jr., A.H., 1990. Stimulation by parathyroid hormone of $^{45}\text{Ca}^{2+}$ uptake in osteoblast-like cells: possible involvement of alkaline phosphatase. *Endocrinology* 126, 1941–1949.
- Gorski, J., 1992. Acidic phosphoproteins from bone matrix: a structural rationalization of their role in biomineralization. *Calif. Tissue Int.* 50, 391–396.
- Groeneveld, M.C., Everts, V., Beertsen, W., 1995. Alkaline phosphatase activity in the periodontal ligament and gingiva of the rat molar: its relation to cementum formation. *J. Dent. Res.* 74, 1374–1381.
- Hunter, G.K., Goldberg, H.A., 1993. Nucleation of hydroxyapatite by bone sialoprotein. *Proc. Natl. Acad. Sci. USA* 90, 8562–8565.
- Hunter, G.K., Hauschka, P.V., Poole, R.A., Rosenberg, L.C., Goldberg, H.A., 1996. Nucleation and inhibition of Hydroxyapatite formation by mineralized tissue proteins. *Biochem. J.* 317, 59–64.
- JCPDS, 1995. Joint Committee on Powder Diffraction Standards No. 9-432 file for calcium hydroxyapatite.
- Jono, S., Peinado, C., Giachelli, C.M., 2000. Phosphorylation of osteopontin is required for inhibition of vascular smooth muscle cell calcification. *J. Biol. Chem.* 275, 20197–20203.
- Kagayama, M., Li, H.C., Zhu, J., Sasano, Y., Hatakeyama, Y., Mizoguchi, I., 1997. Expression of osteocalcin in cementoblasts forming acellular cementum. *J. Periodont. Res.* 32, 273–278.
- Kramer, I.R.H., Pindborg, J.J., Shear, M., 1992. In: *Histological Typing of Odontogenic Tumors*. World Health Organization, International Histological Classification of Tumours, second ed. Springer, Berlin, p. 23.
- Linde, A., 1982. On enzymes associated with biological calcification. In: Veis, A. (Ed.), *The Chemistry and Biology of Mineralized Connective Tissue*. Elsevier, New York, pp. 559–570.
- Liu, H.W., Yacobi, R., Savion, N., Narayanan, A.S., Pitaru, S., 1997. A collagenous cementum-derived attachment protein is a marker for progenitors of the mineralized tissue-forming cell lineage of the periodontal ligament. *J. Bone Miner. Res.* 12, 1691.
- Lowry, O.H., Roberts, N.R., Wu, M.-L., Hixon, W.S., Crawford, E.J., 1954. The quantitative histochemistry of brain I. Enzyme measurement. *J. Biol. Chem.* 207, 19–37.
- MacNeil, R.L., Berry, J., D'Errico, J., Strayhorn, C., Piotrowski, B., Somerman, M.J., 1995. Role of two mineral-associated adhesion molecules, osteopontin and bone sialoprotein, during cementogenesis. *Connect. Tissue Res.* 33, 1–7.
- MacNeil, R.L., D'Errico, J.A., Ouyang, H., Berry, J., Strayhorn, C., Somerman, M.J., 1998. Isolation of murine cementoblasts: unique cells or uniquely-positioned osteoblasts? *Eur. J. Oral Sci.* 106 (Suppl. 1), 350–356.
- McAllister, B., Narayanan, A.S., Miki, Y., Page, R.C., 1990. Isolation of a fibroblast attachment protein from cementum. *J. Periodont. Res.* 25, 99–105.
- Nanci, A., 1999. Content and distribution of noncollagenous matrix proteins in bone and cementum: relationship to speed of formation and collagen packing density. *J. Struct. Biol.* 126, 256–269.
- Oldberg, A., Franzen, A., Heinegard, D., 1988. The primary structure of a cell-binding bone sialoprotein. *J. Biol. Chem.* 263, 19430–19432.
- Olson, S., Arzate, H., Narayanan, A.S., Page, R.C., 1991. Cell attachment activity of cementum proteins and mechanism of endotoxin inhibition. *J. Dent. Res.* 70, 1272–1277.
- Pitaru, S., Narayanan, A.S., Olson, S., Savion, N., Hekmati, H., Alt, I., Metzger, 1995. Specific cementum attachment protein enhances selectively the attachment and migration of periodontal cells to root surfaces. *J. Periodont. Res.* 30, 360–368.
- Posner, A.S., 1969. Crystal chemistry of bone mineral. *Physiol. Rev.* 49, 760–792.
- Saito, M., Iwase, M., Maslan, S., Nozaki, N., Yamauchi, M., Handa, K., Takahashi, O., Sato, S., Kawase, T., Teranaka, T., Narayanan, A.S., 2001. Expression of cementum-derived attachment protein in bovine tooth germ during cementogenesis. *Bone* 29, 242–248.
- Roach, H.I., 1994. Why does bone matrix contain non-collagenous proteins? The possible roles of osteocalcin, osteonectin, osteopontin and bonesialoprotein in bone mineralization and resorption. *Cell Biol. Int.* 18, 617–628.
- Serre, C.M., Papillard, M., Chavassieux, P., Voegel, J.C., Boivin, G., 1998. Influence of magnesium substitution on collagen-apatite biomaterial on the production of a calcifying matrix by human osteoblasts. *J. Biomed. Mater. Res.* 42, 626–633.
- Shakibaei, M., 1998. Inhibition of chondrogenesis by integrin antibody in vitro. *Exp. Cell Res.* 240, 95–106.
- Shapiro, H.S., Chen, J., Wrana, J.L., Zhang, Q., Blum, M., Sodek, J., 1993. Characterization of porcine bone sialoprotein: primary structure and cellular expression. *Matrix* 13, 431–440.
- Tesch, W., Vandenbos, T., Roschgr, P., Fratzl-Zelman, N., Klaushofer, K., Beertsen, W., Fratzl, P., 2003. Orientation and mineral crystallites and mineral density during skeletal development in mice deficient in tissue nonspecific alkaline phosphatase. *J. Bone Miner. Res.* 18, 117–125.
- Vandenbos, T., Beertsen, W., 1999. Alkaline phosphatase activity in human periodontal ligament: age effect and relation to cementum growth rate. *J. Periodont. Res.* 34, 1–6.
- van Dijk, K., Schaeken, H.G., Marèe, C.H.M., Verhoeven, J., Wolke, J.C.G., Habraken, F.H.P., Jansen, J.A., 1995. Influence of Ar pressure on r.f. magnetron-sputtered $\text{Ca}_5(\text{PO}_4)_3\text{OH}$ layers. *Surf. Coat. Technol.* 76, 206–210.
- Weismann, H.P., Tkotz, T., Joos, U., Zierold, K., Stratmann, U., Szwart, T., Plate, U., Höhling, H.J., 1997. Magnesium in newly formed dentin mineral of rat incisor. *J. Bone Miner. Res.* 12, 380–383.
- Wu, D., Ikezawa, K., Parker, T., Saito, M., Narayanan, A.S., 1996. Characterization of a collagenous cementum-derived attachment protein. *J. Bone Miner. Res.* 11, 686–692.

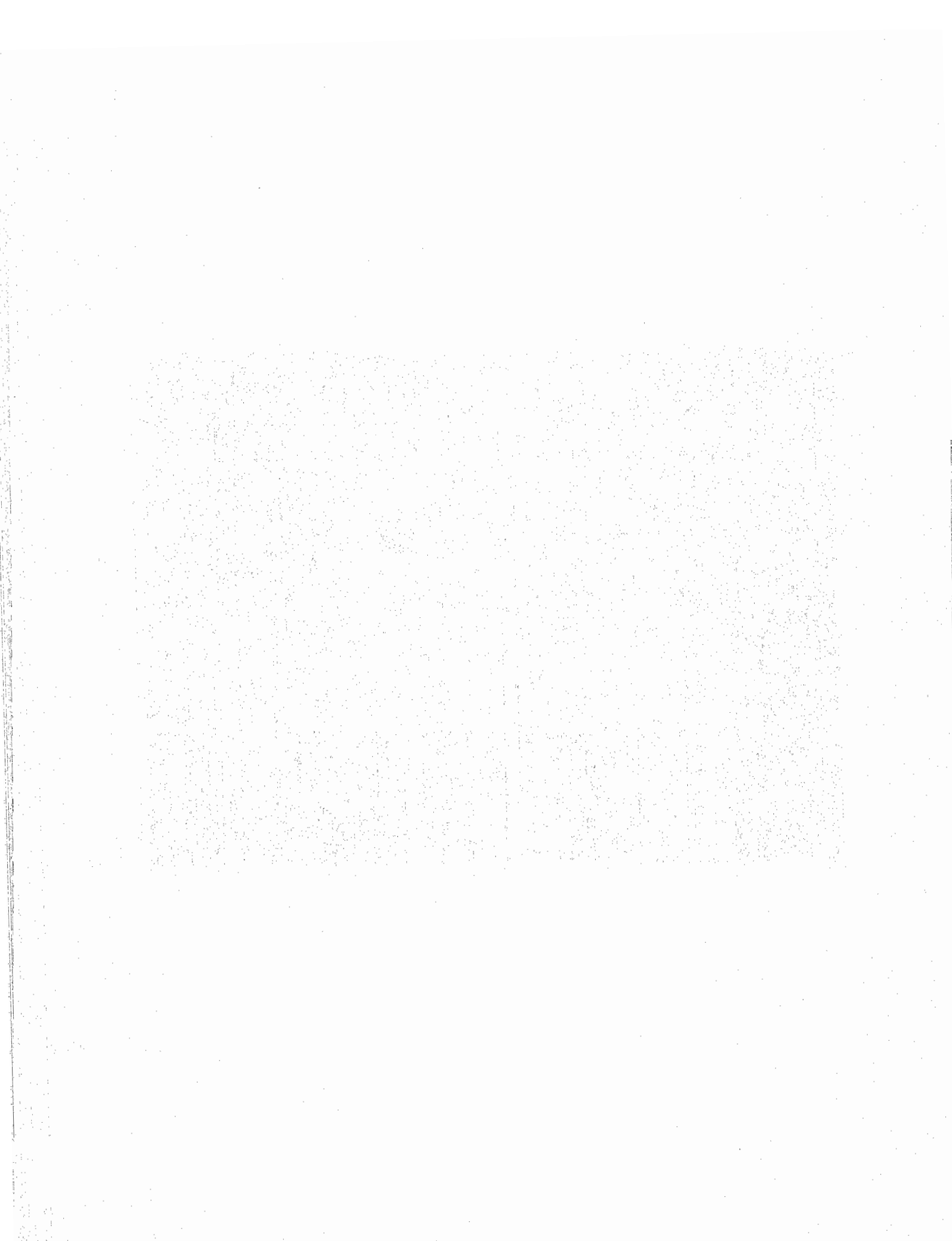




Volume 81 • Number 8 • August 2002

Immunolocalization of a Human Cementoblastoma-conditioned Medium-derived Protein

H. Arzate, L.F. Jiménez-García, M.A. Álvarez-Pérez,
A. Landa, I. Bar-Kana, and S. Pitaru



RESEARCH REPORTS

Biological

H. Arzate^{1*}, L.F. Jiménez-García²,
M.A. Álvarez-Pérez¹, A. Landa³,
I. Bar-Kana⁴, and S. Pitaru⁴

¹Laboratorio de Biología Celular y Molecular, División de Estudios de Posgrado e Investigación, Facultad de Odontología, UNAM, Cd. Universitaria, 04510, México DF, Mexico; ²Departamento de Biología, Facultad de Ciencias, UNAM, Mexico; ³Departamento de Microbiología y Parasitología, Facultad de Medicina, UNAM; and ⁴The Maurice and Gabriela Goldschleger School of Dental Medicine, Tel Aviv University, Israel;
*corresponding author, harzate@servidor.unam.mx

J Dent Res 81(8):541-546, 2002

ABSTRACT

Little is known about the molecular mechanisms that regulate the cementogenesis process, because specific cementum markers are not yet available. To investigate whether a cementoblastoma-conditioned medium-derived protein (CP) could be useful as a cementum biological marker, we studied its expression and distribution in human periodontal tissues, human periodontal ligament, alveolar bone, and cementoblastoma-derived cells. In human periodontal tissues, immunoreactivity to anti-CP was observed throughout the cementoid phase of acellular and cellular cementum, cementoblasts, cementocytes, cells located in the endosteal spaces of human alveolar bone, and in cells in the periodontal ligament located near the blood vessels. Immunopurified CP promoted cell attachment on human periodontal ligament, alveolar bone-derived cells, and gingival fibroblasts. A monoclonal antibody against bovine cementum attachment protein (CAP) cross-reacted with CP. These findings indicate that CP identifies potential cementoblast progenitor cells, is immunologically related to CAP species, and serves as a biological marker for cementum.

KEY WORDS: cementoblasts, cementum protein, periodontium.

Immunolocalization of a Human Cementoblastoma-conditioned Medium-derived Protein

INTRODUCTION

Cementum is the calcified tissue that covers the root surfaces of teeth. Two types of cementum are recognized, acellular and cellular, based on the presence or absence of cells and the source of collagen fibers (Bosshardt and Schroeder, 1996). The cementum matrix contains collagen types I and III (Christner *et al.*, 1977) and non-collagenous proteins such as fibronectin (FN) (Daculsi *et al.*, 1999), osteocalcin, vitronectin (MacNeil *et al.*, 1995), osteopontin (OPN), and bone sialoprotein (BSP) (D'Errico *et al.*, 1997). However, these molecules are not cementum-specific. Because cementum lacks specific markers and resembles bone, it has not been possible to identify and isolate cementoblastic populations *in vivo* or *in vitro*. Recent studies suggest that cementum may contain unique molecules that are specific for this tissue (McAllister *et al.*, 1990). One such molecule is the cementum attachment protein (CAP). CAP is a 56-kDa protein that has been purified from human and bovine cementum (Olson *et al.*, 1991) and characterized as a collagen-like protein (Wu *et al.*, 1996). Monoclonal antibodies raised against CAP species stain positively putative cementoblastic cell populations *in vitro* (Liu *et al.*, 1997; Bar-Kana *et al.*, 1998, 2000), the cementoid layer, and the adjacent cementoblastic cell layer *in vivo* (Arzate *et al.*, 1992a). CAP has been shown to promote several biological activities, such as cell attachment, chemotaxis, and differentiation (Olson *et al.*, 1991; Pitaru *et al.*, 1995; Arzate *et al.*, 1996).

Recently, a new cell line with cementoblastic characteristics was established from a human cementoblastoma tumor (Arzate *et al.*, 1998). This cell line has been shown to express CAP and to form mineralized tissue *in vitro* similar to human cementum (Arzate *et al.*, 1998, 2000). These findings indicated that the cementoblastoma cell line produces a 56-kDa protein species, that this species is CAP or a related molecule, and that it can act as an antigen for producing new antibodies capable of recognizing cementoblastic populations *in vivo* and *in vitro*. The purpose of this investigation was to test this hypothesis and to use the new antibody as a cementum biological marker.

MATERIALS & METHODS

The procedures to obtain human cementoblastoma, periodontal ligament, gingiva, and alveolar bone specimens were approved by the Review Board of the School of Dentistry, National Autonomous University of Mexico. Informed consent was obtained from all patients. The protocol was reviewed and approved by the Animal Care Committee of the National Autonomous University of Mexico. Human autopsy specimens used in this study were obtained from a 29-year-old man in conformity with the policy of the Research Review Board, National Cancer Institute, Mexico City.

Received August 14, 2001; Last revision June 11, 2002;
Accepted June 17, 2002

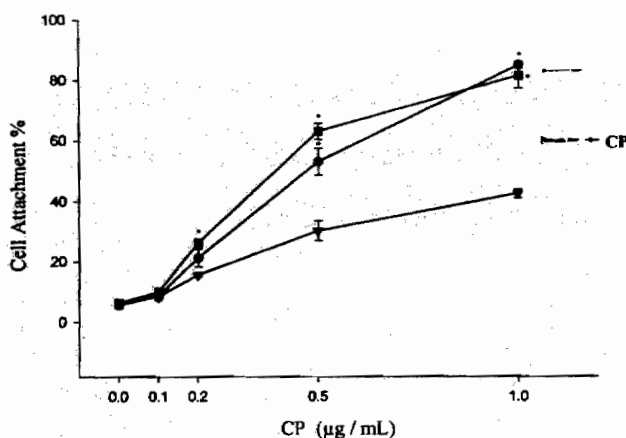


Figure 1. Attachment of periodontal ligament cells, alveolar bone-derived cells, and gingival fibroblasts to protein(s) bound to an anti-CP column. Cementoblastoma-derived cells conditioned medium (500 mL) were used for CP purification. Attachment activity at different protein concentrations is shown. Silver-stained gel showed protein(s) from cementoblastoma-derived cells present in conditioned medium which bound to an anti-CP column. Arrow indicates CP migration. Periodontal ligament cells ■, alveolar bone-derived cells ●, and gingival fibroblasts ▼. Asterisk (*) indicates significant differences in cell attachment between periodontal ligament and alveolar bone-derived cells vs. gingival fibroblasts at $P < 0.05$.

Antibody Preparation

Partially purified CP preparation containing CP migrating with $56,000 M_r$ was obtained by electro-elution, as described previously (Arzate et al., 1996). New Zealand rabbits were immunized as described by Dunbar and Schwobel (1990). Antibody production was monitored through ELISA and immunoblot. IgG antibodies were purified through protein A-sepharose chromatography (Sigma Chemical Co., St. Louis, MO, USA). The antibody fraction will be referred to as anti-CP antibody.

Cell Culture

Human alveolar bone and cementoblastoma-derived cells were obtained as previously described (Arzate et al., 1998). Human periodontal ligament and gingival fibroblasts were obtained from a premolar extracted for orthodontic reasons from a 25-year-old male patient. Cells were cultured by the conventional explant technique (Narayanan and Page, 1976). Cells were grown in DMEM medium supplemented with 10% FBS. All cell types from the 2nd passage were used for the experimental procedures.

Immunoaffinity Chromatography and Immunoblotting of CP

A 500-mL quantity of conditioned medium was collected from plates of each cell type containing cells at confluent density, and CP was immunopurified as described previously (Arzate et al., 1992b). Protein concentrations were determined by means of the Nano Orange Protein Assay Kit (Molecular Probes, Eugene, OR, USA). Cross-reactivity and expression of CP in human cementoblastoma, periodontal ligament cells, and alveolar bone-derived cells were assessed by immunoblotting as previously described (Arzate et al., 1992b), except that anti-CP antibody was used at a 1:300 dilution. For assessment of the specificity of anti-CP antibody, calf skin type I collagen (Boehringer Mannheim, Germany), bovine FN (Life Technologies, Rockville, MD, USA), and human bone extract were

blotted and tested with anti-CP antibody. Antibodies against bovine type I collagen, FN, OPN, and BSP served as controls. To determine the uniqueness of the CP, we performed immunoblots with polyclonal antibodies against rat type I collagen (Chemicon International Inc., Temecula, CA, USA), human OPN (LF-123), human BSP (LF-100), both a gift from Dr. Larry W. Fisher (NIH, Bethesda, MD, USA), and human FN (Dako, Glostrup, Denmark). Immunoblots with anti-CP antibody were compared with those with a monoclonal antibody against bovine CAP (3G9), a gift from Dr. A.S. Narayanan (Seattle WA, USA).

Cell Attachment Assay

Periodontal ligament, alveolar bone-derived cells, and gingival fibroblasts were plated at 2×10^4 density on 24-multiwell Costar plates not treated for tissue culture (Costar Corp., Cambridge, MA, USA) and coated with 1.0, 0.5, 0.2, and 0.1 $\mu\text{g}/\text{mL}$ of immunoaffinity-purified CP. Cell attachment was evaluated according to Hayman et al. (1982). Wells coated with 5 $\mu\text{g}/\text{mL}$ of calf skin type I collagen served as a positive control, and serum-free medium was the negative control.

Processing and Immunostaining of Human Tissues

Specimens were fixed in 10% formaldehyde. Hard tissues were decalcified with 10% EDTA, pH 7.4, dissolved in 0.5% formaldehyde at 4°C for 5 wks, and processed as previously described (Arzate et al., 1998).

Longitudinal and transverse sections 5 μm thick were cut and mounted in 2% 3-aminopropyltriethoxysilane-coated glass slides (Sigma Chemical Co., St. Louis, MO, USA). Sections were de-waxed in xylene and, before complete rehydration, were incubated with antigen retrieval solution as described by Shi et al. (1992). Immunocytochemical procedures were as described elsewhere (Arzate et al., 1998).

Immunostaining of Human Cementoblastoma, Periodontal Ligament, and Alveolar Bone-derived cells *in vitro*

Human cementoblastoma, periodontal ligament, alveolar bone-derived cells, and gingival fibroblasts were plated at low density (5×10^2) on Lab-Tek chamber slides (Life Technologies, Rockville, MD, USA) allowed to attach overnight, and cultured for 3 days. Rabbit pre-immune serum or slides lacking first antibody were used as negative controls. Experiments were done in triplicate. We determined the number of cells cross-reacting with anti-CP antibody by scoring 5 different microscopic fields with a 20X lens.

Statistical Analysis

Cell attachment was expressed as % relative to positive control (type I collagen). Experiments were run in triplicate. We used one-way ANOVA to test variability and performed Tukey's test to assess statistical significance at a level of $P < 0.05$ ($n = 3$). Experimental data for the immunostaining of human cementoblastoma, periodontal ligament, and alveolar bone-derived cells *in vitro* are presented as mean ($n = 5$) \pm SE of 3 independent experiments.

RESULTS

Cell Attachment Assay

As shown in Fig. 1, the attachment of periodontal ligament cells, alveolar bone-derived cells, and gingival fibroblasts to plates incubated with immunopurified CP was dose-dependent. The number of periodontal ligament cells attaching to 0.1, 0.2, 0.5, and 1.0 $\mu\text{g}/\text{mL}$ of CP represented 10, 26, 63, and 86%,

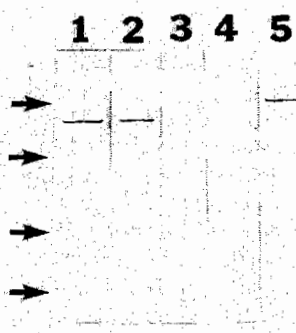


Figure 2. Immunoblotting of immunoadsorbed fractions with anti-CP polyclonal antibody. **Lane 1:** Immunoadsorbed conditioned medium from cementoblastoma-derived cells conditioned medium (0.9 µg/500 mL) showed an intense 56-kDa species cross-reacting with anti-CP antibody. **Lane 2:** Periodontal ligament cells immunoadsorbed conditioning medium (0.4 µg/500 mL) expressed the 56-kDa protein. **Lane 3:** Alveolar bone-derived cells conditioning medium (0.1 µg/500 mL) did not cross-react with the 56-kDa species. **Lane 4:** Control for human serum was negative. **Lane 5:** Immunoadsorbed conditioning medium from cementoblastoma-derived cells showed that a 70-kDa band cross-reacted with a monoclonal antibody (3G9) raised against bovine CAP. From top to bottom, arrows indicate the migration of protein standards of 68, 44, 32, and 22 kDa, respectively.

respectively, relative to the positive control cultures, alveolar bone cells represented 8, 21, 53, and 89%, and gingival fibroblasts 8, 16, 30, and 42%. No statistical differences were observed between periodontal ligament cells and alveolar bone-derived cells. However, gingival fibroblast attachment was significantly lower at 0.2, 0.5, and 1.0 µg/mL of CP when compared with periodontal ligament cells and alveolar bone-derived cells ($P < 0.05$).

Immunoblotting

Specificity of the anti-CP antibody was tested by immunoblotting (Fig. 2). Anti-CP antibody cross-reacted with a single band of 56 kDa in protein(s) obtained from immunoadsorbed conditioned medium of cementoblastoma cells (lane 1). Immunoadsorbed protein(s) obtained from periodontal ligament cell conditioned medium immunoreacted positively (lane 2). Alveolar bone-derived cells immunoadsorbed conditioned medium (lane 3) and human serum (lane 4) were negative. There was no cross-reactivity of the anti-CP antibody

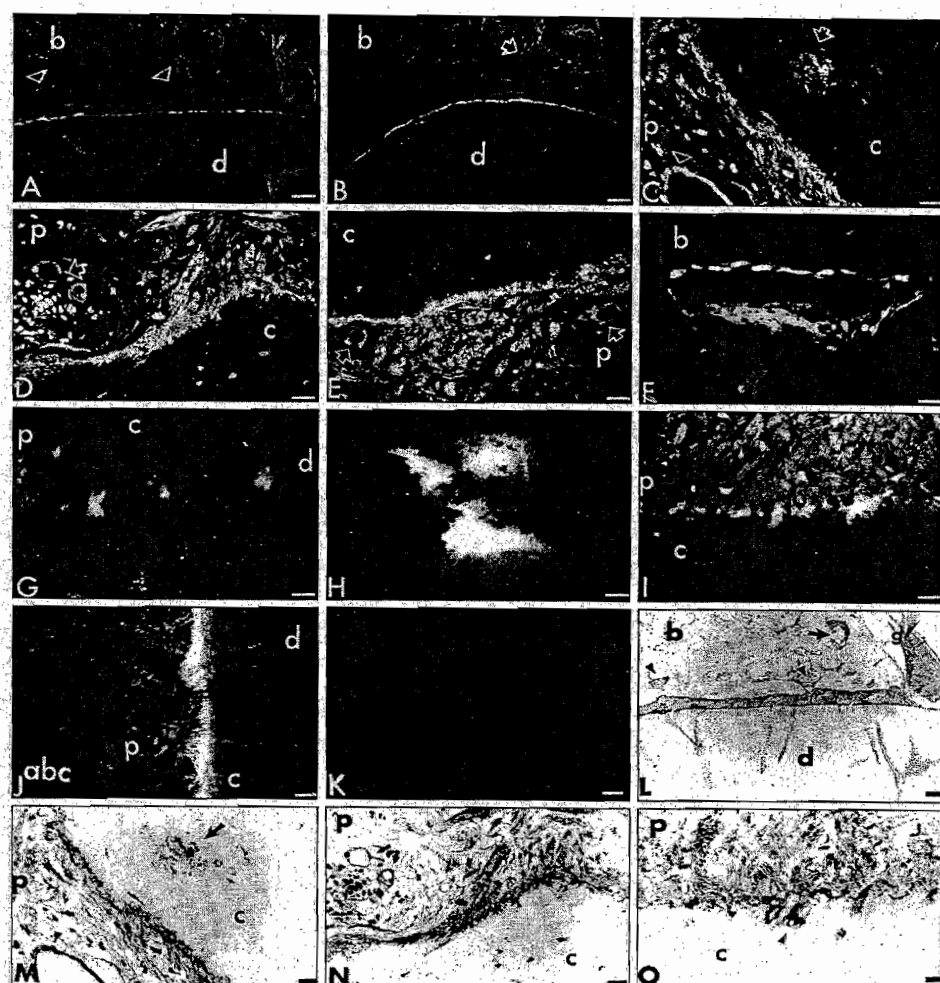


Figure 3. Immunostaining of CP in human periodontal tissues. **[A]** Longitudinal section of a human tooth. Cementoid surface is strongly stained. Open vascular channels and endosteal spaces in alveolar bone are positive (arrowheads and arrow, respectively). **[B]** Transverse section of a human tooth shows both cementoid and bone endosteal spaces stained positive. **[C]** A few periodontal ligament cells are positive as well as cementoblasts lining the cellular cementum. Cells located adjacent to the periodontal ligament blood vessels are strongly positive (arrowhead). A cementocyte with cytoplasmic elongations localized within the cellular cementum is shown to be positive (arrow). **[D,E]** Colony-like cell formation (possibly pre-cementoblasts) in the vicinity of blood vessels (arrow). **[F]** Cells surrounding endosteal spaces in alveolar bone cross-reacted strongly to anti-CP antibody. **[G]** Cementocytes inside the cementum matrix are positive. **[H]** Higher magnification of strongly labeled cementocytes showing cytoplasmic processes interconnecting them. **[I]** Cementoblasts just becoming embedded in the cementum matrix cross-reacted more strongly than periodontal ligament cells and pre-cementoblasts. **[J]** Acellular cementum was strongly stained with anti-CP antibody. **[K]** Control using pre-immune rabbit serum was negative. Histological H & E-stained sections show longitudinal aspects of periodontal structures: open vascular channels (arrowheads), endosteal spaces in alveolar bone (arrow) (**L**), a cementocyte, and periodontal ligament blood vessel (**M**). Cells representing pre-cementoblasts located in the vicinity of periodontal ligament blood vessels (**N**), and a cementoblast becoming embedded in cementum matrix (arrowhead) (**O**).

with type I collagen, FN, OPN, and BSP (data not shown). Immunoblots with immunoadsorbed CP did not cross-react with antibodies against type I collagen, OPN, BSP, and FN (not shown). The monoclonal antibody against bovine CAP recognized a 70-kDa species in CP preparation (lane 5).

Immunostaining of Human Periodontal Structures

The immunostaining of human periodontal tissue sections revealed that CP expression was localized to the cementoid

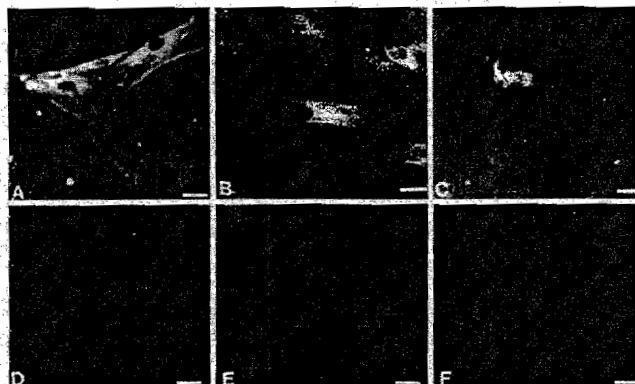


Figure 4. Photomicrographs showing localization of CP in cementoblastoma-derived cells. Positive immunostaining of CP in cementoblastoma-derived (A) and periodontal ligament cells (B). Alveolar bone-derived cells staining appears close to the background levels (C). Controls using pre-immune rabbit serum were negative for the 3 cell types (D, E, and F for cementoblastoma, periodontal ligament cells, and alveolar bone-derived cells, respectively). Magnification 20X. Bar = 100 μ m.

phase of the acellular and cellular cementum (Figs. 3A, 3B). A few spindle-shaped periodontal ligament cells located close to a blood vessel in the region of cellular cementum as well as cementoblasts lining the cementum surface were positive (Fig. 3C). Cell clusters located between blood vessels and 1-3 cell layers from the cementoblast layer stained more intensely than the neighboring periodontal ligament cells (Figs. 3D, 3E). Elongated cells located within the endosteal spaces of the alveolar bone exhibited strong positive staining (Fig. 3F). Cementocytes embedded in the cellular cementum mineralized matrix and those close to the cementum-dentin junction were positive (Fig. 3G). Cementocytes in their lacunae and their interconnecting cytoplasmic processes showed strong immunostaining (Fig. 3H). Cells representing a transitory stage between cementoblasts and cementocytes just becoming embedded in the calcified cementum matrix were observed in cellular cementum. These cells stained more intensely than cells present in the periodontal ligament (Fig. 3I). Acellular cementum (cementoid layer) was intensely stained (Fig. 3J). Control sections where pre-immune rabbit serum was used were negative (Fig. 3K). Other human tissues, such as brain, liver, large intestine, pancreas, kidney, spleen, aorta, tendon, femur, rib, and osteosarcoma, immunoscreened for the expression of CP, revealed no significant immunofluorescence (not shown).

Immunostaining of Cementoblastoma, Periodontal Ligament, and Alveolar Bone-derived Cells *in vitro*

Intense immunoreactivity of CP was observed in the cytoplasm and on the cell surfaces of cementoblastoma-derived cells (Fig. 4A). Positive cells represented approximately 95% (94.7 ± 2.6). In periodontal ligament cell cultures, $5.8 \pm 0.9\%$ cells stained with the anti-CP antibody (Fig. 4B). Cultures of alveolar bone-derived cells were largely negative, and they contained $3.4 \pm 0.6\%$ positive cells (Fig. 4C). Gingival fibroblasts were negative (not shown). Negative controls where non-immune sera were used as a first antibody were negative (Figs. 4D, 4E, 4F for cementoblastoma, periodontal ligament, and alveolar bone-derived cells, respectively).

DISCUSSION

The results of this study indicate that cementoblastoma-derived cells produce a 56-kDa protein. CP was shown to promote attachment of periodontal ligament cells, alveolar bone-derived cells, and gingival fibroblasts in a dose-dependent manner. The 56-kDa protein purified from cementoblastoma-derived cells conditioned medium was used to produce an anti-CP antibody. This antibody did not cross-react at the immunoblotting level with any major extracellular matrix component of periodontal tissues, namely, collagen type I, FN, BSP, and OPN. None of the osteogenic and non-osteogenic human tissues cross-reacted with the anti-CP antibody. Furthermore, antibodies against FN, OPN, BSP, and collagen type I did not cross-react with CP preparation, indicating that cell attachment is due to CP. These findings point to the specificity of the anti-CP antibody to cementum and cementoblastic lineage.

Anti-CAP monoclonal antibodies have been shown to recognize the cementoid phase of human cementum as well as a few cells located within the endosteal spaces of human alveolar bone (Arzate *et al.*, 1992a). The present study demonstrated that CP is distributed throughout the entire root surface, including cellular and acellular cementum. The CP antibody positively stained cells located near the blood vessels in the periodontal ligament. In certain areas, clumps of positively stained cells which were localized between the blood vessels and active cementoid formation were observed. These clumps may represent expanding clones of the cementoblastic lineage. This assumption is further supported by a series of previous reports. First, the work of McCulloch and Melcher (1983) indicates that the progenitor pool in the periodontal ligament is located in the paravascular zone, whence cells migrate toward their target tissues, cementum, alveolar bone, and periodontal ligament. Second, the works of Liu *et al.* (1997) and Bar-Kana *et al.* (2000) demonstrated that there was a direct correlation between the capacity of periodontal ligament-derived progenitor clones to bind CAP and express CAP in culture and their capacity to produce mineralized cementum-like tissue *in vitro*. Analysis of these collective data suggests that the cementoblastic lineage expresses CP during its growth and maturation, both *in vitro* and *in vivo*, and that CP might be a key factor in these processes. This concept is supported by the findings of McCulloch (1985), McCulloch *et al.* (1987), Melcher *et al.* (1987), and Lang *et al.* (1995), who demonstrated that cells from the endosteal spaces of the alveolar bone migrate through vascular channels into the periodontal ligament and contribute to the paravascular pool. They also showed that alveolar bone-derived cells are capable of forming cementum-like tissue *in vitro* and *in vivo*, suggesting that at least some of the early progenitors of the cementoblastic lineage originate in the endosteal spaces of the alveolar bone.

In the present study, we found that 3% of alveolar bone cells stained positively for CP *in vitro*, and that some cells lining the endosteal spaces of the alveolar bone and the vascular channels also stained positively for CP. If it is assumed that CP is a marker for the cementoblastic lineage, then the results of our study strengthen the hypothesis that progenitors originating in the alveolar bone contribute to the cementoblastic lineage.

In the cementoid phase, cementoblasts just becoming embedded in the cementum matrix and cementocytes stained more intensely than the cementoblasts lining the cementum, indicating that cementum matrix formation and maturation are associated with CP synthesis and secretion. Since the calcification of cementum has been postulated to be under the control of cementoblasts lining the cementum and freshly embedded cementocytes, it is possible that CP plays an important role in the mineralization process of cementum.

Western blots showed that conditioned medium from cementoblastoma cells and periodontal ligament cells contained an antigen that cross-reacted with anti-CP antibody. However, this antigen was not detected in alveolar bone cell medium. This may be due to the small amount of protein loaded on gels. The poor yield from immunoaffinity chromatography may reflect low levels of CP production in these cultures, and that only 3% of the cells produce CP (Fig. 4C). Nevertheless, these results indicate that osteoblasts and osteocytes do not express CP protein, *in vivo* and *in vitro*, and that cementoblasts and osteoblasts are therefore phenotypically different. This statement is supported by recent findings which revealed that the mineralized matrix deposited by putative cementoblasts is morphologically, compositionally, and ultrastructurally different from that deposited by human alveolar bone-derived cells *in vitro* and human bone marrow stromal cells (Arzate *et al.*, 1998, 2000; Grzesik *et al.*, 2000). Analysis of these data, together with our previous work on this cell line, demonstrates that cell populations with cementoblastic phenotype have the capacity to produce a protein (CP) that is immunologically related to CAP, since a monoclonal antibody against CAP cross-reacted with CP as a 70-kDa species. However, at this point it is not clear whether the difference in molecular size between these two species is due to differences in post-translational processing of the protein or whether the 70-kDa species is the precursor of CP. Since other molecules such as BSP have multiple molecular forms (Mintz *et al.*, 1993) and CAP has also been reported as a 65-kDa species in the developing tooth germ (Saito *et al.*, 2001), the possibility that CP and CAP could be related molecules appears valid. In summary, these studies demonstrate that CP is widely distributed throughout cementum, has the capacity to identify putative cementoblastic populations both *in vivo* and *in vitro*, and is immunologically related to CAP. Our studies also indicate that antibodies to CP could be useful to identify these populations and to elucidate the cellular and molecular mechanisms that control cementogenesis during homeostasis and wound healing.

ACKNOWLEDGMENTS

This study is supported in part by grants from DGAPA-UNAM IN200599, IN200501, and CONACyT 30735-M.

REFERENCES

- Arzate H, Olson SW, Page RC, Gown AM, Narayanan AS (1992a). Production of a monoclonal antibody to an attachment protein derived from human cementum. *FASEB J* 6:2990-2995.
- Arzate H, Olson SW, Page RC, Narayanan AS (1992b). Isolation of human tumor cells that produce cementum proteins in culture. *Bone Miner* 18:15-30.
- Arzate H, Chimal-Monroy J, Hernández-Lagunas L, Díaz de León L (1996). Human cementum protein extract promotes chondrogenesis and mineralization in mesenchymal cells. *J Periodontal Res* 31:144-148.
- Arzate H, Álvarez-Pérez MA, Aguilar-Mendoza ME, Álvarez-Fregoso O (1998). Human cementum tumor cells have different features from human osteoblastic cells *in vitro*. *J Periodontal Res* 33:249-258.
- Arzate H, Álvarez-Pérez MA, Álvarez-Fregoso O, Wusterhaus-Chávez A, Reyes-Gasga J, Ximénez-Fylie LA (2000). Electron microscopy, micro-analysis and x-ray diffraction characterization of the mineral-like tissue deposited by human cementum tumor-derived cells. *J Dent Res* 79:28-34.
- Bar-Kana I, Savion N, Narayanan AS, Pitaru S (1998). Cementum attachment protein manifestation is restricted to the mineralized tissue forming cells of the periodontium. *Eur J Oral Sci* 106(Suppl 1):357-364.
- Bar-Kana I, Narayanan AS, Grosskopf A, Savion N, Pitaru S (2000). Cementum attachment protein enriches putative cementoblastic populations on root surfaces *in vitro*. *J Dent Res* 79:1482-1488.
- Bosshardt DD, Schroeder H (1996). Cementogenesis reviewed: a comparison between human premolars and rodent molars. *Anat Rec* 245:267-292.
- Christner P, Robinson P, Clark CC (1977). A preliminary characterization of human cementum collagen. *Calcif Tissue Res* 23:147-150.
- D'Errico JA, MacNeil RL, Takata T, Berry J, Strayhorn C, Somerman MJ (1997). Expression of bone associated markers by tooth root lining cells, *in situ* and *in vitro*. *Bone* 20:117-126.
- Daculsi G, Pilet P, Cottrel M, Guicheux G (1999). Role of fibronectin during biological apatite crystal nucleation: ultrastructural characterization. *J Biomed Mater Res* 47:228-233.
- Dunbar BS, Schwoebel ED (1990). Preparation of polyclonal antibodies. *Meth Enzymol* 182:663-670.
- Grzesik WJ, Cheng H, Oh JS, Kuznetsov SA, Mankani MH, Uzawa K, *et al.* (2000). Cementum-forming cells are phenotypically distinct from bone-forming cells. *J Bone Miner Res* 15:52-59.
- Hayman EG, Engvall E, A'Hearn E, Barnes D, Pierschbacher M, Ruoslahti E (1982). Cell attachment on replicas of SDS polyacrylamide gels reveals two adhesive plasma proteins. *J Cell Biol* 95:20-23.
- Lang H, Schuler N, Arnhold S, Nolden R, Meertens T (1995). Formation of differentiated tissues *in vivo* by periodontal cell populations cultured *in vitro*. *J Dent Res* 74:1219-1225.
- Liu HW, Yacobi R, Savion N, Narayanan AS, Pitaru S (1997). A collagenous cementum-derived attachment protein is a marker for progenitors of the mineralized tissue-forming cell lineage of the periodontal ligament. *J Bone Miner Res* 12:1691-1699.
- MacNeil RL, Berry J, D'Errico J, Strayhorn C, Piotrowski B, Somerman MJ (1995). Role of two mineral-associated adhesion molecules, osteopontin and bone sialoprotein, during cementogenesis. *Connect Tissue Res* 33:1-7.
- McAllister B, Narayanan AS, Miki Y, Page RC (1990). Isolation of a fibroblast attachment protein from cementum. *J Periodontal Res* 25:99-105.
- McCulloch CA (1985). Progenitor cell populations in the periodontal ligament of mice. *Anat Rec* 211:258-262.
- McCulloch CA, Melcher AH (1983). Cell density and cell generation in the periodontal ligament of mice. *Am J Anat* 167:43-58.
- McCulloch CA, Nemeth E, Lowenberg B, Melcher AH (1987). Paravascular cells in endosteal spaces of alveolar bone contribute to periodontal ligament cell populations. *Anat Rec* 219:233-242.

- Melcher AH, McCulloch CA, Cheong T, Nemeth E, Shiga A (1987). Cells from bone synthesize cementum-like and bone-like tissue *in vitro* and migrate into periodontal ligament *in vivo*. *J Periodontal Res* 22:246-247.
- Mintz KP, Grzesik WJ, Midura RJ, Robey PG, Termine JD, Fisher LW (1993). Purification and fragmentation of nondenatured bone sialoprotein: evidence for a cryptic, RGD-resistant cell attachment domain. *J Bone Miner Res* 8:985-995.
- Narayanan AS, Page RC (1976). Biochemical characterization of collagens synthesized by fibroblasts derived from normal and diseased human gingiva. *J Biol Chem* 251:5464-5471.
- Olson S, Arzate H, Narayanan AS, Page RC (1991). Cell attachment activity of cementum proteins and mechanism of endotoxin inhibition. *J Dent Res* 70:1272-1277.
- Pitaru S, Narayanan AS, Olson S, Savion N, Hekmati H, Alt I, et al. (1995). Specific cementum attachment protein enhances selectively the attachment and migration of periodontal cells to root surfaces. *J Periodontal Res* 30:360-368.
- Saito M, Iwase M, Maslan S, Nozaki N, Yamauchi M, Handa K, et al. (2001). Expression of cementum-derived attachment protein in bovine tooth germ during cementogenesis. *Bone* 29:242-248.
- Shi SR, Cote C, Kalra KL, Taylor CL, Tandon AK (1992). A technique for retrieving antigens in formalin-fixed, routinely acid-decalcified, celloidin-embedded human temporal bone sections for immunohistochemistry. *J Histochem Cytochem* 40:787-792.
- Wu D, Ikezawa K, Parker T, Saito M, Narayanan AS (1996). Characterization of a collagenous cementum-derived attachment protein. *J Bone Miner Res* 11:686-692.

RESEARCH REPORTS

Biomaterials & Bioengineering

H. Arzate^{1*}, M.A. Alvarez-Pérez², O. Alvarez-Fregoso³, A. Wusterhaus-Chávez⁴, J. Reyes-Gasga⁵, and L.A. Ximénez-Fyvie¹

¹Laboratorio de Biología Celular y Molecular, División de Estudios de Posgrado e Investigación, Facultad de Odontología, UNAM, Cd. Universitaria, 04510 México DF; ²Instituto de Fisiología Celular, UNAM, México; ³Instituto de Investigación en Materiales, UNAM, México; ⁴CMN "20 de Noviembre", ISSSTE, México; and ⁵Instituto de Física, UNAM, México;

*corresponding author, harzate@servidor.unam.mx

J Dent Res 79(1): 28-34, 2000

ABSTRACT

The nature and characteristics of the mineralized-like tissue deposited by cementoblasts are not well-known due to the difficulties in obtaining and culturing cells representing the cementum phenotype. We hypothesized that a putative cementoblastic cell line derived from a human cementoblastoma could serve as a suitable model to study the physical, chemical, and morphological features of the cementum-like tissue deposited *in vitro*. The cementoblastoma cell line was studied by transmission electron, high resolution, scanning, and atomic force microscopy and compared with human cellular cementum, human osteoblasts, and human alveolar bone. The analyses of the crystals and mineral-like tissue in the cell line were performed by x-ray diffraction microscopy and energy-dispersive x-ray micro-analysis. TEM examination of cementoblastoma cells revealed the presence of electron-dense intracellular vesicles surrounded by a membrane that contained filaments and needle-like structures. The diffraction patterns obtained from the intracellular material and human cellular cementum were similar, with D-spacings of 3.36 and 2.8, consistent with those of hydroxyapatite (3.440 and 2.814). The composition of the mineral-like tissue had a Ca/P ratio of 1.60 for cementoblastoma cells and 1.97 for human cellular cementum. Na (5.29%) and Cl (1.47%) were present in the composition of cementoblastoma cells. Human cellular cementum additionally contained Mg (4.95%). Osteoblastic cells showed a Ca/P ratio of 1.6280. Na represented 4.52% and Cl 1.22% of its composition. Human alveolar bone had a Ca/P ratio value of 2.01. Na (6.63%), Mg (2.10%), and Cl (0.84%) were also present. All samples examined represented biological-type hydroxyapatite. Based on the compositional and morphological features, these findings indicate that cementoblastoma-derived cells express the human cellular cementum phenotype.

KEY WORDS: cementoblast, osteoblast, mineralization, hydroxyapatite, and cell culture.

Received November 12, 1998; Last Revision June 3, 1999;
Accepted June 4, 1999

Electron Microscopy, Micro-analysis, and X-ray Diffraction Characterization of the Mineral-like Tissue Deposited by Human Cementum Tumor-derived Cells

INTRODUCTION

Cementoblasts are believed to be derived from multipotential stem cells in the endosteal spaces of the paravascular vessels of the alveolar bone (McCulloch *et al.*, 1987). These stem cells have the capacity of self-renewal and, under the influence of unknown factors, are thought to give rise to progenitors of each cell type that comprise the periodontium, such as osteoblasts, cementoblasts, and periodontal ligament fibroblasts (Gould *et al.*, 1977). Cementoblast progenitor cells have been found in the paravascular zones in the adult periodontal ligament of mice (McCulloch *et al.*, 1983; Melcher *et al.*, 1987), although mice do not constitute a parallel model for the study of cementogenesis in humans (Bosshardt and Schroeder, 1996).

Cells representing the cementum phenotype have not been isolated and propagated in culture, due in part to the lack of a cementum biological marker and in part to the technical difficulties in obtaining a pure population of cementoblasts. The conditions necessary to isolate cementoblasts have not yet been established, although several attempts have been made to obtain a population of cementoblasts and culture them *in vitro* (Arzate *et al.*, 1992a; D'Errico *et al.*, 1997; Grzesik *et al.*, 1998; MacNeil *et al.*, 1998). We recently proposed an alternative approach to obtain cells that express the cementoblast phenotype. Cells from a human cementoblastoma were isolated. This cell line may represent a cloned cell population of human cementoblasts. Preliminary *in vitro* studies have shown that these cells expressed several markers associated with mineral tissue formation, such as alkaline phosphatase (ALP) and osteopontin (OPN). Importantly, the cementoblastoma-derived cells expressed cementum attachment protein (CAP), which is restricted to cementum (Arzate *et al.*, 1992b). The preliminary data showed that cementoblastoma-derived cells deposited mineral-like tissue *in vitro* and had characteristics different from those of human alveolar bone cells *in vitro* (Arzate *et al.*, 1998).

Since very little is known about the nature of the mineralized-like tissue produced by cultured putative cementoblasts, this present work was designed to study the ultrastructural characteristics of cementoblastoma-derived cells and to investigate both the characteristics and the nature of the mineral-like tissue formed by these cells. The findings were compared with those of human cellular cementum, human osteoblastic-derived cells, and human alveolar bone. The characterization and analysis were performed by transmission electron microscopy (TEM), high-resolution transmission electron microscopy (HRTEM), scanning electron microscopy (SEM), atomic force microscopy (AFM), energy-dispersive x-ray micro-analysis (EDX), and x-ray diffraction microscopy (XRD).

MATERIALS & METHODS

Cell Culture

Human cementoblastoma and alveolar bone specimens were obtained according to the protocols approved by the Internal Review Board of the School of Dentistry, National Autonomous University of México. Human alveolar bone and

cementoblastoma-derived cells were obtained from a 38-year-old male patient with a mandibular cementoblastoma. The osteoblastic and cementoblastoma-derived cells were cultured by the explant technique described elsewhere (Narayanan and Page, 1976). Cells were cultured in Dulbecco's modified Eagle's medium (DMEM) (Sigma Chem. Co., St. Louis, MO, USA) supplemented with 10% fetal bovine serum (FBS) and antibiotic solution (penicillin 100 U/mL, streptomycin 100 µg/mL). Confluent monolayers of cells were passaged by trypsinization (Trypsin-EDTA, Gibco Laboratories, Grand Island, NY, USA), washed with full medium, and recultured in 75-cm² tissue culture flasks in a humidified incubator at 37°C in an atmosphere of 5% CO₂ and air. Cells at the 2nd passage were used for all experimental procedures.

Atomic Force Microscopy (AFM)

AFM was used to determine the morphology and homogeneity of the mineral-like tissue deposited by cementoblastoma-derived and osteoblastic cells. AFM (Park Scientific Instruments, Santa Barbara, CA, USA) was used with an AutoProbe in contact and constant mode (5 nanometers). Cementum tumor and osteoblastic cells were plated at 2×10^4 in 24-well culture plates (Costar Corporation, Cambridge, MA, USA) onto a silicon (1,1,1) monocrystal substrate and cultured for 14 days in DMEM supplemented with 10% FBS, antibiotics, 50 µg/mL ascorbic acid, 10 mM of β-glycerophosphate, and 10⁻⁷ M dexamethasone. We monitored the cultures at 3, 7, and 11 days to detect calcium salt precipitation in the cultures by using Alizarin red S staining at pH 4.1. The medium was changed every other day. After 14 days of incubation, osteoblastic and cementoblastoma-derived cells were rinsed three times with ice-cold phosphate-buffered saline (PBS); culture plates were fixed *in situ* by the addition of 70% ethyl alcohol and air-dried. To reveal similarities between the human cementum tumor cell cultures and human cementum, we processed a piece of 3-mm² of human cellular cementum as described above for examination with AFM. A piece of human alveolar bone (3 mm²) was also examined with AFM to show differences with human cementum and cementoblastoma-derived cells.

Energy-dispersive X-ray Micro-analysis (EDX)

The composition of the mineral-like tissue formed by the cementoblastoma-derived and osteoblastic cells was analyzed. Cells were plated onto a silicon (1,1,1) monocrystal substrate at initial density 2×10^4 in 24-well plates and cultured for 14 days in DMEM supplemented with 10% FBS, antibiotics, 50 µg/mL ascorbic acid, 10 mM of β-glycerophosphate, and 10⁻⁷ M dexamethasone. The cultures were analyzed by means of a Leica-Cambridge 440 scanning electron microscope fitted with a Pentafet energy-dispersive x-ray micro-analysis microprobe. After the cultures were terminated, they were washed with PBS, fixed in 70% ethyl alcohol, and air-dried. The surfaces of the cultures as well as the human cellular cementum and human alveolar bone were covered with a thin gold film about 100 nm thick, to avoid electron disturbances that could affect micro-analysis and SEM images. All analyses were carried out at 20 kV for 300 sec (Cuisinier *et al.*, 1991; Van Dijk *et al.*, 1995).

Transmission Electron Microscopy (TEM)

Cementoblastoma-derived cells were plated at 2×10^4 initial density in DMEM supplemented as described above in 24-well culture plates. The medium was replaced with fresh medium every other day, and cultures were kept under these conditions for 14 days. They were then briefly washed with PBS and fixed first *in situ* by the addition of 2.5% glutaraldehyde (buffered at pH 7.4 with 0.1 M

sodium cacodylate) at 4°C for 30 min. Second, the cells were fixed with 1% OsO₄ in the same buffer at 4°C for 1 hr. The samples were then dehydrated briefly in ascending concentrations of ethyl alcohol, followed by propylene oxide as a clearing agent. Cultures were embedded in epoxy resin. Semithin sections about 2 µm thick were obtained and stained with toluidine blue for light microscopy orientation. Ultra-thin sections (about 80 to 90 nm thick) cut with a diamond knife (Diatome, Biel, Switzerland) were mounted on Formvar-coated 150-mesh copper grids and examined with and without uranyl acetate and lead citrate (U-Pb) staining. Examination and recording were performed with a Phillips 201 and a Jeol 100 CX fitted with an SEM unity (STEM). A JEOL 400EX transmission electron microscope was used for the high-resolution analysis of the cultures.

Selected Area Diffraction Patterns by TEM

To reveal the formed mineral phase, we used selected areas of ultra-thin and unstained sections, mounted as described above, for electron diffraction and nanodiffraction techniques. D-spacings of diffraction patterns were calibrated against those of the gold standard obtained with identical diffraction conditions. The mineral phase was analyzed by means of a JEOL 100 CX analytical transmission microscope. All analyses were performed at 100 kV.

RESULTS

Transmission Electron Microscopy (TEM)

Light microscopy monitoring, together with Alizarin red S staining, showed that cementoblastoma-derived cells had formed the first mineralized structures (nodules) after 4 to 7 days in culture. The TEM examination revealed that cementoblastoma-derived cells contained all the cytoplasmic organelles characteristic of protein synthesis and secretion. Arrays of rough endoplasmic reticulum were disposed around the nuclear membrane. Golgi complex was observed in perinuclear areas. Primary lysosomes and mitochondria predominated in various cytoplasmic areas (Fig. 1). Membrane-bound vesicular structures were found intracellularly (Fig. 2). The vesicles had round to oval shapes, with diameters of 50 to 100 nm. The vesicles were electron-dense. Filament and needle-like crystals were observed in the vesicles (Fig. 2 inset). Examination of these nanocrystals at higher resolution with TEM showed both homogeneous and heterogeneous spatial crystal arrangements (Fig. 3).

Electron Diffraction and EDX Micro-analysis

Selected area diffraction patterns from unstained sections of the cementoblastoma-derived cells were obtained for the analysis of mineral deposits at 14 days of culture. Because of the nanosize of the formed crystals, they revealed patterns of concentric double rings. The inner double rings represent D-spacing (3.36 and 2.8, respectively) values consistent with those of hydroxyapatite (3.440 and 2.814) (Fig. 4). These D-spacings are in agreement with those registered from the HRTEM images as shown in Fig. 3.

X-ray EDX Micro-analysis

The Ca/P ratio and composition of the mineral-like tissue deposited by cementoblastoma-derived cells revealed prominent energy peaks for calcium and phosphorus similar to those for biological apatite (Fang *et al.*, 1994).

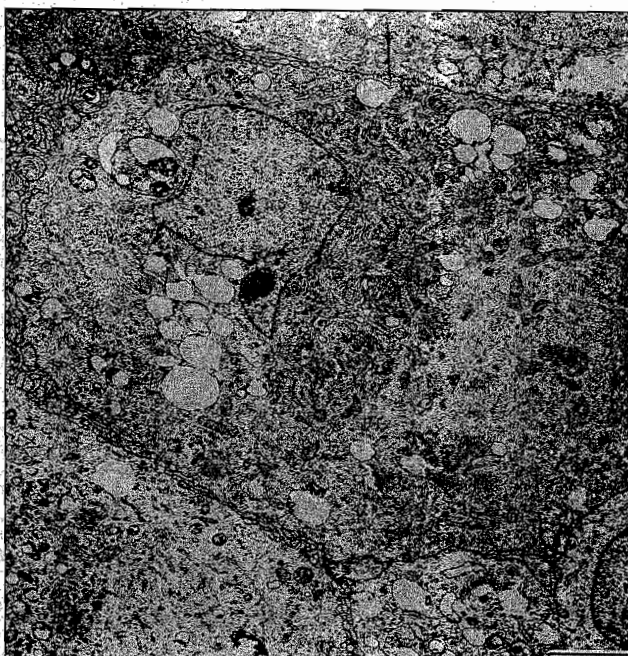


Figure 1. Electron micrograph of a cementoblastoma-derived cell having a nucleus with diffused heterochromatin and cytoplasm with rough endoplasmic reticulum, various amounts of mitochondria, and Golgi complex. 12,230X. Bar = 2.5 μ m.

Cementoblastoma-derived cells had 36.64 and 22.48 atomic percentages of Ca and P, respectively. Other elements such as Na (5.29%) and Cl (1.47%) were present in its global composition. Human cellular cementum revealed Mg 4.95, Na 8.43, Cl 2.92, P 28.18, and Ca 55.52 atomic percentages in its composition. The Ca/P ratio values (1.6056 for cementum cells and 1.9700 for human cellular cementum) correspond well with the biological hydroxyapatite value as determined by EDX. Osteoblastic cells showed 34.2 and 21.3 atomic percentages of Ca and P, respectively, with a Ca/P ratio of 1.6280. Na represented 4.52 and Cl 1.22 atomic percentage. Human alveolar bone had Na 6.63, Mg 2.10, Cl 0.84, P 35.33, and Ca

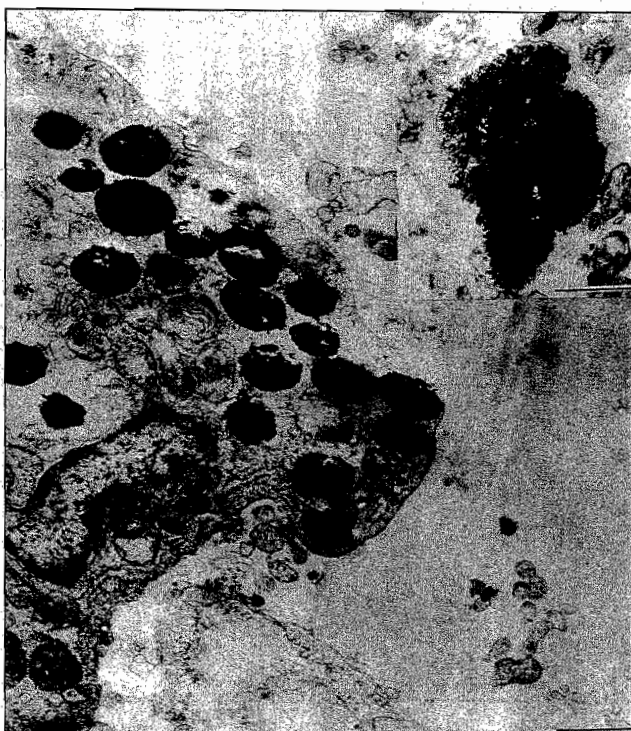


Figure 2. Electron micrograph of cementoblastoma-derived cells shows intracytoplasmic electron-dense granules with a rough shape. 14,000X. Bar = 1.0 μ m. Intracellular vesicle surrounded by a membrane. Note filament and needle-like structures inside the vesicle (inset). 30,000X. Bar = 0.3 μ m.

55.11 atomic percentage in its composition. Human alveolar bone had a Ca/P ratio value of 2.01. Both osteoblastic cells and alveolar bone values correspond to those of biological-type hydroxyapatite as determined by EDX (Figs. 5A, 5B).

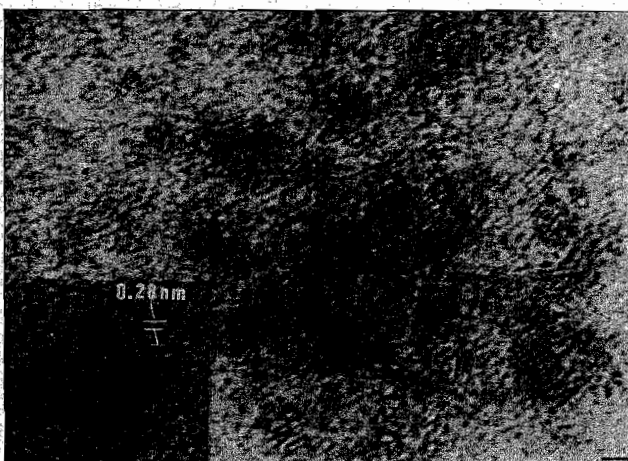


Figure 3. High-resolution transmission electron microscopy (HRTEM). A representative image from cementum cells showing a heterogeneous and homogeneous (inset) arrangement of hydroxyapatite crystals. Bar = 50 nm.

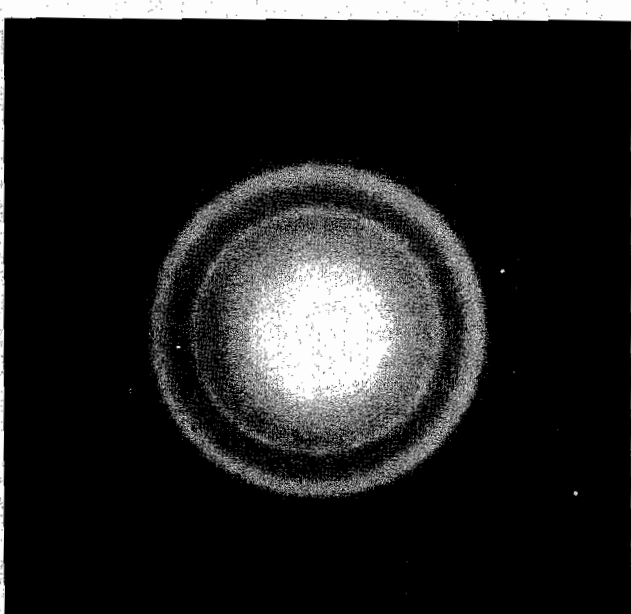


Figure 4. Electron diffraction pattern from mineralized intracellular vesicles observed in cementoblastoma-derived cells.

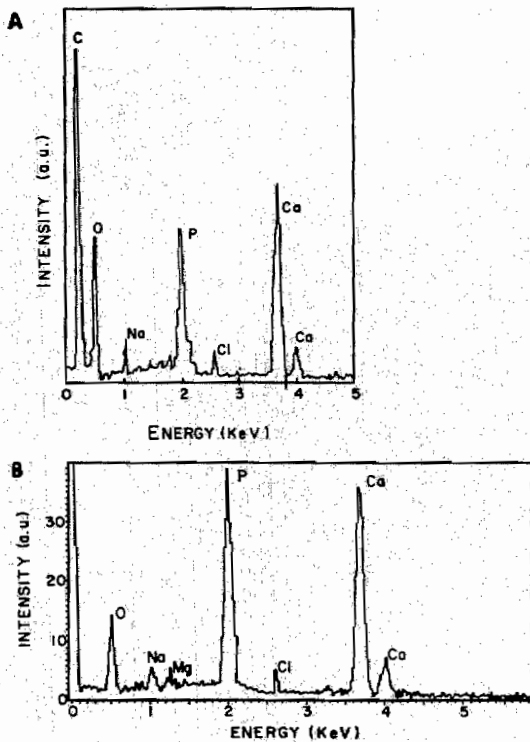


Figure 5. (A) Representative energy-dispersive x-ray micro-analysis spectrum of mineralized areas of cementoblastoma-derived and osteoblastic cells cultured on a silicon (1,1,1) substrate, showing prominent peaks of calcium (Ca), phosphorus (P), and peaks representing sodium (Na) and chloride (Cl). (B) Human cellular cementum and human alveolar bone additionally presented a peak of magnesium (Mg) in its global composition.

X-ray Diffraction Analysis

The crystallinity of the mineralization process was evaluated by x-ray diffraction. The mineral deposited by cementoblastoma-derived cells showed crystallinity with both non-homogeneous (2,1,1, 2,1,0, 2,0,1, etc.) and preferential orientation (2,1,0) of hydroxyapatite crystallites. The heterogeneous diffraction pattern obtained from both cementoblastoma-derived cells and human cellular cementum showed a differential organization of the mineral phase (Fig. 6A). The well-defined diffraction peak obtained from the cementoblastoma-derived cells and human cellular cementum resembles a textured preferentially oriented and homogenized layer of mineral (Fig. 6B). Both patterns were indexed with the hydroxyapatite standard patterns of the JCPDS (Joint Committee on Powder Diffraction Standards No. 9-432 file for calcium hydroxyapatite) (JCPDS, 1998).

Atomic Force Microscopy

The morphology of the mineral deposited by cementoblastoma-derived cells cultured onto a silicon (1,1,1) monocrystal substrate revealed small granular particles ($1 \pm 0.5 \mu\text{m}$) and highly crystalline plaques with needle-like morphology ($35 \pm 15 \mu\text{m}$) for both cementoblastoma-derived cells and human cellular cementum. Cementum cell cultures and human cellular cementum showed a layered structure demarcated by incremental cell lines (Figs. 7A, 7B, respectively). The crystal morphology revealed the submicron size ($0.2 \mu\text{m}$) of the

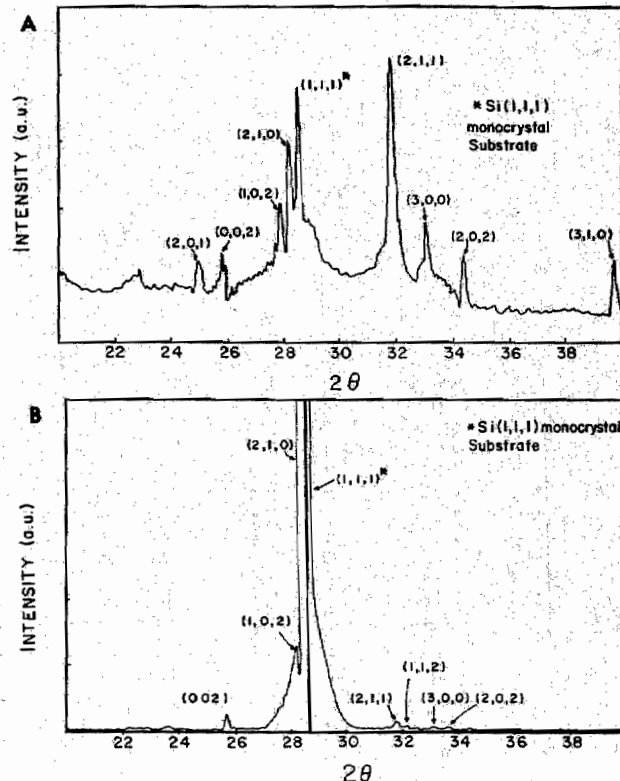


Figure 6. A representative analysis of the crystallinity by means of the x-ray diffraction technique from mineralized areas of cementoblastoma-derived cells and human cellular cementum, showing the XRD pattern with broad peaks, indicating (A) heterogeneous grain size and (B) a better crystallinity with (2,1,0) preferential orientation and homogeneous crystallites.

granular spherical particles that form the agglomerates (Fig. 8A). The frontal needle-like crystals had a grain submicron size average about $0.5 \pm 0.3 \mu\text{m}$ (Fig. 8B). Human cellular cementum revealed similar hydroxyapatite crystal morphology. They showed agglomerates with a granular disposition that resembled that of the cementum tumor cell cultures. The microsize of the granules observed in human cellular cementum was heterogeneous to a size range between $0.2 \mu\text{m}$ and $0.002 \mu\text{m}$ (Figs. 8C, 8D). Osteoblastic cells showed needle-like crystals oriented perpendicular to the silicon (1,1,1) monocrystal substrate and organized in plaque-like structures with a size range of $2.2 \pm 0.3 \mu\text{m}$. Human alveolar bone had well-oriented longitudinal crystals with a size range between 2.0 and $4.0 \mu\text{m}$, and with a lamellar pattern. (Figs. 8E, 8F, respectively). The examination of the cementoblastoma-derived cell cultures with SEM revealed mineralized areas which were formed by agglomerates of homogeneous size with spherical and ring-like shapes (Fig. 9A). Human cellular cementum showed similar agglomerates of heterogeneous size and morphology (Fig. 9B).

DISCUSSION

Human cementoblastoma-derived cells showed membrane-bound intracellular vesicular structures after 14 days in culture. The vesicles showed heavy electron-dense mineralized material that contained filaments and needle-like crystals. The function of these vesicles is still obscure. However, it is possible that they

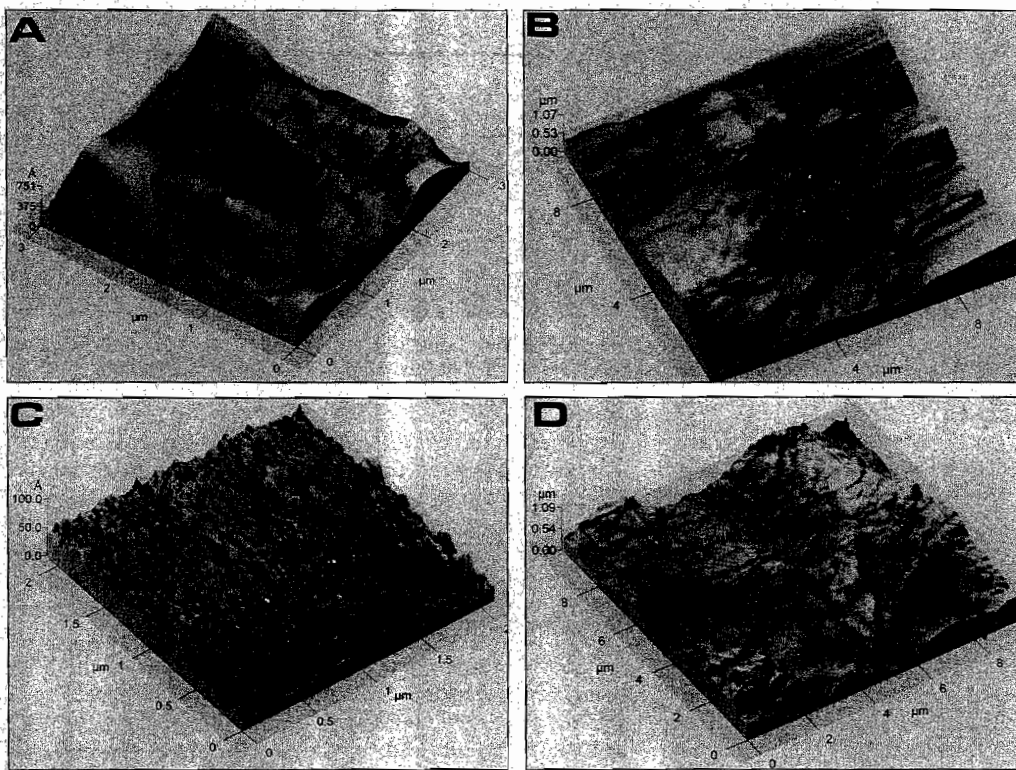


Figure 7. (A) AFM three-dimensional images showed lamellar arrangement of the mineral-like tissue formed by cementoblastoma-derived cells. (B) Human cellular cementum showing similar spatial disposition of the mineral agglomerates and also parallel alignment of the mineral plaques. (C) Osteoblastic cells showed longitudinal needle-like arrangement of the apatite crystals. (D) Human alveolar bone showing apatite crystals oriented similar to those observed in osteoblastic cell cultures.

represent Ca/P storing mitochondria (Lehninger, 1970; Matthews *et al.*, 1970; Brighton and Hunt, 1976; Appleton and Morris, 1979; Landis *et al.*, 1980; Wuthier, 1982). This concept is supported, since the calcium complex is located predominantly in mitochondria as well as in cell membranes, and represents the

initial mineralization site. It also suggests that intracellular calcium plays a significant role in matrix calcification (Sasagawa, 1988). It is possible that, during cementogenesis, cementoblasts liberate Ca/P storing vesicles by physiological cell death to increase the amount of mineral constituents at sites of mineralization, and that those crystals could serve as initial extracellular nucleation centers for hydroxyapatite crystals (Zimmermann *et al.*, 1991; Zimmermann, 1994). Although the importance of cell necrosis in the process of mineralization is as yet unclear, it is important to note that a secretion process from these vesicles was not observed. As shown in the AFM images, the mineral accumulation had morphological processes ranging from amorphous-globular to

crystalline filaments and needle-like morphology. From these results, we assume that this transformation phase takes place within intracellular vesicular structures. This finding provides additional evidence that initial mineralization requires a micro-environment limited by a membrane (vesicular) structure derived from the cells. This is not a unique finding, since intracellular vesicles have been observed in osteoblasts

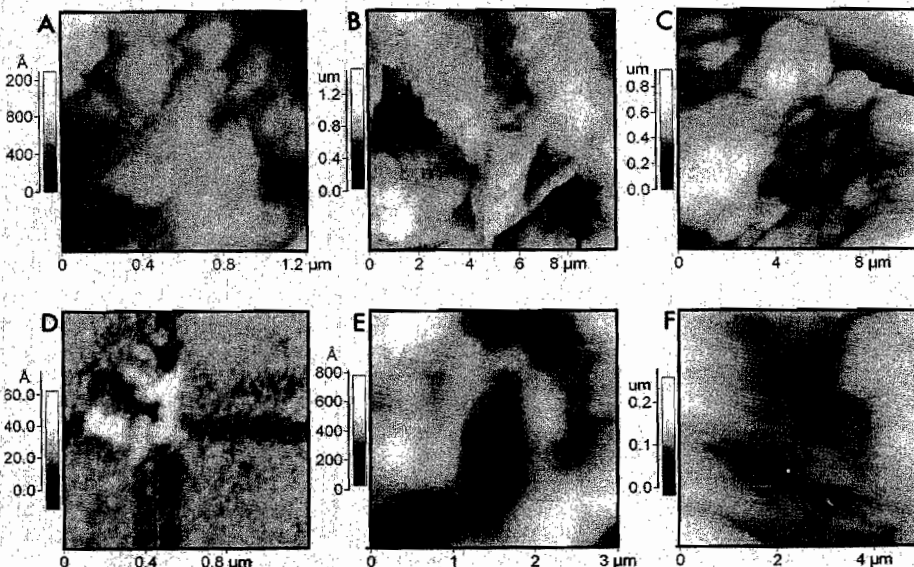


Figure 8. The morphologic features obtained by atomic force microscopy showed that the cementoblastoma cells and human cellular cementum mineral deposits were composed of large agglomerates of tiny submicron-size granular particles (A and D, respectively). Other mineralized areas showed large plaques with some needle-like and small granular particles (B and C, for cementoblastoma-derived cells and human cellular cementum, respectively). (E) Osteoblastic cells showed needle-like crystals oriented perpendicular to the silicon (1,1,1) monocrystal substrate and organized in plaque-like structures with micron size particles. (F) Human alveolar bone had well-oriented longitudinal crystals with a micron size range and with a filament-like pattern.

and associated with transitional stages between mitochondria and intracellular vesicles surrounded by double membranes (Volpe *et al.*, 1988). The occurrence of intracellular vesicles has also been observed in odontoblasts and associated with the mineralization process (Hayashi *et al.*, 1993). AFM images and x-ray EDX microanalysis demonstrated that cementoblastoma-derived cells and human cellular cementum had compositional and morphological features in common. Both showed similar composition and Ca/P ratios. Importantly, the cementoblastoma-derived cells produced biological-type apatite. The morphological features observed in the cementoblastoma cultures resembled those of human cellular cementum. Crystals and a layered structure demarcated by incremental lines were also evident. This lamellar pattern is characteristic of human cellular cementum (Yamamoto *et al.*, 1998). Osteoblastic cells and human alveolar bone showed needle-like crystals with longitudinal arrangement of the mineral-like tissue. However, the morphological features observed in human osteoblastic cells and human alveolar bone were clearly different from those observed in human cementoblastoma-derived cells and human cellular cementum. An important finding in the osteoblastic cells and cementoblastoma-derived cultures was that they do not have Mg in their global composition. We could thus assume that magnesium could interact in the formation, stability, and maturation of biological hydroxyapatite and related Ca/P ratio. This could explain the lower Ca/P ratio values obtained from the cultures when compared with those obtained from human cellular cementum and alveolar bone (LeGeros and Kojkowska, 1989).

It has previously been demonstrated that globular-like structures, which represent initial nucleation centers of hydroxyapatite crystals, are localized intracellularly (Arzate *et al.*, 1998). XRD images showed both a heterogeneous and homogeneous preferential orientation of hydroxyapatite crystals. A similar spatial arrangement of hydroxyapatite crystals was observed in human cellular cementum. The organic structure of the mineral-like tissue formed by the cementoblastoma-derived cells was shown to be granular and needle-like. These features matched those demonstrated in human cellular cementum (Bonucci, 1971, 1987; Goldberg *et al.*, 1980; Bishop and Warshawsky, 1982; Hayashi *et al.*, 1986; Hayashi, 1985, 1989). The composition, morphological appearance of the mineral-like tissue, and size and shape of the hydroxyapatite crystals formed by cementoblastoma-derived cells, when compared with those of human cellular cementum, strongly support the contention that the mineral-like tissue formed by the cementoblastoma-derived cells is human cellular cementum, produced *in vitro*. In the culture system reported here and in our culture conditions, cementoblastoma-derived and osteoblastic cells were able to grow and differentiate when they were plated onto a silicon monocrystal substrate. In addition, they were able to produce biological-type hydroxyapatite. However, when plastic substrate was used, there was an absence of Na and Cl in the global composition of the mineral-like tissue deposited by the cells. This suggests that the substrate influenced the secretory

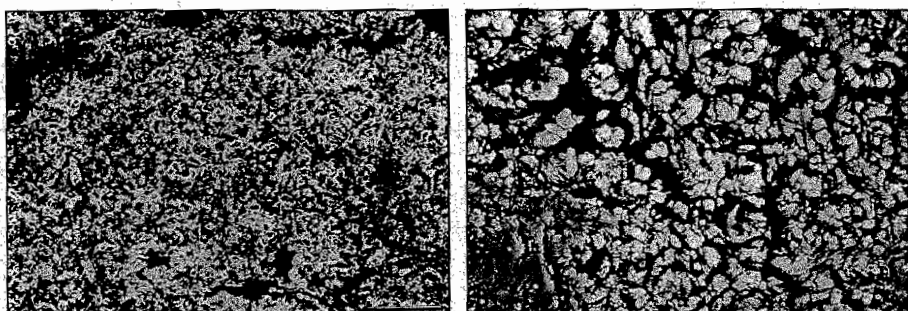


Figure 9. Mineralized features observed by SEM in (A) cementoblastoma-derived cells and (B) human cellular cementum, showing spherical and ring-like shapes. Bar = 100 μm (A) and 10 μm (B).

properties of the cells to produce biological-type hydroxyapatite. This culture system, then, could be useful to study how the inducers-precursors of the mineralization process influence the morphology and composition of mineralized-like tissue. The electron diffraction patterns of the intracellular mineral deposits showed concentric inner rings and D-spacings identical to those of hydroxyapatite. These results clearly showed that the crystals formed in this system represent combined organic-inorganic structures, which contain a solid phase deposit, which is a biological-type apatite. The combined data from chemical, x-ray diffraction, TEM, HRTM, electron diffraction, and SEM analyses have allowed for the precise identification of the crystalline components of the cementum-like tissue deposited by the putative cementoblasts and from human cellular cementum.

We have further characterized the ultrastructural features, nature, and physical structure of the mineral deposited by cementoblastoma-derived cells, which appear to be almost identical to those characteristics of cellular cementum. Although cementum and alveolar bone cells share a common stem cell, from the morphological and compositional differences between cementoblastoma-derived and osteoblastic cells and from their similarities to human cellular cementum, our results lead us to conclude that the cementoblastoma-derived cells expressed the cellular cementum phenotype. Differences between present results and those from other mineralizing cells may indicate molecular variations in the mineralization pathways. A new approach to the analysis of the three-dimensional structure, the composition of the mineral-matrix complex, and the arrangement of the apatite crystallites during the cementogenesis process *in vitro* is proposed.

ACKNOWLEDGMENTS

The authors are indebted to R. Fragoso, M.A. Leyva, P. Mexia, R. Hernández, G. Mondragón, C. Angeles, L. Baños, and A. Caballero from CINVESTAV-México, IF-UNAM, ININ-México, and IIM-UNAM for their assistance during the course of this study. Their support is appreciated. This work was supported by DGAPA-UNAM Grant IN200597 and CONACYT Grant 0057P-M to H.A.

REFERENCES

- Appleton J, Morris DC (1979). The use of the potassium pyroantimonate-osmium method as a means of identifying and localizing calcium at the ultrastructural level in the cells of calcifying systems. *J Histochem Cytochem* 27:676-680.

- Arzate H, Olson SW, Page RC, Narayanan AS (1992a). Isolation of human tumor cells that produce cementum proteins in culture. *Bone Miner* 18:15-30.
- Arzate H, Olson SW, Page RC, Gown AM, Narayanan AS (1992b). Production of a monoclonal antibody to an attachment protein derived from human cementum. *FASEB J* 6:2990-2995.
- Arzate H, Alvarez-Pérez MA, Aguilar-Mendoza ME, Alvarez-Fregoso O (1998). Human cementum tumor cells have different features from human osteoblastic cells *in vitro*. *J Periodont Res* 33:249-258.
- Bishop MA, Warshawsky H (1982). Electron microscopic studies on the potential loss of crystallites from routinely processed sections of young enamel in the rat incisor. *Anat Rec* 202:177-186.
- Bonucci E (1971). The locus of initial calcification in cartilage and bone. *Clin Orthop* 78:108-139.
- Bonucci E (1987). Is there a calcification factor common to all calcifying matrices? *Scanning Microsc* 1:1089-1102.
- Bosshardt DD, Schroeder HE (1996). Cementogenesis reviewed: a comparison between human premolars and rodent molars. *Anat Rec* 245:267-292.
- Brighton CT, Hunt RM (1976). Histochemical localization of calcium in growth plate mitochondria and matrix vesicles. *Fed Proc* 35:143-147.
- Cuisinier FJ, Glaisher RW, Voegel JC, Hutchison JL, Bres EF, Frank RM (1991). Compositional variations in apatites with respect to preferential ionic extraction. *Ultramicroscopy* 36:297-305.
- D'Errico JA, MacNeil RL, Takata T, Berry J, Strayhorn C, Somerman MJ (1997). Expression of bone associated markers by tooth root lining cells, *in situ* and *in vitro*. *Bone* 20:117-126.
- Fang Y, Agrawal DK, Roy DM (1994). Thermal stability of synthetic hydroxyapatite. In: *Handbook of bioactive ceramics*. Vol. III. Boca Raton, FL: CRC Press, pp. 269-282.
- Goldberg M, Molon Noblot M, Septier D (1980). Effects of 2 methods of demineralization on the preservation of glycoproteins and proteoglycans in the intertubular and peritubular dentin in the horse [in French]. *J Biol Buccale* 8:315-330.
- Gould TR, Melcher AH, Brunette DM (1977). Location of progenitor cells in periodontal ligament of mouse molar stimulated by wounding. *Anat Rec* 188:133-141.
- Grzesik WJ, Kuznetsov SA, Uzawa K, Mankani M, Gehron Robey P, Yamauchi M (1998). Normal human cementum-derived cells: isolation, clonal expansion, and *in vitro* and *in vivo* characterization. *J Bone Miner Res* 13:1547-1554.
- Hayashi Y (1985). Ultrastructural characterization of extracellular matrix vesicles in the mineralizing fronts of apical cementum in cats. *Arch Oral Biol* 30:445-449.
- Hayashi Y (1989). Ultrastructural demonstration of the carbohydrate in developing rat enamel using soybean agglutinin-gold complexes. *Arch Oral Biol* 34:517-522.
- Hayashi Y, Bianco P, Shimokawa H, Termine JD, Bonucci E (1986). Organic-inorganic relationships, and immunohistochemical localization of amelogenins and enamelin in developing enamel. *Basic Appl Histochem* 30:291-299.
- Hayashi Y, Imai M, Goto Y, Murakami N (1993). Pathological mineralization in a serially passaged cell line from rat pulp. *J Oral Pathol Med* 22:175-179.
- JCPDS (1998). Joint Committee on Powder Diffraction Standards No. 9-432 file for calcium hydroxyapatite.
- Landis WJ, Paine MC, Glimcher MJ (1980). Use of acrolein vapors for the anhydrous preparation of bone tissue for electron microscopy. *J Ultrastruct Res* 70:171-180.
- LeGeros RZ, Kojkowska R (1989). Synergistic effect of magnesium and carbonate on some properties of apatites (abstract). *J Dent Res* 68(Spec Iss):1003.
- Lehnninger AL (1970). Mitochondria and calcium ion transport. *Biochem J* 119:129-138.
- MacNeil RL, D'Errico JA, Ouyang H, Berry J, Strayhorn C, Somerman MJ (1998). Isolation of murine cementoblasts: unique cells or uniquely-positioned osteoblasts? *Eur J Oral Sci* 106(Suppl 1):350-356.
- Matthews JL, Martin JH, Sampson HW, Kunin AS, Roan JH (1970). Mitochondrial granules in the normal and rachitic rat epiphysis. *Calcif Tissue Res* 5:91-99.
- McCulloch CA, Melcher AH (1983). Cell migration in the periodontal ligament of mice. *J Periodont Res* 18:339-352.
- McCulloch CA, Nemeth E, Lowenberg B, Melcher AH (1987). Paravascular cells in endosteal spaces of the alveolar bone contribute to periodontal ligament cell populations. *Anat Rec* 219:233-242.
- Melcher AH, McCulloch CA, Cheong T, Nemeth E, Shiga A (1987). Cells from bone synthesize cementum-like and bone-like tissue *in vitro* and may migrate into periodontal ligament *in vivo*. *J Periodont Res* 22:246-247.
- Narayanan AS, Page RC (1976). Biochemical characterization of collagens synthesized by fibroblasts derived from normal and diseased human gingiva. *J Biol Chem* 251:5464-5471.
- Sasagawa I (1988). The appearance of matrix vesicles and mineralization during tooth development in three teleost fishes with well-developed enameloid and orthodentine. *Arch Oral Biol* 33:75-86.
- Van Dijk K, Schaecken HG, Maree CHM, et al. (1995). Influence of Ar pressure on r.f. magnetron-sputtered $\text{Ca}_5(\text{PO}_4)_3\text{OH}$ layers. *Surf Coat Technol* 76:206-210.
- Volpe P, Krause KH, Hashimoto S, Zorzato F, Pozzan T, Meldolesi J, et al. (1988). "Calciosome," a cytoplasmic organelle: the inositol 1,4,5-trisphosphate-sensitive Ca^{2+} store of nonmuscle cells? *Proc Natl Acad Sci USA* 85:1091-1095.
- Wuthier RF (1982). A review of the primary mechanism of endochondral calcification with special emphasis on the role of cells, mitochondria and matrix vesicles. *Clin Orthop* 169:219-242.
- Yamamoto T, Domon T, Takahashi S, Islam NM, Suzuki R, Wakita M (1998). The regulation of fiber arrangement in advanced cellular cementogenesis of human teeth. *J Periodont Res* 33:83-90.
- Zimmermann B (1994). Occurrence of osteoblast necroses during ossification of long bone cortices in mouse fetuses. *Cell Tissue Res* 275:345-353.
- Zimmermann B, Wachtel HC, Noppe C (1991). Patterns of mineralization *in vitro*. *Cell Tissue Res* 263:483-493.

